A Doctoral Thesis on

DRY AUTOTHERMAL REFORMING OF FUELS

SUBMITTED TO THE

University of Pune

FOR THE DEGREE OF
DOCTOR OF PHILOSOPHY

(In Chemical Engineering)

BY

GANESH R. KALE

National Chemical Laboratory, Pune
(Registered with University of Pune)

This research work was carried out with place of research
Chemical Engineering & Process Development Division
National Chemical Laboratory, Pune – 411008, INDIA.

June 2014

Dedicated to my Parents, family and NCL

CERTIFICATE OF THE GUIDE

CERTIFIED that the work incorporated in the thesis **DRY AUTOTHERMAL REFORMING OF FUELS** submitted by Mr. Ganesh R. Kale was carried out by the candidate under my supervision/ guidance. Such material as has been obtained from other sources has been duly acknowledged in the thesis.

Dr. B. D. Kulkarni
(Supervisor/ Research Guide)

DECLARATION BY THE CANDIDATE

I declare that the thesis entitled **DRY AUTOTHERMAL REFORMING OF FUELS** submitted by me for the degree of Doctor of Philosophy is the record of work carried out by me during the period from July 2005 to February 2014 under the guidance of Dr. B.D. Kulkarni and has not formed the basis for the award of any degree, diploma, associateship, fellowship, titles in this or any other University or other institution of Higher learning.

I further declare that the material obtained from other sources has been duly acknowledged in the thesis.

(Ganesh R. Kale) Date: 6 June 2014

Acknowledgement

A doctorial degree is a vital component of a researcher's life. I started this research work with great enthusiasm a few years ago and now I feel very happy to complete this research thesis. I am highly indebted to my research guide Dr. B D Kulkarni for guiding me in this research work, correcting my ideas and constantly encouraging me to think in positive direction, without which I would not have succeeded this far. I have taken a lot of his time during the past few years to learn invaluable research themes and ideas, patience to pursue them till completion and importance of updating research skills. I also wish to thank members of the research committee, Dr. Tambe and Dr. Inamdar for their continuous help and suggestions for completing this research thesis.

I am also indebted to my parents, my wife and my children who have wholeheartedly supported me to reach this most important milestone in my life and missed me at home on many important occasions.

My special thanks to Mr. Ajit Joshi, Mr Prakash Bhujang, Mr. Prashant Kulkarni and Mr. Ganpat Mane who have helped me in all aspects of life in these years. I cannot forget the kind help and advice of Mr V G Kulkarni, Mr. G M Chaphekar and Dr. S N Shintre, who have interacted with me many times to ensure that I stay on path to complete this degree.

I also wish to thank Dr. V V Ranade, Dr. P V Rao, Dr. M S Qureshi, Dr. Imran Rehman, Dr. Gurunath and Dr. Sunil Bhongale for their kind support and advice. I also thank my students for helping me in various aspects of research activities and calculations through which I gained better understanding on many research themes. I sincerely thank my colleagues Prof. Ratnadip Joshi, Dr. Harshavardhan Pol and Dr. Deenadayalan for their help me in this Ph.D venture.

Lastly, I also thank those whom I may have missed mentioning unknowingly.

Ganesh R. Kale

Abstract

CO_2 is a greenhouse gas that is emitted worldwide by various chemical processes and is responsible for problems like global warming and climate change. The serious need to cut CO_2 emissions from the chemical processes is already under implementation. Simultaneously the development of CO_2 utilization processes to convert CO_2 to value added chemicals is also a crucial requirement for chemical industries.

This research work is focused on the CO_2 utilization by dry autothermal reforming (DATR) which is similar to steam reforming, autothermal reforming and dry reforming. A basic thermodynamic basis, similar to these processes, is adopted and is further expanded in depth. The main assumption of thermodynamic chemical equilibrium (which defines the maximum possible conversion in chemical processes) is applied to the DATR process. Application of DATR to some well known areas in chemical industry is also studied in this research. Traditional fuels such as coal, LPG, gasoline and bio fuels like ethanol and glycerol are used in this study.

The research work starts with a general product distribution study in a DATR process at different operating parameters. This establishes the thermodynamic feasibility of DATR. It expands further to study the distribution of thermoneutral points for DATR process operation and the product yield trends at the thermoneutral points. Thermoneutral temperatures are very important process operational points in autothermal processes. The application of DATR in fuel processor development to generate syngas to fuel the Solid Oxide fuel cells, and its comparison to the traditional autothermal reforming is studied. Further, the application of DATR in coal gasification and its comparison with steam coal gasification in mixtures and the generation of value added products is also studied. The coupling of DATR to chemical looping combustion (CLC) to sequester the generated CO_2 for value added product generation is further studied in this research work. The conclusions of the thesis with a few recommendations as possible directions for future research are discussed in the last chapter.

Dry Autothermal reforming of fuels

Ganesh R. Kale

June 6, 2014

Contents

List of Figures

List of Tables

Chapter 1

Introduction

CHAPTER 1: Introduction

1.1 Introduction

Carbon based fossil fuels like coal, oil and gas are widely combusted to generate thermal energy (based on their heat of combustion), which is then converted to other forms of energy. The flue gas emitted from the combustion process mainly consists of N_2, CO_2, along with nitrogen oxides, sulfur oxides, CO, H_2, excess oxygen and some particulate matter and is released to the atmosphere increasing CO_2 emissions that lead to global warming and climate change issues that have emerged as a major problem for rich industrialized nations as well as developing countries. Reducing CO_2 emissions to atmosphere is a solution to slow the impacts of climate change, however it has many limitations. Carbon sequestration through plants was a well established culture, but nowadays the rate at which these CO_2 emissions occur cannot be helped by biological systems like trees as they are regularly deforested. Pure CO_2 generation using clean energy techniques like chemical looping combustion is also researched but the CO_2 utilization is not much researched area. There is a need of an innovative way to sequester carbon dioxide. CO_2 utilization by chemical reactions / processes is a crucial necessity today as these reactions are fast and can be scaled up to larger capacities easily.

CO_2 utilization has been a hot topic for research in many countries. There are several chemical reactions / processes that are being researched to convert CO_2 to value added chemicals. One of the most important products of CO_2 utilization is syngas (H_2 + CO). Syngas is a useful value added product for many applications. Syngas has been used as raw material to produce hydrocarbons, as fuel in IC engines, for synthesis of LPG, gasoline, alcohols, DME, as fuel in gas turbines, for use in coal liquefaction, for use in co-firing and reburning in a coal fired boiler, for synthesis of methanethiol, as fuel in fuel cells and is also used to synthesize biofuels by syngas fermentation. Dry reforming is one of the most popular catalytic process to convert CO_2 to syngas. Many research studies about dry reforming are reported in literature.

Jankhah et al. (2008) have studied the thermodynamic equilibrium analysis and experimentation of thermal and catalytic ethanol cracking and dry reforming using a carbon steel catalyst precursor and reported that highest hydrogen and carbon (carbon nanofilaments) yields were obtained at 550ºC. Wang et al. (2009) have studied the thermodynamics of ethanol reforming with carbon dioxide for hydrogen production and have reported the optimum conditions which gave over 94% yield of syngas with complete conversion of ethanol without carbon deposition. De Oliveira-Vigier et al. (2005) have experimentally studied the dry reforming of ethanol using a recyclable and long lasting SS 316 catalyst and have obtained hydrogen yield that is 98% of the theoretical value. Blanchard et al. (2008) have experimentally studied the ethanol dry reforming using a carbon steel catalyst to produce syngas and also nanocarbons. Bellido et al. (2009) have experimentally studied the dry reforming of ethanol using Ni/Y_2O_3-ZrO_2 catalysts and achieved a maximum CO_2 conversion of 61% on 5NiYZ catalyst at 800°C. However dry reforming is a highly endothermic process that suffers a great drawback of carbon formation and catalyst deactivation and hence has many limitations. Hence the process has failed to commercialise.

Steam reforming of fuels has been practiced for a long time in chemical industry primarily for hydrogen generation. It is a catalytic endothermic process. It also had some limitations due to carbon formation and highly endothermic reaction. But further research in this area developed an advanced version in this category - autothermal steam reforming that uses oxygen (air) insitu to generate heat by partial oxidation to supply energy to the endothermic steam reforming. A similar strategy was devised to overcome the problems of dry reforming. The advanced version is named as dry autothermal reforming (DATR) and is studied in detail in this thesis. This thesis is aimed to study the feasibility of dry autothermal reforming of fuels and its applications in different industrial sectors. Secondly, since steam reforming, autothermal reforming and dry reforming do not have any specific fuel limitations, it was also crucial to ascertain the wide applicability of DATR

using different fuels. Hence a number of fuels (biofuels – (glycerol and ethanol), Lignite coal, hydrocarbons – (LPG (propane) and gasoline (isooctane) have been used in this research study. Figure 1.1 shows the conceptual design of DATR process.

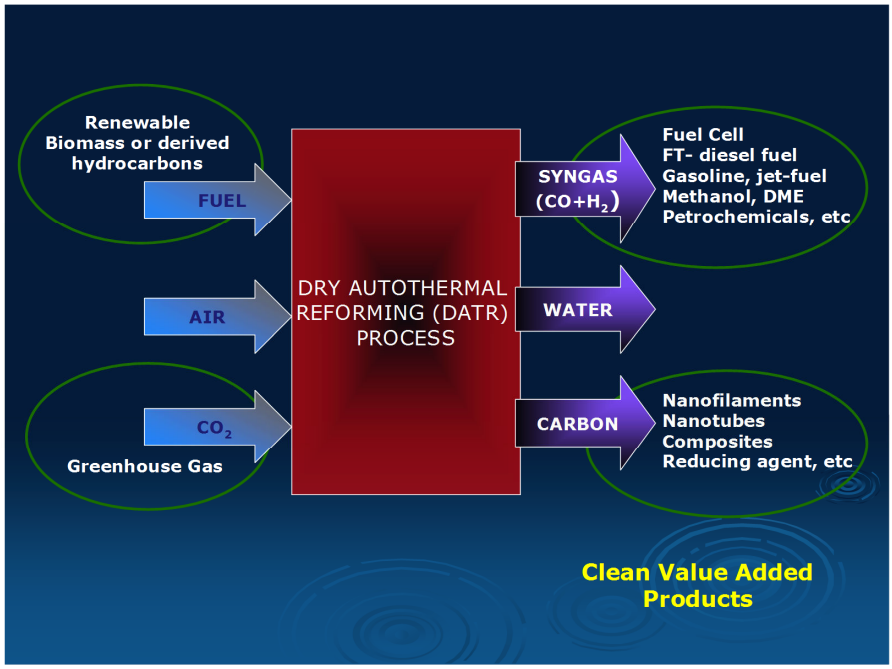

Figure 1.1: Conceptual process design of DATR

1.2 Methodology

Development of new chemical reactions / processes is a very costly matter. The studies start with basic theoretical calculations which further grow to experimental studies, catalyst development programs, bench scale studies, reactor and process design, pilot plant studies and commercialization. Further, it is very important to device a process that may have applications in various industrial sectors. This thesis aims at studying the CO_2 utilization by DATR for some important fuels and evaluate the applications in some high value processes.

Thermodynamics is the backbone for chemical industry. Thermodynamics studies the feasibility of chemical reactions at different temperatures. Many processes have been designed using the thermodynamic studies. Thermodynamics provides the domain for process operation and also defines the maximum and minimum yields and conversions of desired / byproducts. Thermodynamic equilibrium studies for process development have earlier been reported using Gibbs free energy minimization algorithm or simultaneous solution of non-linear reaction equations coded to Matlab programs, equilibrium reactor module of Design II, HYSYS, Aspen Plus, fluent or HSC Chemistry software. Sometimes simultaneous solution of non-linear reaction equations based on equilibrium constants might become complex and tedious.

Another procedure taking account of chemical species and suitable for general computer solution is based on minimization of the total Gibbs energy G_t (Perry 1997) is shown by the expression:

$$(dG_t)_{T,\,P} = 0$$

It shows that all irreversible processes occurring at constant T (temperature) and P (pressure) proceed in a direction where the total Gibbs energy of the system decreases and the equilibrium state has the minimum total Gibbs energy attainable at the given T and P. Although the choice of a set of species is equivalent to the choice of a set of independent reactions among the species, different assumptions might produce different results.

HSC Chemistry version 5.1 (2002) has been used for this thermodynamic study. This software is very user friendly (Smith, 1996). Equilibrium calculations in the Gibbs routine are made using the Gibbs energy minimization method. The Gibbs program finds the most stable species combination and seeks the phase compositions where the Gibbs energy of

the system reaches its minimum at a fixed mass balance (a constraint minimization problem), constant pressure and temperature. Hence, no specific chemical reaction equations are needed in the input.

The optimum process operating conditions can be generated using these models including feasibility studies at different conditions of temperature, pressure, input feed ratios, fuels etc. The product compositions are analyzed and the optimum process conditions for maximizing desired products and minimizing undesired products at minimized energy requirements and negligible pollution for traditional fuels such as coal, LPG, gasoline or bio fuels like ethanol and glycerol were found in this study.

HSC Chemistry software is low cost effective software used for this research work. The software is recognized software at international level and has a very good thermodynamic database of many compounds. Several researchers have used this software for their research studies. The chemical equilibrium module of the software is effective in calculating equilibrium compositions in a complex reforming systems such as steam reforming, dry reforming, dry autothermal reforming, etc without the need of specific reaction equations. This is a major advantage of the software as the exact number and nature of chemical reactions in any process are very difficult to determine.

The objectives of the present research work were as follows:

i) To study the thermodynamic feasibility of DATR process using a fuel (e.g. glycerol),
ii) To study the thermoneutral point analysis in DATR using a fuel (e.g. ethanol),
iii) To study the application of DATR in fuel processor development,
iv) To study the application of DATR in Chemical looping combustion system,
v) To study the application of DATR in coal gasification process,

1.3 Summarized details of each chapter

The thermodynamic feasibility of dry autothermal reforming is studied in **Chapter 2** using glycerol as a fuel. Glycerol is a byproduct of biodiesel production process. Biofuels like ethanol and biodiesel are gaining significance due to the consistent decline in fossil fuels like oil and natural gas reserves worldwide. Glycerol is projected to be extensively available byproduct after the commercialization of biodiesel production processes. This has prompted researchers to find ways for utilization of glycerol. Thermodynamic equilibrium data for dry autothermal reforming of glycerol was generated for temperature range 600–1000 K, 1 bar pressure, OCGR [feed O_2/C(C of glycerol only) ratio] 0.1 to 0.5 and CGR [feed CO_2/glycerol ratio] 1 to 5 and analyzed. The objective of this chapter was to identify the thermodynamic domain of the process operation, study the variation of product distribution pattern and describe the optimum conditions to maximize yield of the desired product and minimize the undesired product formation. The concept of thermoneutral point was introduced at the end of this chapter.

Thermoneutral point is the condition where the endothermic reactions balance the exothermic reactions to make the net enthalpy of chemical reaction zero. Autothermal processes are generally operated at thermoneutral conditions to maximize energy efficiency. However, very little literature is available regarding thermoneutral points and product trends at those points. The concept of the thermoneutral point in dry autothermal reforming was studied in detail in the **Chapter 3** using ethanol as a fuel. The main goal of this work was to analyze the thermoneutral conditions for DATR of ethanol process to produce a variety of value added products like hydrogen, syngas and CNF's whose yield can be maximized at different operating conditions and input ratios. This study intended to study the variation of components in the product stream at thermoneutral conditions, presenting product yields and product

distribution trends at various pressures to find the best operating thermoneutral point for the desired product.

Chapter 4 deals with the application of DATR in fuel processor systems. Hydrogen energy and fuel cells are considered to be the future energy sources. Syngas (H_2 + CO) production using hydrocarbon reforming has been a popular research area for more than three decades. Various hydrocarbon fuels have been evaluated for their capacity to fulfil the requirements of fuel processor system. Liquid fuels like gasoline have high energy density and are the most favourable choice for fuel processors as reported in literature. This chapter aimed to explore the thermodynamics of an alternate syngas generation process i.e. DATR and its comparison to popular autothermal reforming process of isooctane for use in gasoline fuel processors to power the Solid Oxide Fuel Cell (SOFC). A thermodynamic analysis of isooctane as feed hydrocarbon for autothermal reforming and dry autothermal reforming processes for feed OCIR (oxygen to carbon in isooctane ratio) from 0.5 to 0.7 at 1 bar pressure under analogous thermoneutral operating conditions was done using Gibbs free energy minimization algorithm in HSC Chemistry. The trends in thermoneutral points (TNP), important product gas compositions at TNPs and fuel processor energy requirements were compared and analyzed.

Coal is a valuable energy resource widely available in India. Coal gasification is an industrially commercialized technology that uses coal, steam and air to produce syngas from coal. The thermodynamics of CO_2 utilization in dry autothermal reforming (gasification) of coal and its comparison with steam gasification as well as the combined gasification (use of steam and CO_2 simultaneously) was done in **Chapter 5** using lignite coal. This study was done within the gasifier operating temperature range of 450 – 950ºC at 1 bar pressure. This thermodynamic study was done in the OCR (oxygen to carbon (in coal) ratio) range from 0.5 – 0.7, SCR (steam to carbon (in coal) ratio) range from 1 – 3 and CCR (CO_2 to carbon (in coal) ratio) range from 1 – 3 to compare the gasification processes under analogous conditions. The product

composition and energy aspects of autothermal gasification processes were evaluated. The OCR and SCR for steam gasification and OCR and CCR for dry autothermal gasification are chosen as controlling parameters for the gasifier for temperature and product composition variation.

The thermodynamics of another important application of dry autothermal reforming (DATR) for CO_2 utilization in the chemical looping combustion (CLC) process was studied in **Chapter 6**. CLC is an emerging area for energy generation that has several advantages like no direct mixing of fuel and air. The process operates continuously and many oxygen carriers have been evaluated for long term durability of oxidation–reduction cycles. The fuel reactor product stream mainly consisting of steam and CO_2 is usually cooled to condense out water and the pure CO_2 stream is compressed, liquefied and injected deep underground into porous rock for sequestration without any separation expense. The thermodynamic feasibility of CLC using propane as fuel and $CaSO_4$ as oxygen carrier was investigated by a short cut technique and the thermodynamic feasibility of a new process scheme combining chemical looping combustion (CLC) and DATR (with steam) of propane was also studied in this chapter. The CO_2 (and steam) generated in the CLC was used for dry autothermal reforming of propane in an autothermal way within the temperature range (400–1000 ºC) at 1 bar pressure to generate syngas of desired ratio < 3.0 which is extremely desirable for petrochemical manufacture. The novel process scheme generated (a) huge thermal energy in CLC that can be used for various applications, (b) pure N_2 and syngas rich streams can be used for petrochemical manufacture and (c) CO_2 utilization in DATR.

Chapter 7 discusses the major conclusions and recommendations for future work and lists the publications from the work done in this thesis.

1.4 References

Bellido J. D. A., Tanabe E. Y., and Assaf E. M., 2009, Carbon dioxide reforming of ethanol over Ni/Y2O3-ZrO2 catalysts, Applied Catalysis B, 90(3-4), 485–488.

Blanchard J., Oudghiri-Hassani H., Abatzoglou N., Jankhah S., Gitzhofer F., 2008, Synthesis of nano carbons via ethanol dry reforming over a carbon steel catalyst, Chem. Eng. J., 143(1), 186–194.

De Oliveira-Vigier K., Abatzoglou N., 2005, Dry-reforming of ethanol in the presence of a 316 stainless steel catalyst, Can. J. Chem. Eng., 83(6), 978–984.

HSC Chemistry [Software] 2002, version 5.1 Pori: Outokumpu research Oy.

Jankhah S., Abatzoglou N., 2008, Thermal and catalytic dry reforming and cracking of ethanol for hydrogen and carbon nanofilaments production, Int. J. Hydrogen Energy, 33(18), 4769–4779.

Perry R.H., Green D.W., 1997, Chemical engineers' handbook, 7th edition, McGraw-Hill, USA.

Smith, W.R., 1996, Computer software reviews, HSC chemistry for windows, 2.0, J. Chem. Inf. Comput. Sci., 36 (1), 151–152.

Wang W.J., Wang Y.Q., 2009, Dry reforming of ethanol for hydrogen production: thermodynamic investigation, Int. J. Hydrogen Energy, 34(13), 5382–5389.

Chapter 2

Thermodynamic analysis of dry autothermal reforming of Glycerol

CHAPTER 2: Thermodynamic analysis of dry autothermal reforming of Glycerol

Abstract

Dry autothermal reforming of glycerol uses a combination of dry (CO_2) reforming and partial oxidation reactions to produce syngas rich product stream. The objective of the chapter is to evaluate the thermodynamic feasibility of dry autothermal reforming of glycerol by identifying the thermodynamic domain of the DATR process operation, study the variation of product distribution pattern and describe the optimum conditions to maximize yield of the desired product and minimize the undesired product formation. Glycerol is used as fuel in this study. The thermodynamic equilibrium data for dry autothermal reforming of glycerol was generated for temperature range 600–1000 K, 1 bar pressure, OCGR [feed O_2/C (C of glycerol only) ratio] 0.1 to 0.5 and CGR [feed CO_2/glycerol ratio] 1 to 5 and analyzed. Higher OCGR and higher CGR yielded a syngas ratio, with lower carbon and methane formation, while lower CGR and lower OCGR yielded good hydrogen and total hydrogen, with low water and CO_2 in the product gas. The best thermoneutral condition for DATR of glycerol operation was seen at a temperature of 926.31 K at 1 bar pressure, OCGR=0.3 and CGR=1 that gave 2.67 mol of hydrogen, 4.8 mol of total hydrogen with negligible methane and carbon formation.

CHAPTER 2: Thermodynamic analysis of dry autothermal reforming of Glycerol

2.1 Glycerol as fuel

Glycerol is a byproduct of biodiesel production process. Biofuels like ethanol and biodiesel are gaining significance due to the consistent decline in fossil fuels like oil and natural gas reserves worldwide. Glycerol will be extensively available as byproduct after the commercialization of biodiesel production processes. This has prompted researchers to find ways for utilization of glycerol to valuable products. Researchers working in the field of hydrogen and syngas production have now started focusing on the use of glycerol for hydrogen and syngas production by various techniques.

Some of the important glycerol utilization techniques reported in literature are as follows:

2.1.1 Catalytic & Experimental studies

Dauenhauer et al. (2006) have studied the autothermal reforming of glycerol and its solutions in water over platinum and rhodium based catalysts supported on alumina foams at a contact time of ~10 ms. Simonetti et al. (2007) have studied the rate of glycerol conversion to syngas mixtures under kinetically controlled reaction conditions over carbon-supported platinum and platinum-rhenium catalysts. Zhang et al. (2007) have studied the hydrogen production from steam reforming reactions of ethanol and glycerol using ceria-supported Ir, Co and Ni catalysts. Valliyappan et al. (2008a) have studied the pyrolysis of glycerol for H_2 and syngas production in various flow rates of N_2 (30-70 ml/min), temperatures (650-800 ºC) and types and sizes of packing material in a tubular reactor at atmospheric pressure. Slinn et al. (2008) have reported that steam reforming of impure glycerol was a viable alternative for use of glycerol. Lehnert et al. (2008) have studied the catalytic conversion of glycerol to hydrogen by aqueous-phase reforming (APR) on several platinum based catalysts. Byrd et al. (2008) have studied the hydrogen production by supercritical water reforming of glycerol over a Ru/Al_2O_3 catalyst with low

methane and carbon monoxide formation. Wen et al. (2008) have studied the activities and stabilities of Pt, Ni, Co, and Cu catalysts and the effect of support on activity and stability for H_2 production by aqueous-phase reforming of glycerol using a fixed-bed flow reactor. Luo et al. (2008) have studied the effect of metal loadings and operating conditions for hydrogen production from glycerol solution by aqueous phase reforming process over Pt supported catalysts. Cui et al. (2009) have studied the steam reforming of glycerol (1, 2, 3 - propantriol) with non-substituted and partially Ce substituted $La_{(1-x)}Ce_xNiO_3$ mixed oxides and compared the activities with Pt metal catalysts and thermodynamic equilibrium. Fernandez et al. (2009) have investigated the pyrolysis of glycerol over carbonaceous catalysts to produce synthesis gas in a fixed-bed reactor. Iriondo et al. (2009) have studied the performance of monometallic (Ni and Pt) and bimetallic (Pt-Ni) catalysts and also the effect of lanthana-modified alumina support in the glycerol steam reforming process. Luciene et al. (2009) have studied the catalytic activity of Ni/CeO_2-Al_2O_3 catalysts modified with noble metals (Pt, Ir, Pd and Ru) for steam reforming of glycerol. Kunkes et al. (2009) have reported a gas phase catalytic process for glycerol reforming based on the use of two catalyst beds that can be tuned to yield hydrogen and CO_2 or synthesis gas at 573 K and 1 atm pressure. Buffoni et al. (2009) have studied the effect of nickel catalysts supported on commercial alpha-Al_2O_3 and alpha-Al_2O_3 modified by addition of ZrO_2 and CeO_2 to obtain hydrogen by steam reforming of glycerol. Xu et al. (2009) have studied the catalytic gasification of glycerol with supercritical water in a continuous tubular-flow reactor operated at 380-500 °C and 25 MPa pressure with or without Na_2CO_3 catalyst. Dou et al. (2009) have experimentally studied the catalytic steam reforming of glycerol in a continuous flow fixed-bed reactor at atmospheric pressure within a temperature range of 400-700 °C using a commercial Ni-based catalyst and a dolomite sorbent for in-situ CO_2 removal. Swami et al. (2006) have successfully studied steam and autothermal reforming of glucose, glycerol and industrial waste water using Ni/Pd/Cu catalyst at atm pressure within 500–800 °C temperature range. Soares et al. (2006) have reported the catalytic conversion of glycerol to syngas at lower

temperatures. Valliyappan et al. (2008b) have studied catalytic steam gasification in presence of commercial Ni/Al_2O_3 catalyst and reported 15 mol % increased hydrogen yield in steam gasification process than pyrolysis process. Huber et al. (2003) have studied aqueous-phase reforming of glycerol over a tin-promoted Raney-nickel catalyst for hydrogen production. Douette et al. (2007) have experimentally investigated glycerin reforming and formulated a model defining the effect of oxygen to carbon ratio, steam to carbon ratio, and temperature on the process to improve hydrogen yield. Adhikari et al. have experimentally studied glycerin steam reforming using nickel catalysts with MgO, CeO_2 and TiO_2 supports (2008) and also by using Ni/Al_2O_3 and $Rh/CeO_2/Al_2O_3$ based catalysts (2007a). Hirai et al. (2005) have studied hydrogen production by steam reforming of glycerin on ruthenium catalyst. Iriondo et al. (2008) have used different catalyst functionalities to carry out aqueous-phase and vapor phase steam reforming of glycerol and found that the addition of Ce, La and Zr to Ni/ Al_2O_3 improved the initial glycerol conversions in aqueous phase reforming of glycerol while the same catalysts improved hydrogen selectivity in steam reforming of glycerol. Kunkes et al. (2008) have experimentally studied aqueous solutions of glycerol over carbon-supported Pt and Pt-Re catalysts at 483 - 523 K and found that the turnover frequencies for production of H_2, CO, CO_2, and light alkanes (primarily methane) increase with addition of Re to Pt/C as it modifies the interaction of CO with surface sites.

2.1.2 Thermodynamic studies

Adhikari et al. (2007b) have performed thermodynamic equilibrium analysis of glycerol steam reforming process and described that temperature >900 K, atmospheric pressure and a molar ratio of water/glycerin at 9:1 are the best operating conditions for hydrogen production with minimizing methane and carbon formation. X. Wang et al. (2009) have performed a thermodynamic analysis of glycerol dry reforming by the Gibbs free energy minimization method as a function of CO_2 to glycerol ratio, temperature, and pressure. Luo

et al. (2007) have studied the thermodynamic analysis of autothermal reforming (a combination of water aqueous reforming and oxidation), aqueous hydrogen peroxide reforming and water aqueous reforming process and found that water aqueous reforming of glycerol gave the highest hydrogen yield in the absence of methanation. H. Wang et al. (2009) have performed thermodynamic analysis of glycerol autothermal reforming using Gibbs free energy minimization over a temperature range (700–1000 K), steam to glycerol ratio (1–12) and oxygen to glycerol ratio (0.0–3.0) and reported product yields at thermoneutral conditions. X. Wang et al. (2008) have studied the thermodynamic analysis of glycerin steam reforming as a function of water/glycerin molar ratios (1:1−12:1) within temperature range (550−1200 K) and pressure range (1−50 atm) and reported optimum conditions for hydrogen production, syngas production with minimum carbon formation. Chen et al. (2009) have performed thermodynamic analysis of adsorption-enhanced steam reforming of glycerol and shown that the maximum number of moles of hydrogen produced per mole of glycerol can be increased due to the CO_2 adsorption.

2.1.3 Other studies

Marshall and Haverkamp (2008) have reported a 66 % reduction in electrical energy consumption using electrochemical reforming of glycerol solution in a proton exchange membrane (PEM) electrolysis cell compared to water electrolysis in the same cell. Xuan et al. (2009) have discussed the research challenges and future development of biomass fuel processor along with a review of the biomass-derived fuel processing technologies from various perspectives including the feedstock, reforming mechanisms, catalysts and processor configurations. Selembo et al. (2009) have studied the use of glycerol for hydrogen gas production was examined via electrohydrogenesis using microbial electrolysis cells (MECs) which gave hydrogen yield of 3.9 mol-H_2/mol using glycerol and was observed to be higher than that possible by fermentation. Zhu et al. (2009) have reported plasma reforming of glycerol at

low temperature & atm pressure without external heating. Ito et al. (2005) have studied the hydrogen and ethanol production using Enterobacter aerogenes HU-101 from glycerol-containing wastes discharged from biodiesel manufacturing process. Some review articles (S. Adhikari, 2009; Vaidya and Rodrigues, 2009) for hydrogen production using glycerol are also published.

2.2 Thermodynamic analysis

A thermodynamic analysis of glycerol steam reforming (Adhikari, 2007; X. Wang, 2008), glycerol autothermal reforming (H. Wang, 2009) and glycerol dry reforming (X. Wang, 2009) have already been reported. On the similar lines, a thermodynamic study of pure glycerol dry autothermal reforming process was undertaken to evaluate the feasibility of the process. The role of CO_2 in DR has already been discussed in detail by X. Wang et al. (2009) and the same is applicable to this system, oxygen reacts with glycerol to produce energy that is in-situ transferred to dry reforming process. Dry autothermal reforming (DATR) is a better process than dry reforming (DR) for many reasons. DR requires external energy and more carbon is formed in the reactor while DATR does not require external energy and minimum carbon is formed at optimized conditions. The species such as glycerol (g) [1, 2, 3 Propanetriol], glycerol (l), O_2 (g), N_2 (g), CO_2 (g), H_2 (g), CO (g), H_2O (g), CH_4 (g), H_2O (l) and C(s) are considered in this study. The input species are glycerol, oxygen, nitrogen and CO_2 (all in gaseous phase) at particular temperature-pressure conditions reacting to give the products. Any other product – byproduct formation is not considered in this study.

The dry autothermal reforming of glycerol process operation is based on four main thermodynamic parameters like temperature, pressure, OCGR [feed O_2/C (C of glycerol only) ratio] and CGR [feed CO_2 to glycerol ratio]. The process engineer has to choose the best reactor operating conditions. A detailed study of product distribution trends of glycerol DATR process with

respect to change in temperature, OCGR and CGR is essential. This chapter intends to study these things to locate the thermodynamic domain for reactor operation. The material and energy balance calculations were preformed using the inbuilt databases in HSC Chemistry software package. The reaction products are assumed to be in thermodynamic equilibrium at the exit of the reactor. 1 mole of glycerol (gaseous phase) was taken in each case, so the product moles obtained were for 1 mole glycerol input. The operating temperature range for this exercise was 600 to 1000 K, with CGR 1, 3 & 5 and OCGR zero, 0.1, 0.3 and 0.5. Complete (100 %) conversion of glycerol and positive product yields with accurate material balances was observed in all the considered cases, indicating the feasibility of the DATR process. The case of zero OCGR represents the dry reforming of glycerol and these results have already been reported (X. Wang, 2009). The accuracy of the data presented is within reasonable error limit.

2.3 Results and Discussion:

2.3.1. Hydrogen yield

Hydrogen is always a desired product of reforming processes for its end use in fuel cells or syngas manufacture. Steam reforming of natural gas is a popular process for hydrogen production. With availability of cheaper fuel options like glycerol, the hydrogen production processes might shift to use the available feedstock. Table 2.1 shows the hydrogen yield in DATR of glycerol process at various pressures. It was found that the hydrogen yield decreased at higher pressures, making low pressure (1 bar) operation a favorable process parameter. The further thermodynamic studies for DATR of glycerol were done at 1 bar process pressure only. Figure 2.1 shows the effect of oxygen addition on hydrogen production by glycerol dry autothermal reforming at various conditions of process temperature, CGR and OCGR at 1 bar pressure.

OCGR		CGR = 1			CGR = 3			CGR = 5		
	Pressure (bar)	1	3	6	1	3	6	1	3	6
	Temperature (K)	Moles of hydrogen in product gas								
0.1	650	0.37	0.22	0.16	0.35	0.21	0.15	0.33	0.20	0.14
	750	1.00	0.62	0.45	0.95	0.59	0.43	0.92	0.58	0.42
	850	1.92	1.30	0.98	1.84	1.25	0.95	1.81	1.22	0.93
	950	2.88	2.17	1.72	2.69	2.11	1.68	2.43	2.08	1.66
0.3	650	0.41	0.25	0.18	0.38	0.23	0.16	0.36	0.22	0.15
	750	1.09	0.69	0.51	1.02	0.65	0.48	0.98	0.62	0.46
	850	2.04	1.41	1.08	1.95	1.34	1.03	1.89	1.30	1.00
	950	2.73	2.30	1.86	2.37	2.13	1.79	2.08	1.96	1.73
0.5	650	0.44	0.27	0.19	0.40	0.24	0.17	0.38	0.23	0.16
	750	1.15	0.74	0.55	1.08	0.69	0.51	1.03	0.66	0.48
	850	2.09	1.49	1.15	1.95	1.41	1.09	1.82	1.36	1.05
	950	2.26	2.11	1.87	1.92	1.85	1.70	1.67	1.63	1.55

Table 2.1: Hydrogen yield in DATR of Glycerol at different pressures

It is observed that hydrogen production steadily increases with temperature till 850 K and later starts saturating and also declines in later stages. The increase in CGR decreases the hydrogen output. However, hydrogen production trend is same for dry reforming and DATR. The moles of hydrogen produced at 950 K for increase in CGR from 1 to 5, decrease from 2.8 to 2.56 (DR) and decrease from 2.88 to 2.26 (for CGR = 1), 2.69 to 1.92 (for CGR = 3) and 2.43 to 1.67 (for CGR = 5) for OCGR increase from 0.1 to 0.5 in DATR. Taking the extreme conditions, the maximum hydrogen yield at 950 K is 2.88 moles for OCGR = 0.1 and CGR = 1 and the minimum hydrogen yield of 1.67 moles is noted for the other extreme condition of OCGR = 0.5 and CGR = 5 in

DATR process. Hence it can be observed that higher OCGR and higher CGR actually decrease the hydrogen yield in this process.

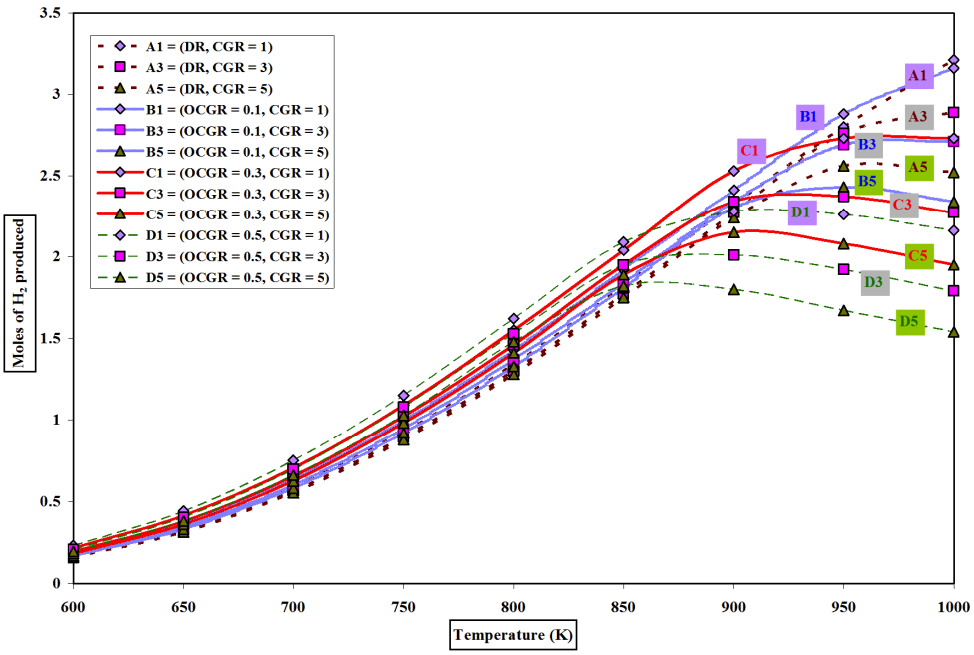

Figure 2.1: Hydrogen yield in DR and DATR of Glycerol

2.3.2 CO yield

Carbon monoxide is an undesired product and poison for applications that require pure hydrogen. However it is very much desired for syngas feeding applications. CO can be converted to hydrogen using a series of WGS reactors, while the very low CO levels can be preferentially oxidized to CO_2 or converted to methane using a methanation catalyst. Figure 2.2 shows the moles of CO produced in the DR and DATR of glycerol process as a function of temperature, CGR and OCGR at 1 bar pressure. It is observed that the CO yield increases with increase in process temperature in all cases. With increase in OCGR at constant CGR, the CO yield decreases. Similarly, at constant OCGR, the CO yield increases with increase in CGR. The moles of CO produced at 950 K for increase in CGR from 1 to 5, increase from 2.09 to

4.18 (DR), decrease from 2.46 to 1.7 (for CGR = 1), 3.39 to 2.07 (for CGR = 3) and 3.83 to 2.32 (for CGR = 5) for OCGR increase from 0.1 to 0.5 in DATR. The maximum CO yield at 950 K was found to be ~3.83 moles for OCGR = 0.1 and CGR = 5 and the minimum CO yield of 1.7 was observed at OCGR = 0.5 and CGR = 1 for DATR process.

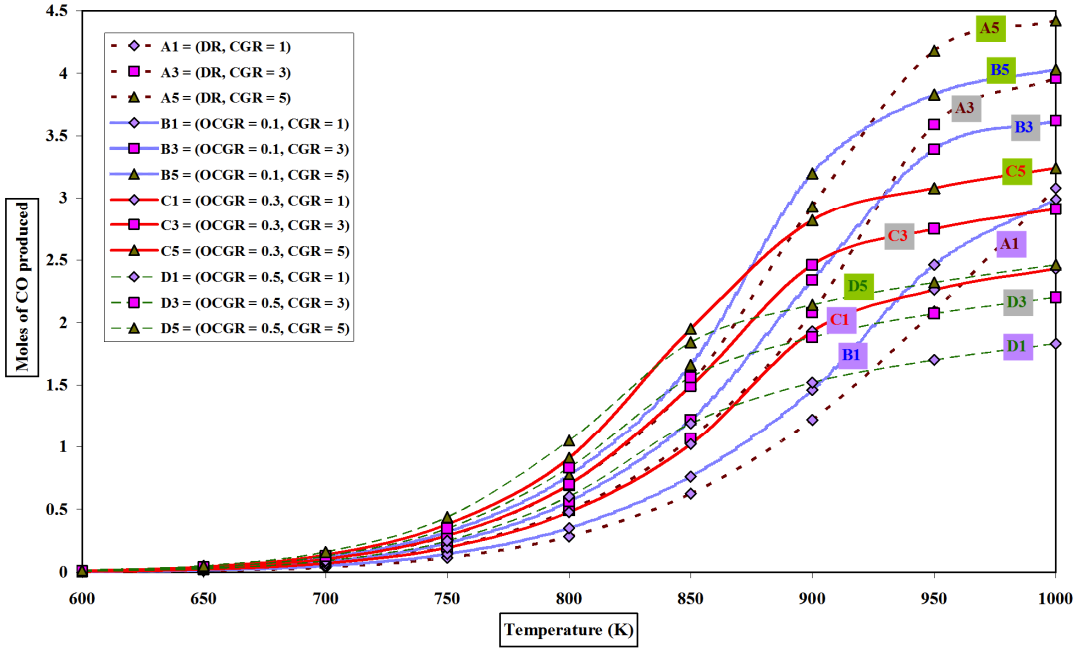

Figure 2.2: CO yield in DR and DATR of Glycerol

2.3.3 Variation of Syngas ratio (H_2/CO) of product gas

Syngas is the basic building block for petrochemicals. Dry reforming gives more CO than steam reforming processes. Hence syngas can be preferably manufactured by glycerol DATR process. Moreover the syngas ratio in the range of 1–3 (desirable for use in petrochemical manufacture) is easily obtained in this process. Figure 2.3 shows the variation of syngas ratio as a function of temperature, CGR and OCGR for DR-DATR of glycerol. The syngas ratio of the product gas shows a regular decline with increase in DR-DATR process temperature. Increase in OCGR at constant CGR and increase

in CGR at constant OCGR also show a decrease in product syngas ratio in the same trend. The product syngas ratio obtained at 950 K for increase in CGR from 1 to 5, decreases from 1.34 to 0.61 (DR) and increases from 1.17 to 1.33 (CGR = 1), 0.79 to 0.93 (CGR = 3) and 0.63 to 0.72 (CGR = 5) for OCGR increase from 0.1 to 0.5 in DATR. The maximum syngas ratio at 950 K is 1.33 obtained at OCGR = 0.5 and CGR = 1 while the minimum syngas ratio of 0.63 is seen at OCGR = 0.1 and CGR = 5 for DATR process. The syngas ratio around 1 (0.63–1.33) is obtained at 950 K for CGR variation from 1–5, making this process favorable for syngas manufacture.

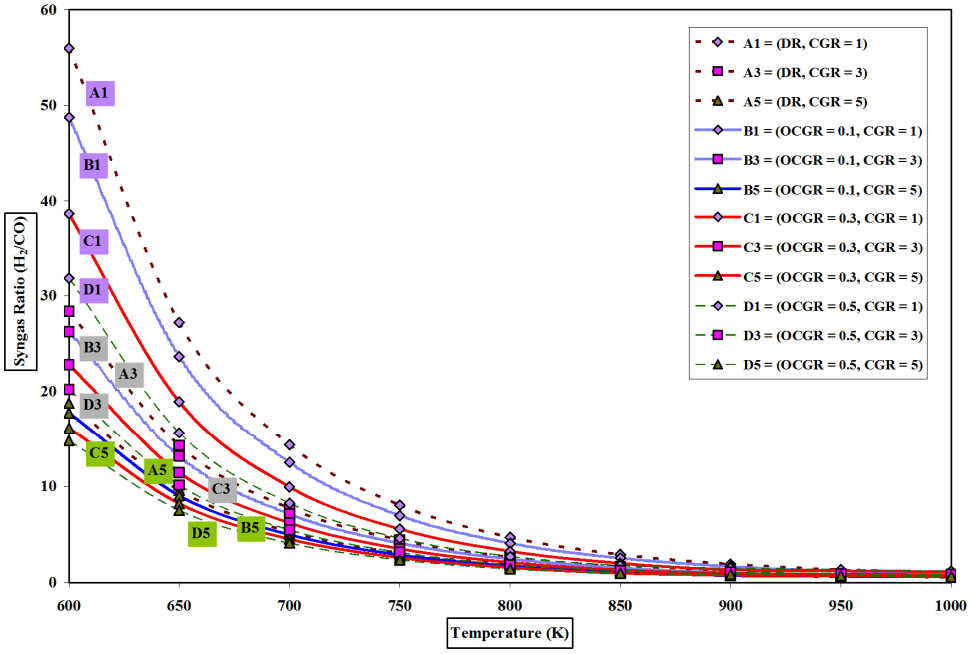

Figure 2.3: Syngas ratio (H_2/CO) in DR and DATR of Glycerol

2.3.4 Total hydrogen (H_2+CO) potential

Total hydrogen potential of a process is the sum of moles of hydrogen and carbon monoxide obtainable in the process. This terminology is useful in identifying and ranking fuels for hydrogen production processes. It is assumed

that almost all the CO can be converted to hydrogen by coupling a series of WGS reactors to the DATR reactor. Figure 2.4 show the variation of total hydrogen moles obtained at different temperatures, OCGR and CGR.

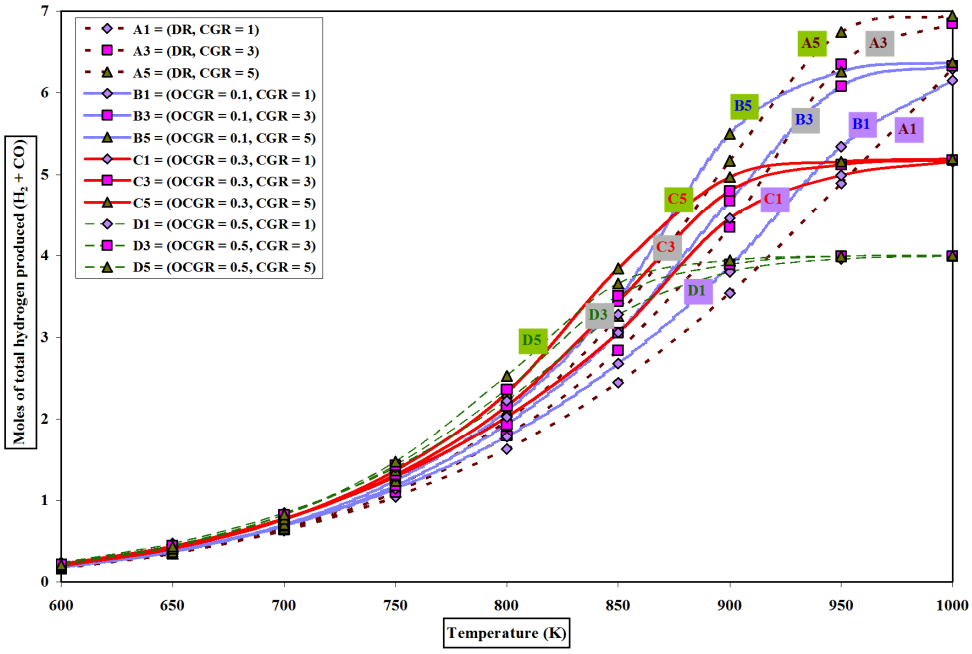

Figure 2.4: Moles of total hydrogen produced in DR and DATR of Glycerol

It is observed that the total hydrogen obtainable increases with increase in OCGR till 850-950 K and later saturates. Increase in CGR at constant OCGR, increases the total hydrogen production although that increase is not significant. The moles of total hydrogen produced at 950 K for increase in CGR from 1 to 5, increase from 4.89 to 6.74 (DR) and decrease from 5.34 to 3.96 (for CGR = 1), 6.08 to 3.99 (for CGR = 3) and 6.26 to 3.99 (for CGR = 5) for OCGR increase from 0.1 to 0.5 in DATR. The maximum total hydrogen obtainable at 950 K is 6.26 at CGR = 5 and OCGR = 0.1, while the minimum is 3.96 at CGR = 1 and OCGR = 0.5.

2.3.5 Methane formation

Methane formation is undesirable due to the loss of hydrogen and carbon moles. Figure 2.5 shows the moles of methane produced at different temperatures, OCGR and CGR. Methane formation seems negligible and decreases with temperature in all the considered cases. The methane formation is lowest at high OCGR and high CGR. The moles of CH_4 produced at 950 K for increase in CGR from 1 to 5, decrease from 0.20 to 0.06 (DR) and decrease from 0.17 to 0.01 (for CGR = 1), 0.08 to 0.00 (for CGR = 3) and 0.04 to 0.00 (for CGR = 5) for OCGR increase from 0.1 to 0.5 in DATR. The maximum CH_4 moles formed at 950 K in DATR is 0.17 at CGR = 1 and OCGR = 0.1, while the minimum is 0.00 at CGR = 3 & 5 and OCGR = 0.5.

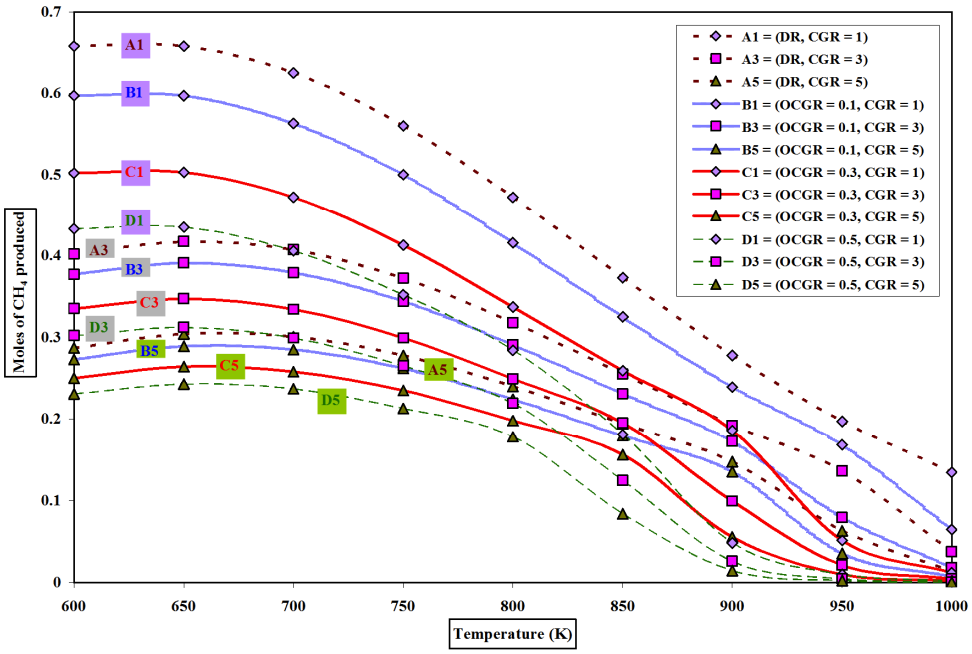

Figure 2.5: Moles of methane produced in DR and DATR of Glycerol

2.3.6 CO_2 obtained in product gas

One of the important aims of dry autothermal reforming is utilization of CO_2 to produce value added products like syngas and hydrogen without the use of

external energy. But the CO_2 production results obtained from thermodynamic study indicate that the regions for positive CO_2 utilization are very narrow. However, even if CO_2 is evolved from the process, the net CO_2 evolved (i.e. the product CO_2 – feed CO_2 moles) from the DATR process is very less. This makes the process more attractive. Figure 2.6 shows the CO_2 obtained in DR-DATR process at different temperatures, OCGR and CGR.

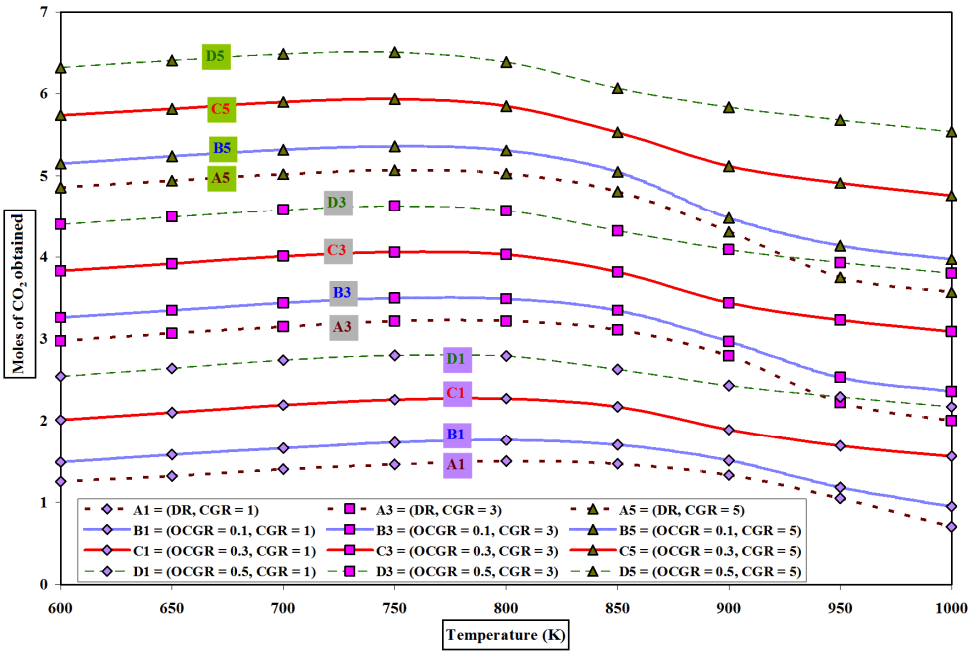

Figure 2.6: Moles of CO_2 obtained in DR and DATR of Glycerol

The CO_2 obtained in the product gas slightly increases till ~750 K and later decreases at higher temperatures. The CO_2 production increases with increase in CGR and also with increase in OCGR. The moles of CO_2 produced at 950 K for increase in CGR from 1 to 5, increase from 1.05 to 3.75 (DR) and increase from 1.18 to 2.29 (for CGR = 1), 2.53 to 3.93 (for CGR = 3) and 4.14 to 5.68 (for CGR = 5) for OCGR increase from 0.1 to 0.5 in DATR. The maximum CO_2 moles emitted at 950 K in DATR is 5.68 at CGR = 5 and OCGR = 0.5, while the minimum is 1.18 at CGR = 1 and OCGR = 0.1.

2.3.7 Water formation

Water formation is sometimes desired to increase humidity of the product gas as the humidified gas has better thermal transport properties. However, water formation takes place at the expense of hydrogen in the system. Figure 2.7 shows the moles of water formed at different temperature, CGR and OCGR in the DR-DATR of glycerol process.

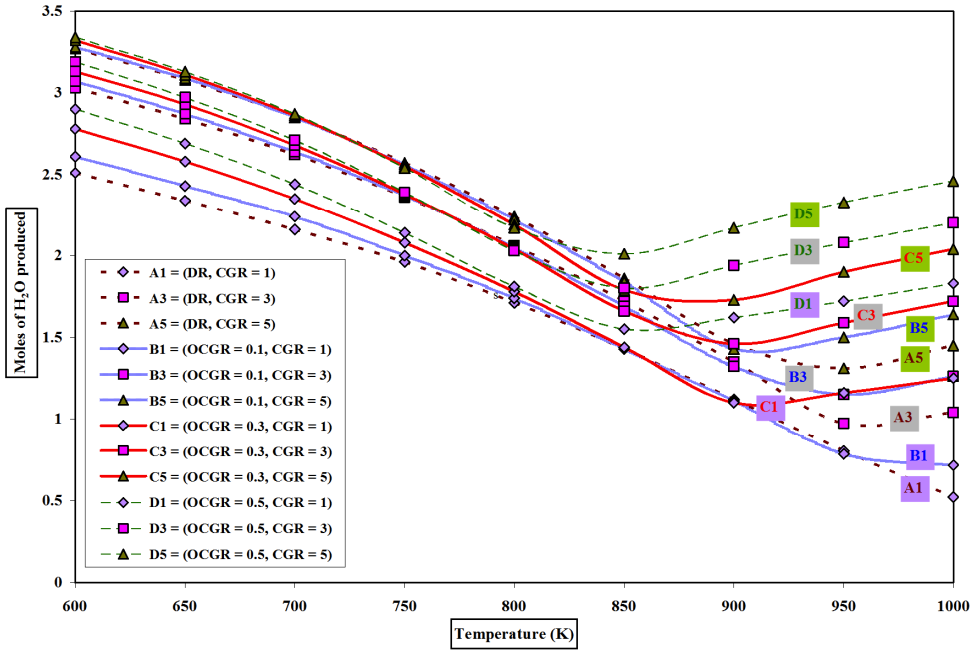

Figure 2.7: Moles of water produced in DR and DATR of Glycerol

The water formation decreases with increase in temperature till 850-950 K and then increases in majority of the cases. Higher CGR and higher OCGR seems to promote more water formation in the process. The moles of water produced at 950 K for increase in CGR from 1 to 5, increase from 0.8 to 1.31 (DR) and increase from 0.78 to 1.72 (for CGR = 1), 1.15 to 2.08 (for CGR = 3) and 1.50 to 2.33 (for CGR = 5) for OCGR increase from 0.1 to 0.5 in DATR. The maximum H_2O moles formed at 950 K in DATR is 2.33 at CGR = 5 and OCGR = 0.5, while the minimum is 0.78 at CGR = 1 and OCGR = 0.1.

2.3.8 Carbon formation

Carbon is also an undesired component of reforming processes as it deactivates the catalyst and increases pressure drop in reactors. Dry reforming process has always had this as major problem. DATR uses in-situ partial oxidation to reduce this problem. The carbon formation at different temperatures, OCGR and CGR is shown in figure 2.8. As seen from the figure, the carbon formation is more in DR than DATR and it increases with increase in CGR, but decreases with increase in OCGR and increase in temperature. At 950 K the carbon formation decreases from 0.66 to 0.00 as CGR increases from 1–5 in DR of glycerol. Similarly at 950 K, the maximum carbon formation of 0.19 moles is observed only in the case of CGR = 1 and OCGR = 0.1, and it decreases to zero for higher OCGR and higher CGR.

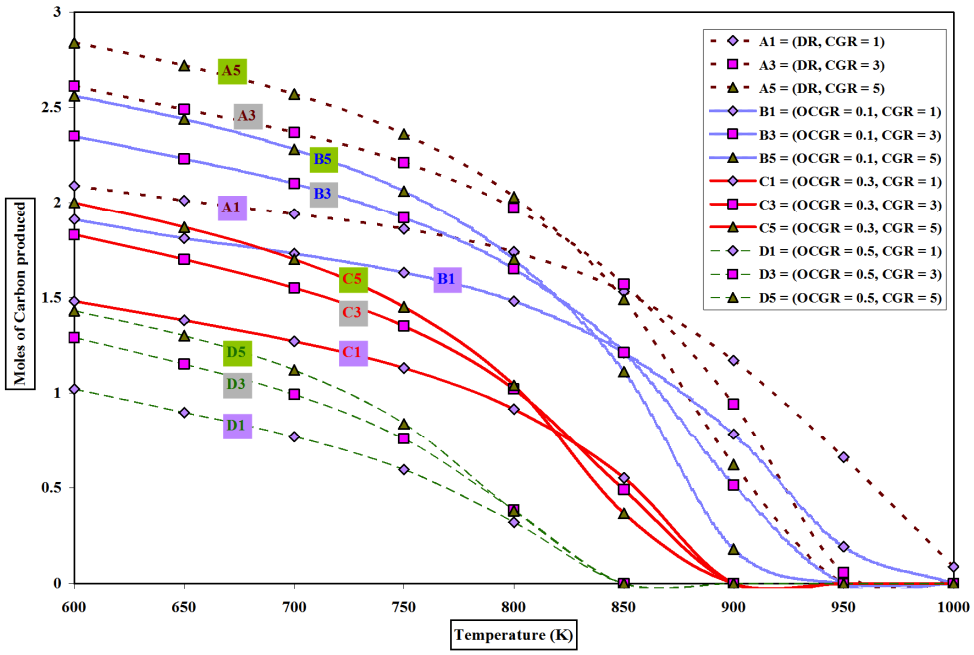

Figure 2.8: Moles of carbon produced in DR and DATR of Glycerol

2.3.9 Process Enthalpy and Thermoneutral points

Reaction enthalpy is always a crucial parameter in reforming processes. Thermoneutral operation of DATR of glycerol requires no external energy for cooling or heating, which makes it valuable from energy consumption point of view. Figure 2.9 shows the variation of enthalpy of DATR of glycerol process with change in OCGR and CGR along the thermoneutral line (zero enthalpy line).

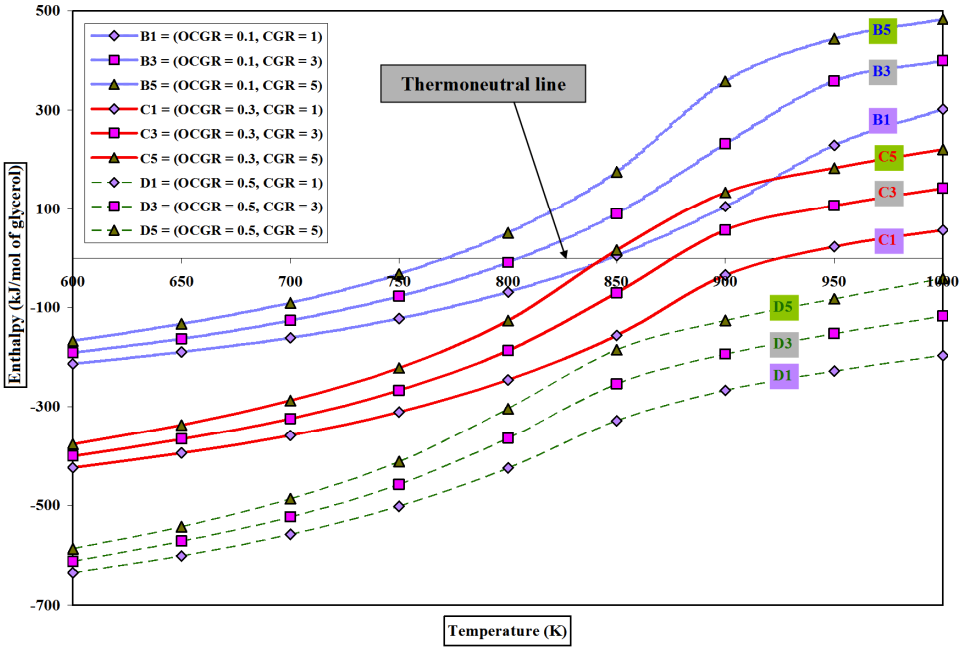

Figure 2.9: Process enthalpy for DATR of Glycerol

The intersection of reaction enthalpy curves with temperature axis shows the thermoneutral temperatures. It is observed that the process exothermicity increases with increase in OCGR at constant CGR. Table 2.2 shows the product gas yields at thermoneutral conditions. It is observed that the reaction endothermicity increases with increase in CGR from 1 to 5, at constant OCGR, and also show a decrease in thermoneutral temperatures. Similarly, the thermoneutral temperatures show an increase with the increase in OCGR

at constant CGR which indicate an increase in exothermicity of the reaction. Lower OCGR and higher CGR gave lower thermoneutral point (temperatures) and vice versa. The thermoneutral temperatures range from 771.48 K (OCGR = 0.1, CGR = 5) to 1346.85 K (OCGR = 0.5, CGR = 1).

OCGR	CGR	Thermoneutral Temperature (K)	Equilibrium product gas composition (moles)							
			$H_2(g)$	CO(g)	Total hydrogen (H_2 + CO)	Syngas ratio (H_2/CO)	$CO_2(g)$	$CH_4(g)$	$H_2O(g)$	C
0.1	**1**	847.15	1.89	0.73	2.62	2.60	1.71	0.33	1.45	1.23
	3	805.56	1.42	0.62	2.04	2.31	3.49	0.29	2.01	1.61
	5	771.48	1.09	0.47	1.56	2.30	5.35	0.25	2.42	1.93
0.3	**1**	926.31	2.67	2.13	4.80	1.25	1.77	0.10	1.13	0.00
	3	873.18	2.18	2.04	4.22	1.07	3.64	0.17	1.48	0.15
	5	845.03	1.84	1.81	3.65	1.02	5.58	0.16	1.84	0.45
0.5	**1**	1346.8	1.660	2.340	4.00	0.71	1.66	0.000	2.340	0.00
	3	1170.2	1.450	2.550	4.00	0.57	3.45	0.000	2.550	0.00
	5	1051.3	1.420	2.580	4.00	0.55	5.42	0.000	2.580	0.00

Table 2.2: Product gas composition in DATR of Glycerol at thermoneutral temperatures (K) & 1 bar pressure

2.4 Conclusions

A thermodynamic analysis of glycerol dry autothermal reforming process has been done to map the effect of OCGR and CGR on product distribution pattern at 1 bar pressure and 600–1000 K temperature range. The study shows the thermodynamic feasibility of the process in the parameter range considered. This process seems favorable for syngas production as it gives a syngas ratio in the desirable range (~1). Hydrogen production can also be achieved. The results show good CO_2 utilization potential. Experimentation will be helpful for comparing the theoretical results obtained here. Higher OCGR and higher CGR are good for syngas production (ratio ~1), lower carbon and methane formation, while lower CGR and lower OCGR give good hydrogen and total hydrogen yields, low water and CO_2 production. The process temperature around 850 K is good for minimizing methane, water and carbon formation. Thermoneutral temperature of 926.31 K at 1 bar pressure, OCGR = 0.3 and CGR = 1 gave 2.67 moles of hydrogen, 4.8 moles of total hydrogen with negligible methane and carbon formation, and was identified as the best thermoneutral condition for DATR operation.

2.5 References

Adhikari S., Fernando S., Haryanto A., 2007, A comparative thermodynamic and experimental analysis on hydrogen production by steam reforming of glycerin, Energy Fuels, 21, 2306-2310.

Adhikari S., Fernando S., Haryanto A., 2007, Production of hydrogen by steam reforming of glycerin over alumina-supported metal catalysts, Catal. Today, 129, 355-364.

Adhikari S., Fernando S.D., To S.D.F., Brick R.M., Steele P.H., Haryanto A., 2008, Conversion of glycerol to hydrogen via a steam reforming process over nickel catalysts, Energy Fuels, 22(2), 1220-1226.

Adhikari S., Fernando S. D., Haryanto A., 2009, Hydrogen production from glycerol: An update, Energy Convers. Manage., 50(10), 2600-2604.

Byrd A. J., Pant K.K., Gupta R. B., 2008, Hydrogen production from glycerol by reforming in supercritical water over Ru/Al_2O_3 catalyst, Fuel, 87(13-14), 2956-2960.

Buffoni I. N., Pompeo F., Santori G. F., Nichio N. N., 2009, Nickel catalysts applied in steam reforming of glycerol for hydrogen production, Catal. Commun., 10(13), 1656-1660.

Cui Y., Galvita V., Rihko-Struckmann L., Lorenz H., Sundmacher K., 2009, Steam reforming of glycerol: The experimental activity of $La_{1-x}Ce_xNiO_3$ catalyst in comparison to the thermodynamic reaction equilibrium, Appl. Catal. B, 90(1-2), 29-37.

Chen H., Zhang T., Dou B., Dupont V., Williams P., Ghadiri M., Ding Y., 2009, Thermodynamic analyses of adsorption-enhanced steam reforming of glycerol for hydrogen production, Int. J. Hydrogen Energy, 34, 7208.

Dauenhauer P.J., Salge J.R., Schmidt L.D., 2006, Renewable hydrogen by autothermal steam reforming of volatile carbohydrates, J. Catal., 244(2), 238-247.

Dou B., Dupont V., Rickett G., Blakeman N., Williams P.T., Chen H., Ding Y., Ghadiri M., 2009, Hydrogen production by sorption-enhanced steam reforming of glycerol, Bioresour. Technol., 100(14), 3540-3547.

Douette A.M.D., Turn S.Q., Wang W.Y., Keffer V.I., 2007, Experimental investigation of hydrogen production from glycerin reforming, Energy Fuels, 21, 3499-3504.

Fernandez Y., Arenillas A., Diez M.A., Pis J.J., Menendez J.A., 2009, Pyrolysis of glycerol over activated carbons for syngas production, J. Anal. Appl. Pyrolysis, 84(2), 145-150.

Hirai T., Ikenaga N.O., Mayake T., Suzuki T., 2005, Production of hydrogen by steam reforming of glycerin on ruthenium catalyst, Energy Fuels, 19, 1761−1762.

HSC Chemistry [software], 2002, Version 5.1 Pori: Outokumpu Research Oy.

Huber G.W., Shabaker J.W., Dumesic J.A., 2003, Raney Ni-Sn catalyst for H_2 Production from Biomass-Derived Hydrocarbons, Science, 300, 2075-2077.

Iriondo A., Barrio V.L., Cambra J.F., Arias P.L., Güemez M.B., Navarro R.M., Sánchez-Sánchez M.C., Fierro J.L.G., 2008, Hydrogen production from glycerol over nickel catalysts supported on Al_2O_3 modified by Mg, Zr, Ce or la, Top. Catal., 49(1-2), 46-58.

Iriondo A., Barrio V.L., Cambra J.F., Arias P.L., Guemez M.B., Navarro R.M., Sanchez-Sanchez M.C., Fierro J.L.G., 2009, Influence of La_2O_3 modified support and Ni and Pt active phases on glycerol steam reforming to produce hydrogen, Catal. Commun., 10(8), 1275-1278.

Ito T., Nakashimada Y., Senba K., Matsui T., Nishio N., 2005, Hydrogen and ethanol production from glycerol-containing wastes discharged after biodiesel manufacturing process, J. Biosci. Bioeng., 100(3), 260-265.

Kunkes E.L., Simonetti D.A., Dumesic J.A., Pyrz W.D., Murillo L.E., Chen J.G., Buttrey D.J., 2008, The role of rhenium in the conversion of glycerol to synthesis gas over carbon supported platinum-rhenium catalysts, J. Catal., 260(1), 164-177.

Kunkes E.L., Soares R.R., Simonetti D.A., Dumesic J.A., 2009, An Integrated Catalytic Approach for Production of Hydrogen by Glycerol Reforming coupled with Water-Gas-Shift, Appl. Catal. B, 90(3-4), 693-698.

Lehnert K., Claus P., 2008, Influence of Pt particle size and support type on the aqueous-phase reforming of glycerol, Catal. Commun., 9(15), 2543-2546.

Luciene P.R.P., Ticianelli E.A., Elisabete M., 2009, Production of hydrogen via steam reforming of biofuels on Ni/CeO_2-Al_2O_3 catalysts promoted by noble metals, Int. J. Hydrogen Energy, 34(12), 5049-5060.

Luo N.J., Zhao X., Cao F.H., Xiao T.C., Fang D.Y., 2007, Thermodynamic study on hydrogen generation from different glycerol reforming processes, Energy Fuels, 21, 3505–3512.

Luo N., Fu X., Cao F., Xiao T., Edwards P., 2008, Glycerol aqueous phase reforming for hydrogen generation over Pt catalyst - Effect of catalyst composition and reaction conditions, Fuel, 87(17-18), 3483-3489.

Marshall A.T., Haverkamp R.G., 2008, Production of hydrogen by the electrochemical reforming of glycerol-water solutions in a PEM electrolysis cell, Int. J. Hydrogen Energy, 33(17), 4649-4654.

Perry R.H., Green D.W., 1997, Chemical engineers' handbook 7th Edition, McGraw Hill.

Selembo P.A., Perez J.M., Lloyd W.A., Logan B.E., 2009, High hydrogen production from glycerol or glucose by electrohydrogenesis using microbial electrolysis cells, Int. J. Hydrogen Energy, 34(13), 5373-5381.

Simonetti D.A., Kunkes E.L., Dumesic J.A., 2007, Gas-phase conversion of glycerol to synthesis gas over carbon-supported platinum and platinum-rhenium catalysts, J. Catal., 247(2), 298-306.

Slinn M., Kendall K., Mallon C., Andrews J., 2008, Steam reforming of biodiesel by-product to make renewable hydrogen, Bioresour. Technol., 99(13), 5851-5858.

Smith W.R., 1996, Computer Software Reviews, HSC Chemistry for Windows, 2.0, J. Chem. Inf. Comput. Sci., 36(1), 151-152.

Soares R.R., Simonetti D.A., Dumesic J.A., 2006, Glycerol as a source for fuels and chemicals by low-temperature catalytic processing, Angew. Chem. Int. Ed., 45, 3982-3985.

Swami S.M., Abraham M.A., 2006, Integrated catalytic process for conversion of biomass to hydrogen, Energy Fuels, 20, 2616−2622.

Vaidya P.D., Rodrigues A.E., 2009, Glycerol reforming for hydrogen production: A review, Chem. Eng. Technol., 32(10), 1463-1469.

Valliyappan T., Bakhshi N.N., Dalai A.K., 2008, Pyrolysis of glycerol for the production of hydrogen or syngas, Bioresour. Technol., 99(10), 4476-4483.

Valliyappan T., Ferdous D., Bakhshi N.N., Dalai A.K., 2008, Production of hydrogen and syngas via steam gasification of glycerol in a fixed-bed reactor, Top. Catal., 49, 59-67.

Wang H., Wang X., Li M., Li S., Wang S., Ma X., 2009, Thermodynamic analysis of hydrogen production from glycerol autothermal reforming, Int. J. Hydrogen Energy, 34, 5683.

Wang X., Li S., Wang H., Liu B., Ma X., 2008, Thermodynamic Analysis of Glycerin Steam Reforming, Energy Fuels, 22, 4285–4291.

Wang X., Li M., Wang M., Wang H., Li S., Wang S., Ma X., 2009, Thermodynamic analysis of glycerol dry reforming for hydrogen and synthesis gas production, Fuel, 88(11), 2148-2153.

Wen G., Xu Y., Ma H., Xu Z., Tian Z., 2008, Production of hydrogen by aqueous-phase reforming of glycerol, Int. J. Hydrogen Energy, 33(22), 6657-6666.

Xu D., Wang S., Hu X., Chen C., Zhang Q., Gong Y., 2009, Catalytic gasification of glycine and glycerol in supercritical water, Int. J. Hydrogen Energy, 34(13), 5357-5364.

Xuan J., Leung M.K.H., Leung D.Y.C., Ni M., 2009, A review of biomass-derived fuel processors for fuel cell systems, Renewable Sustainable Energy Rev.,13(6-7), 1301-1313.

Zhang B., Tang X., Li Y., Xu Y., Shen W., 2007, Hydrogen production from steam reforming of ethanol and glycerol over ceria-supported metal catalysts, Int. J. Hydrogen Energy, 32(13), 2367-2373.

Zhu X., Hoang T., Lobban L.L., Mallinson R.G., 2009, Plasma reforming of glycerol for synthesis gas production, Chemical Communications, 20, 2908-2910.

Chapter 3

Thermoneutral point analysis of ethanol dry autothermal reforming

CHAPTER 3: Thermoneutral point analysis of ethanol dry autothermal reforming

Abstract

Thermoneutral points are vital operational temperatures in autothermal processes. A thermodynamic analysis of dry autothermal reforming of ethanol has been carried out to locate the thermoneutral temperatures and product composition at those points at 1, 3, 6 and 9 bar reaction pressures. The variations of thermoneutral temperatures and individual product yields at those temperatures have been discussed to find the optimum operating parameters for desired product output from the process. The process operated at thermoneutral conditions can give useful products like hydrogen, syngas (of low ratio) and carbon (possibly CNFs) and also provide a way for CO_2 sequestration using renewable ethanol fuel. A maximum of 2.58 moles of syngas of ratio 2.01 obtained at 1 bar, CER=1 and OER=0.5 along with 0.82 moles of carbon, with 0.20 moles of CH_4 and 0.89 moles of water for the thermoneutral temperature of 603.55 °C was found to be the best operating thermoneutral point for value added product generation from this process.

CHAPTER 3: Thermoneutral point analysis of ethanol dry autothermal reforming

3.1 Ethanol as fuel

The spurt of renewable energy has brought biofuels like ethanol, glycerol and biodiesel into limelight. Biofuels are considered as reliable energy sources for the future. Bioethanol, glycerol, etc. can be produced in abundant quantities all around the world once the biofuel revolution commercializes. Ethanol is easy to produce, safe to handle, transport and store. Ethanol does not contain heteroatoms (N, S, etc) or metals, and using it in process will not emit NOx or SOx. Although commercial biodiesel manufacture is being done recently, ethanol manufacture from molasses has been well known in industry. Ethanol is a reliable and preferred feedstock and can be used to generate hydrogen and syngas instead of traditional feeds like coal, oil or gas as their reserves have been depleting over the time. Ethanol to syngas by partial oxidation, steam reforming, autothermal reforming and dry reforming has been studied by many researchers. Some important ethanol to syngas work reported in literature is summarized below:

3.1.1 Thermodynamic studies on steam reforming of ethanol

Vasudeva et al. (1996) have investigated the thermodynamic feasibility of ethanol steam reforming under conditions conducive to carbon formation and have reported that 5.5 moles of hydrogen can be obtained as against the stoichiometric value of 6.0 per mole ethanol feed. Garcia et al. (1991) have conducted thermodynamic analysis of steam reforming of ethanol to produce hydrogen between 1-9 atm, 400-800 K and 0:1-10:1 water to ethanol feed ratio and found that atmospheric pressure and water in excess in the feed gave the best condition for hydrogen production at T > 650 K minimizing methane production preventing carbon formation. Fishtik et al. (2008) have studied the thermodynamics of ethanol steam reforming using an algorithm for deriving a unique set of response reactions (RERs) that can be used to rationalize the effect of process variables on steam reforming of ethanol to produce hydrogen and have reported that at or above 700-800 K, and using

high water/ethanol ratios, the desired reaction of ethanol steam reforming can be made predominant minimizing the effect of undesirable side reactions. Comas et al. (2004) have studied the thermodynamic analysis of ethanol steam reforming using CaO as a CO_2 sorbent and reported that atmospheric pressure, 700 ºC and water/ethanol molar ratio of 4 were the best conditions for hydrogen production in the presence of CaO. De Souza et al. (2006) have studied the physical-chemical, thermodynamic and exergetic analysis of a steam reformer of ethanol to produce hydrogen and reported that the best thermodynamic conditions for steam reforming of ethanol are the same conditions suggested in the physical-chemical analysis. Da Silva et al. (2009) have presented a thermodynamic analysis of ethanol steam reforming to identify conditions for carbon formation and also stated that the work could provide explanations for deviations between thermodynamic analysis and experimental results regarding carbon deposition. Ni et al. (2007) have presented a review on reforming bio-ethanol for hydrogen production. Haryanto et al. (2005) have presented a review of hydrogen production techniques by steam reforming of ethanol.

3.1.2 Kinetics and Process engineering aspect studies

Vaidya et al. (2006a) have discussed the process engineering aspects of ethanol steam reforming along with catalysts, optimum conditions and ways to prevent problems like coking and byproduct formation. Sahoo et al. (2007) have experimentally investigated the kinetics of ethanol steam reforming using Co/Al_2O_3 catalysts in a fixed bed tubular reactor and proposed a kinetic model to describe the steam reforming of ethanol process adequately for a wide range of experimental data. Vaidya et al. (2006b) studied the catalytic steam reforming of ethanol over a Ru/Al_2O_3 catalyst in 873-973 K temperature range. Mathure et al. (2007) have experimentally studied the kinetics of ethanol steam reforming over a commercial nickel-magnesia-alumina ($Ni/MgO/Al_2O_3$) catalyst in a fixed-bed reactor.

3.1.3 Oxidative Steam reforming / autothermal reforming

a. Thermodynamic studies

Liu et al. (2008) have conducted thermodynamic analysis of hydrogen production in oxidative steam reforming of ethanol to calculate the thermoneutral product gas equilibrium moles at 700, 900 and 1100 K and reported that maximum hydrogen with minimum coke and methane were formed at 900 K.

b. Experimental studies

Biswas et al. (2007) have experimentally compared steam reforming and autothermal reforming of ethanol over Ni-CeO_2-ZrO_2 catalyst and reported that the hydrogen yield was higher in ATR at 500 ºC but at higher temperatures higher hydrogen yields were obtained in absence of oxygen. Chen et al. (2009) have experimentally studied the autothermal reforming of ethanol using noble metal (Ir, Ru, Rh, and Pd) catalysts supported on various oxides like gamma-Al_2O_3, CeO_2, ZrO_2 and La_2O_3 and found that La_2O_3 was the best support for the ATR reaction and Ir/La_2O_3 gave excellent hydrogen selectivity with good stability on stream and high conversion approaching thermodynamic limit. Cai et al. (2008) have studied the ethanol autothermal reforming over an Rh/CeO_2 catalyst and reported that the catalysts exhibited stable activity and selectivity for long term operation without deactivation or sintering. Deluga et al. (2004) have also studied ethanol autothermal reforming on rhodium-ceria catalysts and reported that the process has great potential for low-cost H_2 generation applications. Markova et al. (2009) have experimentally studied bio-ethanol autothermal reforming to generate data for regression models to provide optimum values of the process factors to maximize hydrogen. Youn et al. (2006) have investigated the effect of addition of second metal (Ce, Co, Cu, Mg and Zn) to Ni/gamma-Al_2O_3 catalysts for autothermal reforming of ethanol and found that Cu was the most efficient

promoter for hydrogen production. De Lima et al. (2008) have tested the catalytic performance of a $Pt/CeZrO_2$ catalyst for ethanol decomposition, steam reforming, partial oxidation, and oxidative steam reforming and proposed a reaction mechanism based on results obtained under reaction conditions. Cai et al. (2007) have experimentally tested the oxidative steam reforming of ethanol over an Ir/CeO_2 catalyst and reported complete conversion of ethanol at 773K with hydrogen, carbon oxides and methane as only products and stable performance of Ir/CeO_2 without deactivation or coking.

3.1.4 Dry reforming of ethanol

Jankhah et al. (2008) have studied the thermodynamic equilibrium analysis and experimentation of thermal and catalytic ethanol cracking and dry reforming using a carbon steel catalyst precursor and reported that highest hydrogen and carbon (carbon nanofilaments) yields were obtained at 550 ºC. Wang et al. (2009) have studied the thermodynamics of ethanol reforming with carbon dioxide for hydrogen production and have reported that optimum conditions gave over 94% yield of syngas with complete conversion of ethanol without carbon deposition. De Oliveira-Vigier et al. (2005) have experimentally studied the dry reforming of ethanol using a recyclable and long lasting SS 316 catalyst and have obtained hydrogen yield 98% of the theoretical value. Blanchard et al. (2008) have experimentally studied the ethanol dry reforming using a carbon steel catalyst to produce syngas and also nanocarbons.

No study of ethanol dry reforming with oxygen addition (dry autothermal reforming (DATR) of ethanol) has been reported yet although a similar study for glycerol has been reported in the earlier chapter which has stated the advantages of DATR over the DR process and role of CO_2 in the process.

Thermoneutral point is the condition where the endothermic reactions balance the exothermic reactions to make the net enthalpy of reaction zero.

CHAPTER 3: Thermoneutral point analysis of ethanol dry autothermal reforming

Autothermal processes are generally operated at thermoneutral conditions to maximize energy efficiency. However, very little literature is available regarding thermoneutral points and product trends at those points. S. Ahmed et al. (2001) have theoretically explained the advantages of thermoneutral points of reforming reactions. The main goal of the work is to analyze the thermoneutral conditions for DATR of ethanol process to produce a variety of value added products like hydrogen, syngas and CNF's whose yield can be maximized at different operating conditions and input ratios. This paper intends to study the variation of components in the product stream at thermoneutral conditions, presenting product yields and product distribution trends at various pressures to find the best operating thermoneutral point for desired product.

3.2 Methodology

HSC Chemistry software package (version 5.1) has been used to generate the equilibrium data for this study. The input species fed to the software were ethanol (both gaseous and liquid state), air (g) and CO_2 (g). The output species fed to the software are H_2, CO, CO_2, CH_4 (all in gaseous state), H_2O (both gas and liquid state) and C (solid), which are common reaction products of reforming reactions. The software gives the individual product moles, along with overall reaction enthalpy at the T and P condition. Temperature, pressure, CER (feed CO_2 to ethanol ratio) and OER (feed O_2 to ethanol ratio) are the key parameters for the process design. The OER is the equivalent of the equivalence ratio, which is defined by the fuel to oxygen ratio compared to the stoichiometric value by some researchers. It has been decided to operate the process at thermoneutral temperatures only, so the data generation is limited to product compositions at thermoneutral conditions for change in CER, OER and pressure. Thermoneutral point temperatures can be obtained from the temperature Vs reaction enthalpy graph as it is the temperature at which the enthalpy curve touches the temperature axis where the enthalpy is zero. 1 mole of ethanol has been used at all conditions for this study. The

thermodynamic analysis of ethanol dry autothermal reforming has been carried out in the temperature range (450 – 950ºC) at 1, 3, 6 and 9 bar reaction pressures with CER (feed CO_2 to ethanol ratio) 1, 2, 3 and OER (feed O_2 to ethanol ratio) 0.1, 0.3, 0.5. These conditions represent a realistic view for process operation and are carefully chosen to limit the thermoneutral point temperature to < 700ºC which is practical for ethanol feed and also to produce significant carbon (possible CNFs) as they have been reported as useful products by some researchers. The data for variation in yields of products like H_2, CO, CH_4, H_2O and C and also CO_2 conversion at zero enthalpy (thermoneutral) temperatures at different pressures have been generated, analyzed and discussed in the proceeding section. Complete conversion of ethanol and oxygen was found in all cases.

3.3 Results and Discussion

3.3.1 Thermoneutral points for DATR of ethanol

Thermoneutral point (TNP) is the temperature at which zero net enthalpy is obtained in the autothermal process. It is considered as the best point for autothermal process operation. Lower TNPs are generally preferred to reduce heat losses. Figure 3.1 depicts the variation of TNP in DATR of ethanol with change in pressure, CER and OER.

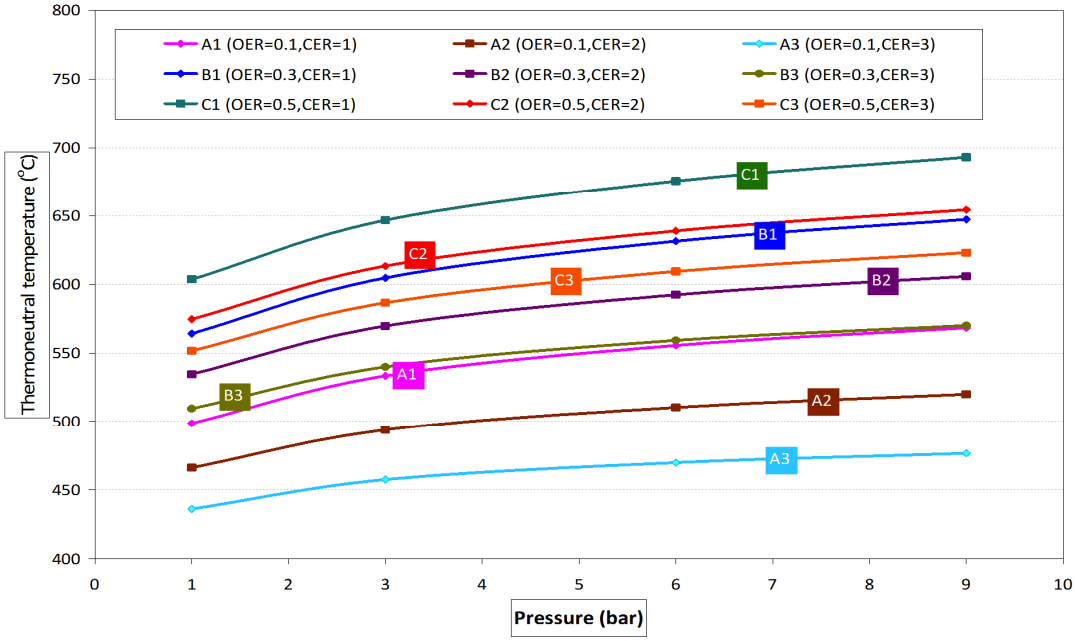

Figure 3.1: Thermoneutral temperatures in DATR of Ethanol

As seen from figure 3.1, the TNP increases with increase in pressure at constant CER and OER and also increases with increase in OER at constant pressure and constant CER. However, the TNP decreases with increase in CER at constant pressure and constant OER. At constant pressure, the TNP shows an increase with a simultaneous increase in CER and OER, but it decreases with increase in CER and decrease in OER at constant pressure. Simultaneous increase in pressure, CER and OER generally increases the TNP except for one (P=6 bar, CER=1, OER=0.3 and P=9 bar, CER=3, OER=0.5) point. The TNP range obtained for increase in pressure from 1 bar to 9 bar, was from 436.05°C to 603.55°C (P=1 bar), from 457.38°C to 646.66°C (P=3 bar), from 469.74°C to 675.61°C (P=6 bar) and from 476.47°C to 693.15°C (P=9 bar) at different CERs and OERs. The TNP range obtained for increase in CER from 1 to 3, was from 498.61°C to 693.15°C (CER=1), from 466.08°C to 654.36°C (CER=2) and from 436.05°C to 623.00°C (CER=3) for the considered pressure and OER range. The TNP range obtained for increase in OER from 0.1 to 0.5, was from 436.05°C to 568.32°C (OER=0.1), from 509.37°C to 647.37°C (OER=0.3) and from 551.51°C to

693.15°C (OER=0.5) for the considered pressure and CER range. The minimum TNP for every pressure were obtained at CER=3 & OER= 0.1 while the maximum TNPs were obtained at CER=1 & OER=0.5. Considering all the data points, the minimum TNP of 436.05 °C was obtained at 1 bar pressure, CER = 3 & OER = 0.1 and the maximum TNP of 693.15 °C was found at 9 bar pressure, CER = 1 & OER = 0.5.

3.3.2 Hydrogen yield at TNP

Hydrogen generation is one of the most desired applications of reforming processes. Thermoneutral operation of the process to give higher hydrogen yield is highly desired. Figure 3.2 shows the variation of hydrogen yield in DATR of ethanol at thermoneutral points at various pressures, CER and OER. The hydrogen yield decreases with increase in pressure at constant CER and OER, and also decreases with increase in CER at constant OER and pressure. But the hydrogen yield increases with increase in OER at constant CER and pressure. Similarly, with simultaneous increase in CER and OER, the hydrogen yield increases at constant pressure. But it decreases when CER is increased and OER is decreased at constant pressure. Simultaneous increase in pressure, CER and OER shows a mixed trend (the hydrogen yield increases at some points and decreases at other points). The hydrogen yield obtained for increase in pressure from 1 bar to 9 bar, was from 0.48 to 1.72 moles (P=1 bar), from 0.36 to 1.51 moles (P=3 bar), from 0.29 to 1.37 moles (P=6 bar) and from 0.26 to 1.29 moles (P=9 bar) at different CERs and OERs. The hydrogen yield obtained for increase in CER from 1 to 3, was from 0.56 to 1.72 moles (CER=1), from 0.38 to 1.45 moles (CER=2) and from 0.26 to 1.24 moles (CER=3) for the considered pressure and OER range. The hydrogen yield obtained for increase in OER from 0.1 to 0.5, was from 0.26 to 0.87 moles (OER=0.1), from 0.58 to 1.38 moles (OER=0.3) and from 0.84 to 1.72 moles (OER=0.5) for the considered pressure and CER range.

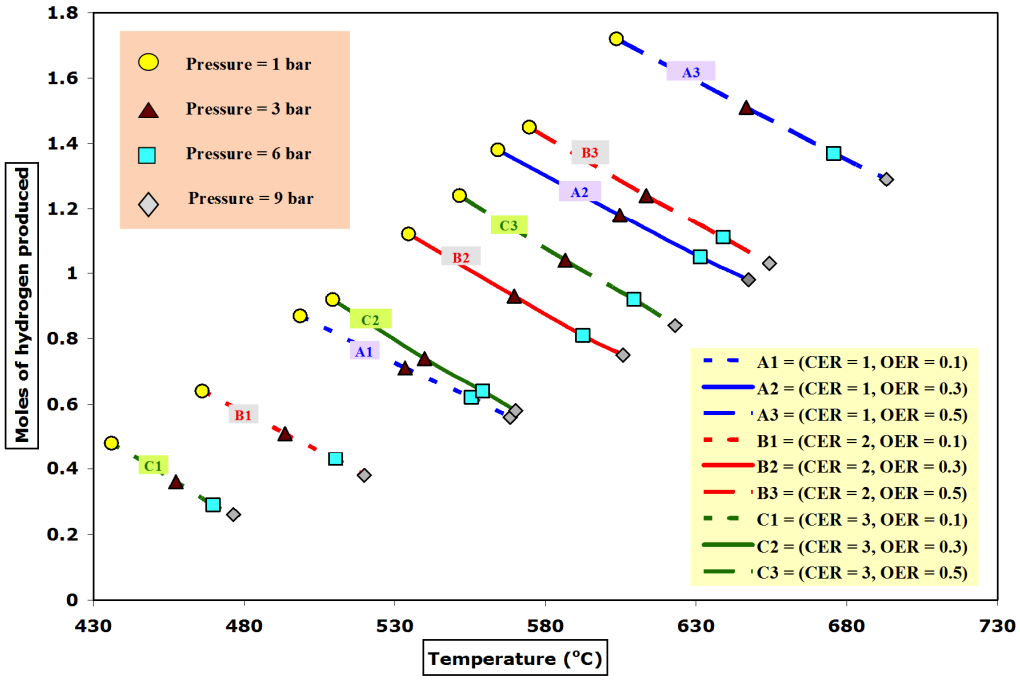

Figure 3.2: Hydrogen yield at thermoneutral temperatures

The minimum hydrogen yield for every pressure was obtained at CER=3 & OER=0.1 and the maximum hydrogen yield was obtained at CER=1 & OER=0.5. Considering all the data points, the maximum hydrogen yield of 1.72 moles was observed at 1 bar pressure, CER= 1 and OER= 0.5, while the minimum hydrogen yield of 0.26 moles was observed at 9 bar pressure, CER = 3 and OER = 0.1.

3.3.3 CO yield at TNP

Carbon monoxide is an undesired gas for PEM fuel cell applications but a desired component of syngas for GTL (Gas-to-Liquids) manufacture. Figure 3.3 shows the variation of CO yield in DATR of ethanol at thermoneutral points with variation in pressure, CER and OER. The CO yield decreases with increase in pressure at constant CER and OER, (but it was constant at CER=1, OER=0.1) and also decreases with increase in CER at constant pressure and constant OER, but the CO yield increases with increase in OER

at constant pressure and constant CER. The CO yield increases at constant pressure when CER and OER are increased simultaneously.

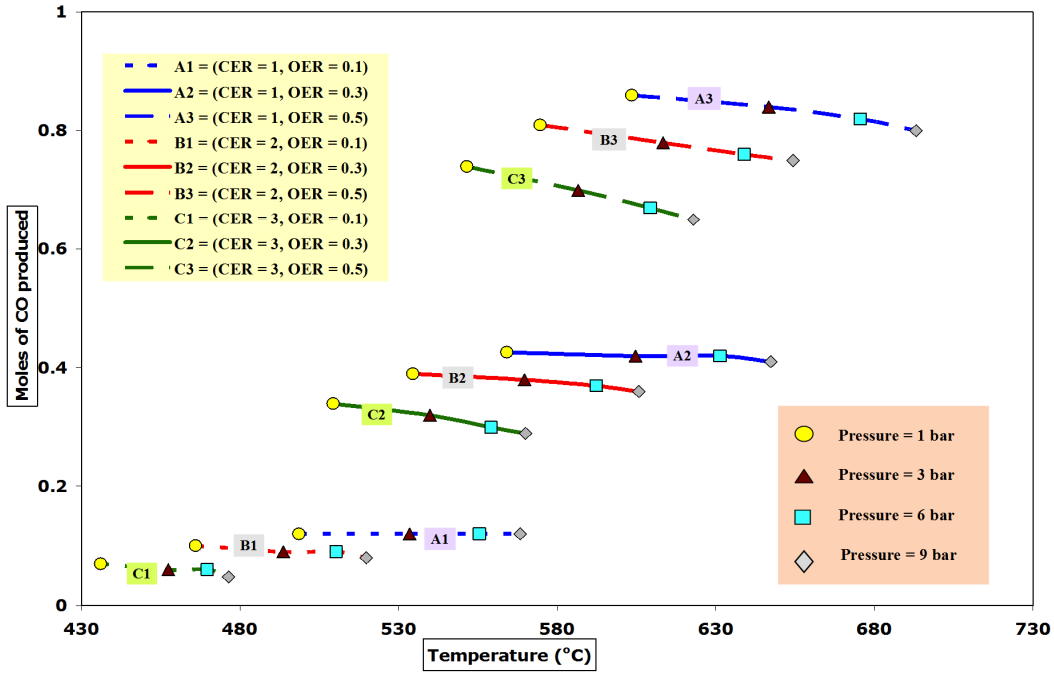

Figure 3.3 Carbon monoxide yield at thermoneutral temperatures

The CO yield decreases when CER is increased and OER is decreased at constant pressure. The CO yield increases when pressure is increased and CER is decreased simultaneously at constant OER. Simultaneous increase in pressure, CER and OER increases the CO yield. The CO yield obtained for increase in pressure for 1 bar to 9 bar, was from 0.07 to 0.86 moles (P=1 bar), from 0.06 to 0.84 moles (P=3 bar), from 0.06 to 0.82 moles (P=6 bar), and from 0.05 to 0.8 moles (P=9 bar). The CO yield obtained for increase in CER from 1 to 3, was from 0.12 to 0.86 moles (CER=1), from 0.08 to 0.81 moles (CER=2) and from 0.05 to 0.74 moles (CER=3) for the considered pressure and OER range. The CO yield obtained for increase in OER from 0.1 to 0.5, was from 0.05 to 0.12 moles (OER=0.1), from 0.29 to 0.43 moles (OER=0.3) and from 0.65 to 0.86 moles (OER=0.5) for the considered pressure and CER range. The minimum CO yield for every pressure was obtained at CER=3 & OER= 0.1 and the maximum CO yield were obtained at CER=1 & OER=0.5.

Considering all the data points, it was observed that a minimum of 0.05 moles of CO were produced at 9 bar pressure, CER = 3 & OER = 0.1, while a maximum of 0.86 moles were produced at 1 bar pressure, CER = 1 & OER = 0.5.

3.3.4 Syngas (H_2 + CO) amount at TNP

Syngas (H_2 + CO) is an important gas for petrochemical manufacture. The conditions for maximizing syngas yield are desired. The variation in the amount of syngas moles obtained in DATR of ethanol at thermoneutral points with variation in pressure, CER and OER is shown in figure 3.4.

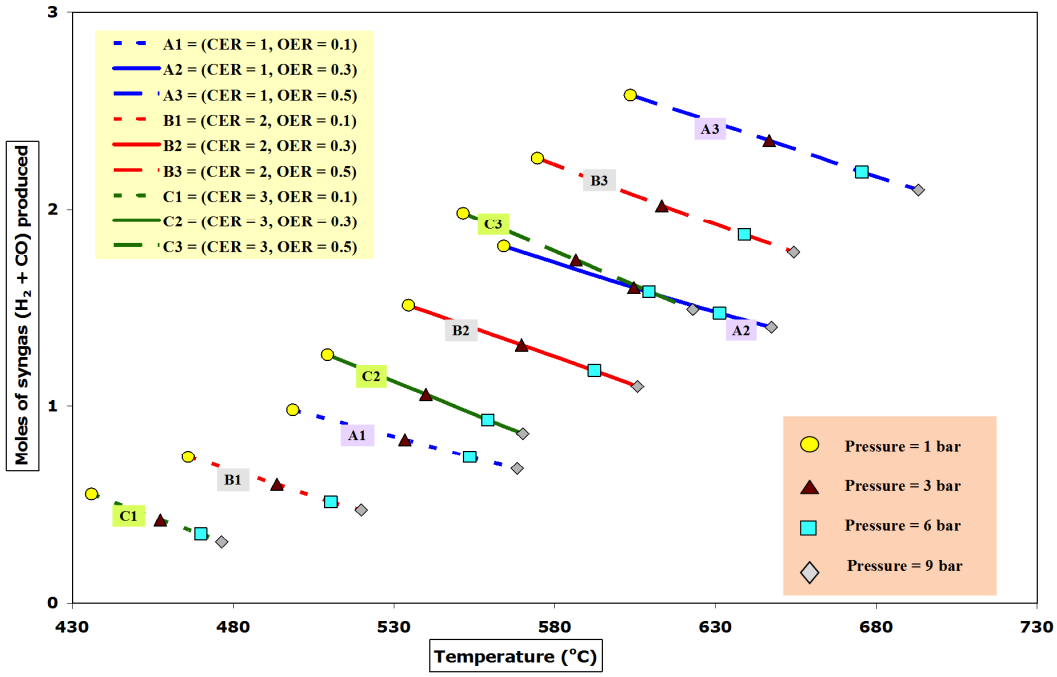

Figure 3.4: Syngas yield at thermoneutral temperatures

As seen from the figure, the moles of syngas decrease with increase in pressure at constant CER and OER, and also decrease with increase in CER at constant pressure and constant OER. But the syngas yield increases with increase in OER at constant pressure and constant CER. The moles of syngas produced increase when CER and OER are increased simultaneously

at constant pressure. On the other hand, the moles of syngas produced decrease when CER is increased and OER is decreased at constant pressure. Simultaneous increase in pressure, CER and OER generally increases the syngas moles except for some points. The amount of syngas moles obtained for increase in pressure from 1 bar to 9 bar, was from 0.55 to 2.58 moles (P=1 bar), from 0.42 to 2.35 moles (P=3 bar), from 0.35 to 2.19 moles (P=6 bar) and from 0.31 to 2.10 moles (P=9 bar). The amount of syngas moles obtained for increase in CER from 1 to 3, was from 0.68 to 2.38 moles (CER=1), from 0.47 to 2.26 moles (CER=2) and from 0.31 to 1.98 moles (CER=3) for the considered pressure and OER range. The amount of syngas obtained for increase in OER from 0.1 to 0.5, was from 0.31 to 0.98 moles (OER=0.1), from 0.86 to 1.81 moles (OER=0.3) and from 1.49 to 2.58 moles (OER=0.5) for the considered pressure and CER range. The minimum syngas moles for all pressures were obtained at CER=3 & OER= 0.1 and the maximum syngas moles were obtained at CER=1 & OER=0.5. Considering all the data points, the minimum amount of syngas obtained was 0.31 moles at 9 bar pressure, CER = 3 & OER = 0.1, while a maximum 2.58 moles of total hydrogen were obtained at 1 bar pressure, CER = 1 & OER = 0.5.

3.3.5 Syngas ratio (H_2/CO) at TNP

Lower syngas (H_2/CO) ratio between 0 – 5 is desired for converting syngas to chemicals by FT synthesis. Figure 3.5 shows the variation of syngas ratio in DATR of ethanol at thermoneutral points with variation in pressure, CER and OER. It was seen that the syngas ratio decreased with increase in pressure at constant CER and OER, the decrease was much more for lower OERs. With increase in OER at constant pressure and constant CER, the syngas ratio decreased considerably. Also with increase in CER at constant pressure and constant OER, the syngas ratio decreased (except at OER = 0.1). It was observed that when CER and OER were increased simultaneously, the syngas ratio decreased at constant pressure. But at constant pressure, when CER was increased and OER was decreased, the syngas ratio increased.

Simultaneous increase in pressure, CER and OER decreases the syngas ratio. The range of syngas ratio obtained for increase in pressure from 1 to 9 bar, was from 1.69 to 7.34 (P=1 bar), from 1.49 to 5.93 (P=3 bar), from 1.37 to 5.23 (P=6 bar) and from 1.30 to 4.82 (P=9 bar).

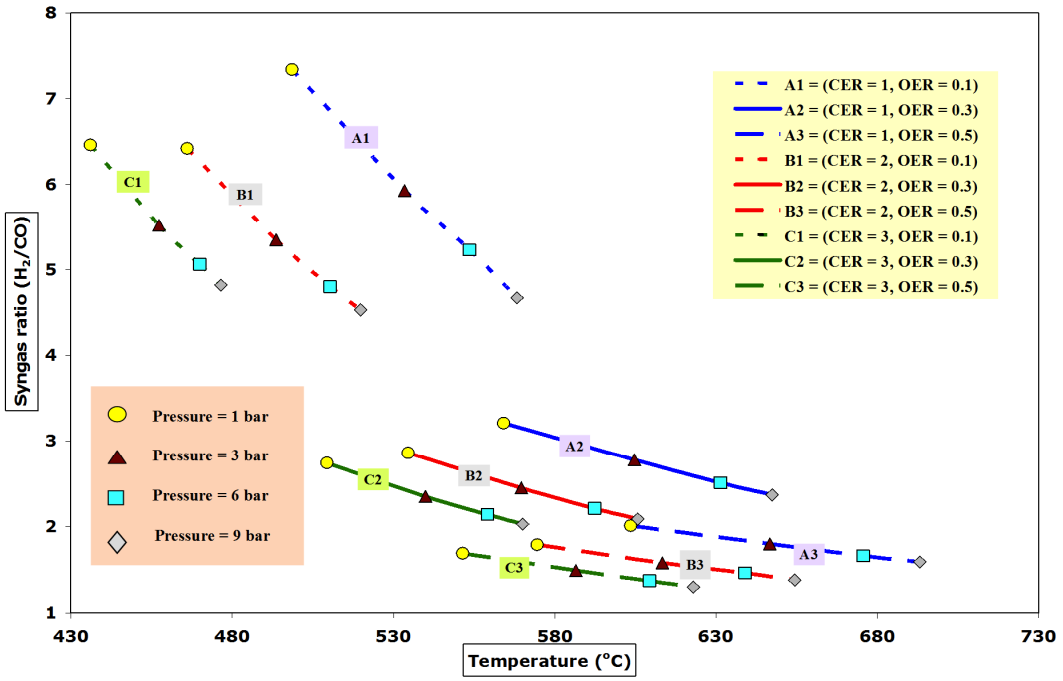

Figure 3.5: Syngas ratio at thermoneutral temperatures

The range of syngas ratio obtained for increase in CER from 1 to 3, was from 1.59 to 7.34 (CER=1), from 1.38 to 6.42 (CER=2) and from 1.3 to 6.46 moles (CER=3) for the considered pressure and OER range. The range of syngas ratio obtained for increase in OER from 0.1 to 0.5, was from 4.53 to 7.34 (OER=0.1), from 2.03 to 3.21 (OER=0.3) and from 1.30 to 2.01 (OER=0.5) for the considered pressure and CER range. It was observed that the range of syngas ratio decreases at higher pressures. The minimum syngas ratio was obtained at CER=3 & OER= 0.5 and the maximum syngas ratio was obtained at CER=1 & OER=0.1 (except at 9 bar) for all pressures considered. Considering all the data points, the minimum syngas ratio obtained was 1.30 at 9 bar pressure, CER = 3 & OER = 0.5, and maximum syngas ratio of 7.34 was observed at 1 bar pressure, CER = 1 & OER = 0.1.

3.3.6 Methane formation at TNP

Methane formation is inevitable in reforming processes. Figure 3.6 depicts the variation of CH_4 formation in DATR of ethanol at thermoneutral points with change in pressure, CER and OER. It was seen that, the CH_4 formation increases with increase in pressure at constant CER and OER. It was observed that with increase in OER at constant pressure and constant CER, the CH_4 formation decreased. Also at constant pressure and constant OER, the CH_4 formation decreased with increase in CER. Similarly at constant pressure when CER and OER were increased, the CH_4 formation decreased gradually. When CER was increased and OER was decreased, the methane formation increased at constant pressure except for P=9 bar. Simultaneous increase in pressure, CER and OER generally decreases the CH_4 formation except for some points. The moles of CH_4 obtained for increase in pressure from 1 to 9 bar was from 0.17 to 0.42 (P=1 bar), from 0.22 to 0.49 (P=3 bar), from 0.25 to 0.52 (P=6 bar) and from 0.27 to 0.55 (P=9 bar). The moles of methane obtained for increase in CER from 1 to 3, was from 0.20 to 0.55 (CER=1), from 0.19 to 0.43 (CER=2) and from 0.17 to 0.35 (CER=3) for the considered pressure and OER range. The moles of methane formed for increase in OER from 0.1 to 0.5, was from 0.28 to 0.55 (OER=0.1), from 0.22 to 0.42 (OER=0.3) and from 0.17 to 0.33 (OER=0.5) for the considered pressure and CER range. The minimum CH_4 yield for all pressure conditions was obtained at CER=3 & OER= 0.5, while the maximum CH_4 was obtained at CER=1 & OER=0.1. Considering all the data points, minimum of 0.17 moles of CH_4 were obtained at 1 bar pressure, CER = 3 & OER = 0.5 and a maximum of 0.55 moles of CH_4 were obtained at 9 bar pressure, CER = 1 & OER = 0.1.

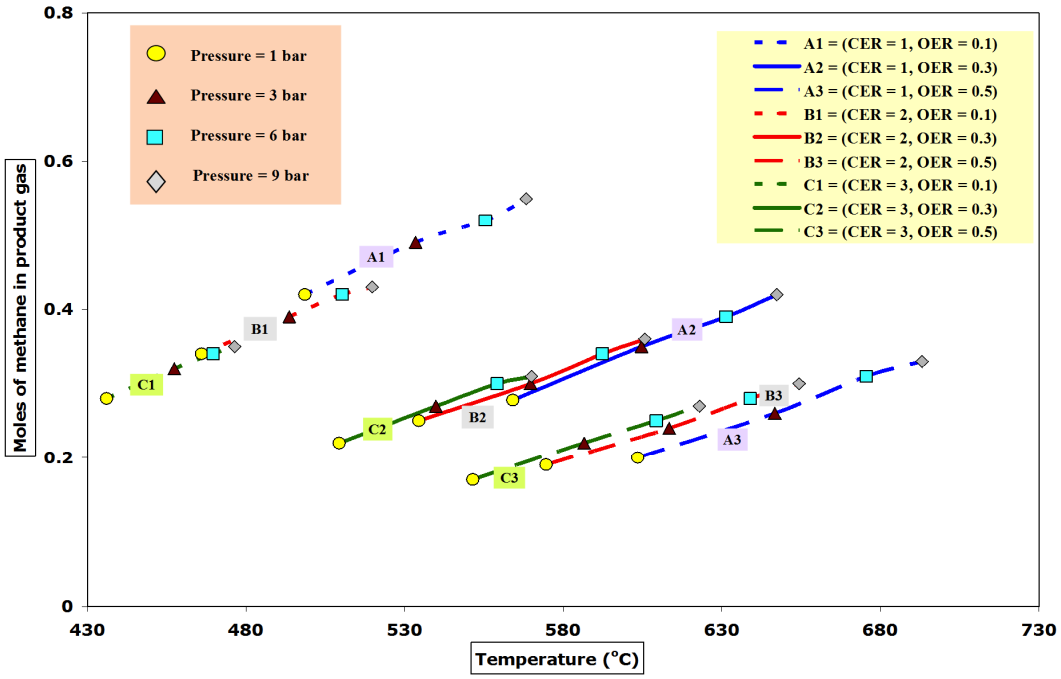

Figure 3.6: Methane yield at thermoneutral temperatures

3.3.7 Water formation at TNP

Water formation is undesirable in reforming processes as it decreases the hydrogen yield. But water formation cannot be avoided. Figure 3.7 depicts the variation in H_2O yield in DATR of ethanol at thermoneutral points at specified pressures, CER and OER. From figure 3.7, it was seen that the moles of H_2O produced increased with increase in pressure at constant CER and OER but the moles of H_2O produced decreased with increase in OER at constant pressure and constant CER. When CER was increased at constant pressure and constant OER, the moles of H_2O produced increased. Similarly, at constant pressure when CER and OER were increased simultaneously, the moles of H_2O produced increased at some points and decreased at other points.

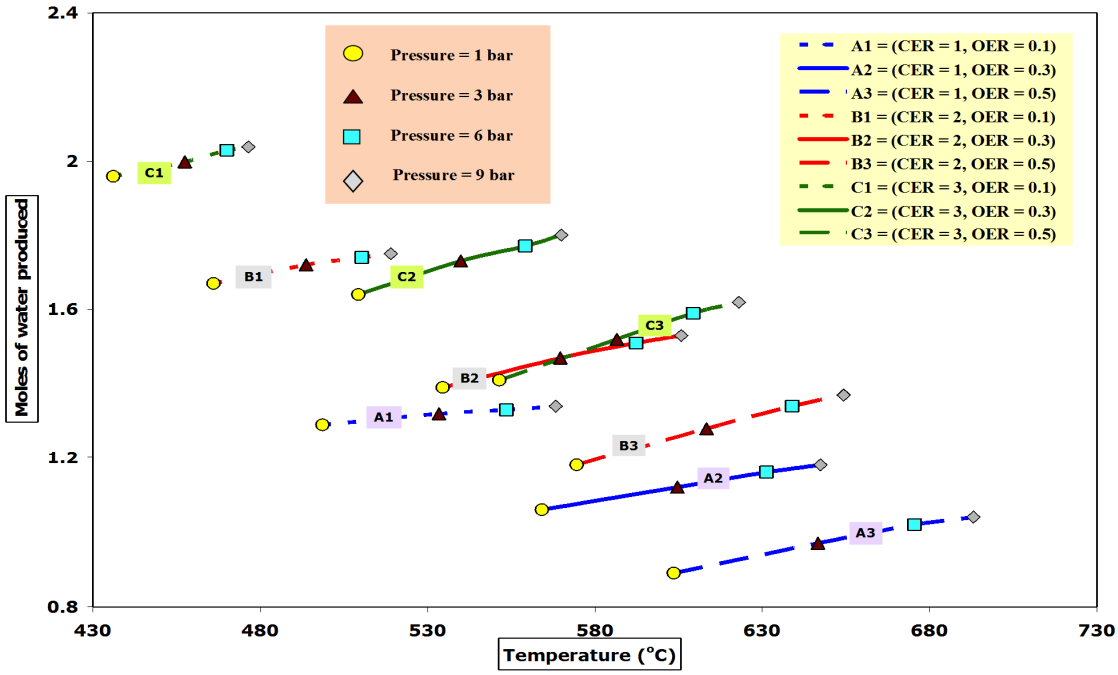

Figure 3.7: Water yield at thermoneutral temperatures

It was observed that at constant pressure when CER was increased and OER was decreased, the moles of H_2O produced gradually increased. Simultaneous increase in pressure, CER and OER generally increases the H_2O except for some points. The moles of H_2O produced for increase in pressure from 1 to 9 bar ranged from 0.89 to 1.96 (P=1 bar), from 0.97 to 2.0 (P=3 bar), from 1.02 to 2.03 (P=6 bar) and from 1.04 to 2.04 (P=9 bar). The moles of water obtained for increase in CER from 1 to 3, was from 0.89 to 1.34 (CER=1), from 1.18 to 1.75 (CER=2) and from 1.41 to 2.04 (CER=3) for the considered pressure and OER range. The moles of water formed for increase in OER from 0.1 to 0.5, was from 1.29 to 2.04 (OER=0.1), from 1.06 to 1.80 (OER=0.3) and from 0.89 to 1.62 (OER=0.5) for the considered pressure and CER range. The minimum moles of H_2O for every pressure were obtained at CER=1 & OER= 0.5 and the maximum H_2O was obtained at CER=3 & OER=0.1. Considering all the data points, the minimum moles of H_2O produced were 0.89 at 1 bar pressure and CER = 1 & OER = 0.5, and a maximum of 2.04 moles of H_2O were obtained at 9 bar pressure and CER = 3 & OER = 0.1.

3.3.8 Carbon formation at TNP

Carbon formation is not desirable in any process as coking may deactivate the catalyst. However, carbon (in the form of CNFs) is a valuable product for some applications. Figure 3.8 shows the variation of the carbon formation in DATR of ethanol at thermoneutral points at different pressures, CER and OER. From figure 3.8, it was observed that, the carbon formation decreases with increase in pressure at constant CER and OER (except for some points). Also, it was observed that at constant pressure and constant CER, the moles of carbon formed decreased with increase in OER. However, as CER was increased at constant pressure and constant OER, the moles of carbon produced increased. It was also observed that at constant pressure when CER and OER were increased simultaneously, the moles of carbon formed decreased. When CER was increased and OER was decreased, the moles of carbon formed at constant pressure increased.

Simultaneous increase in pressure, CER and OER generally decreases the carbon formation except at some points. The moles of carbon formed for increase in pressure from 1 to 9 bar ranged from 0.82 to 2.06 (P=1 bar), from 0.80 to 2.05 (P=3 bar), from 0.79 to 2.05 (P=6 bar) and from 0.78 to 2.04 (P=9 bar). The moles of carbon obtained for increase in CER from 1 to 3, was from 0.78 to 1.56 (CER=1), from 1.00 to 1.85 (CER=2) and from 1.16 to 2.06 (CER=3) for the considered pressure and OER range. The moles of carbon formed for increase in OER from 0.1 to 0.5, was from 1.47 to 2.06 (OER=0.1), from 1.16 to 1.65 (OER=0.3) and from 0.78 to 1.22 (OER=0.5) for the considered pressure and CER range. The minimum carbon formation for all pressures was observed at CER=1 & OER= 0.5, while the maximum carbon formation was observed at CER=3 & OER=0.1. Considering all the data points, the minimum carbon formation was 0.78 moles at 9 bar pressure, CER = 1 & OER = 0.5, while a maximum carbon of 2.06 moles were obtained at 1 bar pressure, CER = 3 & OER = 0.1.

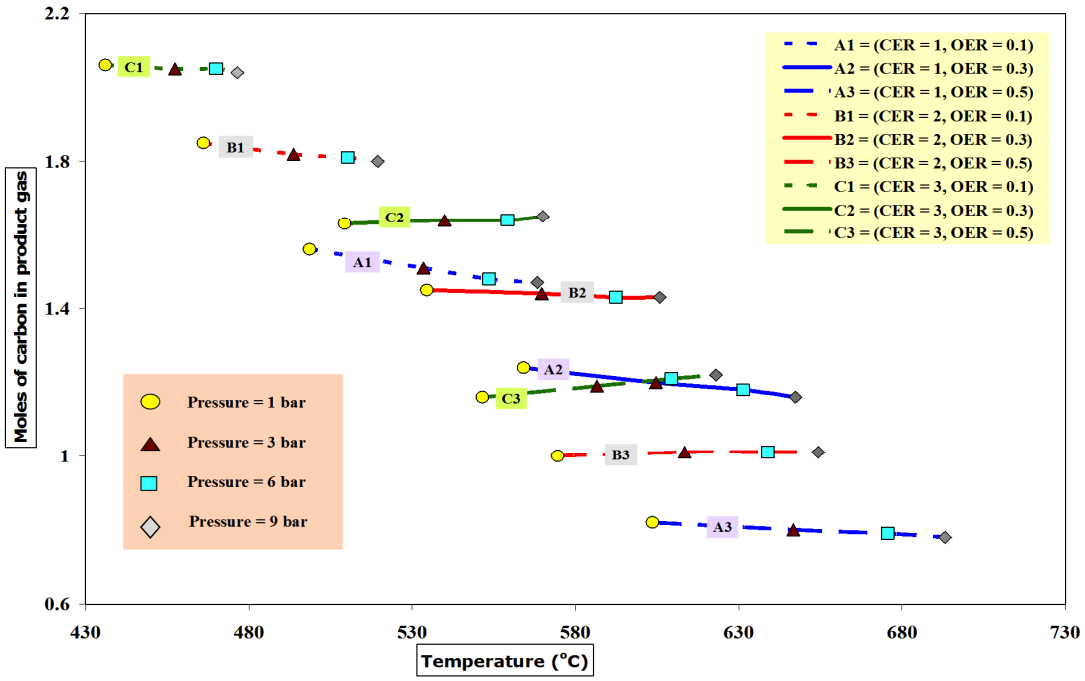

Figure 3.8: Carbon yield at thermoneutral temperatures

3.3.9 CO_2 conversion (%) at TNP

CO_2 conversion in DATR of ethanol is important for CO_2 sequestration. Figure 3.9 represents the variation of CO_2 conversion (%) in DATR of ethanol at thermoneutral point at different pressures, CER and OER. From the figure 3.9, it is seen that, the CO_2 conversion increases with increase in pressure at constant CER and OER It was observed that with increase in OER at constant pressure and constant CER, the CO_2 conversion decreases. Also at constant pressure and constant OER, the CO_2 conversion increases (except for OER = 0.1) with increase in CER of the process. Also at constant pressure when CER is increased and OER is decreased, the CO_2 conversion increases. Simultaneous increase in pressure, CER and OER generally decreases the CO_2 conversion except for some points. The CO_2 conversion (%) obtained for increase in pressure from 1 to 9 bar ranged from -13.0 to 14.5 (P=1 bar), from -10.0 to 15.5 (P=3 bar), from -8.0 to 15.5 (P=6 bar) and from -7.0 to 16.0 (P=9 bar).

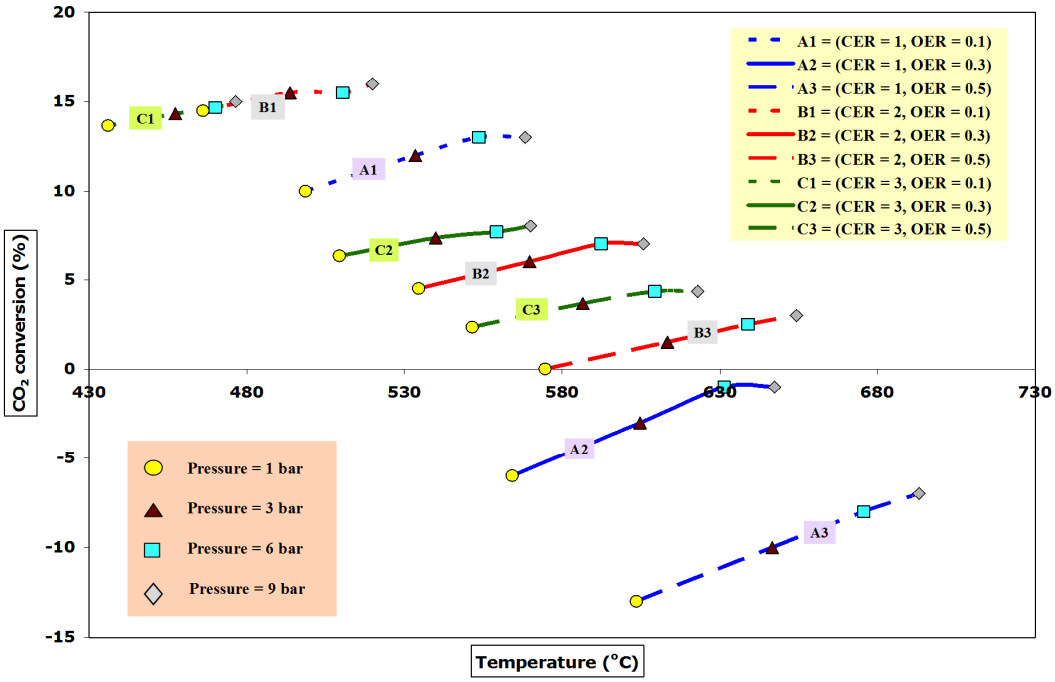

Figure 3.9: Carbon dioxide conversion at thermoneutral temperatures

The CO_2 conversion (%) obtained for increase in CER from 1 to 3, was from -13.00 to +13.00 (CER=1), from 0.00 to 16.00 (CER=2) and from 2.33 to 15.00 (CER=3) for the considered pressure and OER range. The CO_2 conversion (%) obtained for increase in OER from 0.1 to 0.5, was from 10.00 to 16.00 (OER=0.1), from -6.00 to 8.00 (OER=0.3) and from -13.00 to 4.33 (OER=0.5) for the considered pressure and CER range. The minimum CO_2 conversions were obtained at CER=1 & OER= 0.5 and the maximum CO_2 conversions were obtained at CER=2 & OER=0.1 for all the pressures. The CO_2 conversion varied from a minimum of -13 % at 1 bar pressure, CER = 1 & OER = 0.5 to a maximum of 16 % at 9 bar pressure, CER = 2 & OER = 0.1, for all the data points considered.

3.4 Conclusions

The product composition at thermoneutral points for DATR of ethanol at various pressures showed some interesting results. Maximum carbon

formation was observed at OER=0.1 and CER=3 and it decreased with increase in pressure; hence thermo-neutral low pressure operation can be used to produce carbon (possibly CNFs). The syngas ratio ranged between 7.34 to 1.30 and the syngas ratio decreased with increase in pressure, and as lower syngas ratios are desirable for petrochemical manufacture by FT synthesis, thermo-neutral higher pressure operation can be used for this purpose. The maximum syngas (total H_2) was formed at CER=1 and OER=0.5, and it reduced with increase in pressure, so lower pressure TNP operation can be used for hydrogen/syngas manufacture for fuel cells. Higher CO_2 conversion was observed for CER=2 and OER=0.1 and higher pressures making this process effective for CO_2 conversion (CO_2 sequestration). Thermoneutral points ranged from 436.05 to 693.15 °C which are practically achievable temperatures in ethanol chemical processes. Depending upon the desired product requirements, the system pressure and thermoneutral points can be chosen for process operation. Syngas (of a particular ratio), carbon (in the form of CNFs), syngas moles (total H_2) are the usual desired products. A maximum of 2.58 moles of total hydrogen obtained at 1 bar, CER=1 and OER=0.5 producing 0.82 moles of carbon, of syngas ratio 2.01 with 0.20 moles of CH_4 and 0.89 moles of water for the TNP=603.55 °C was found to be the best operating thermoneutral point for value added product generation. Lower pressure TNP operation is favored for higher hydrogen production, lower methane and water formation. Higher pressure TNP operation is favored for lower syngas ratio with higher CO_2 conversion and sometimes lower carbon formation.

Thermoneutral Points (Temperature °C) for DATR of Ethanol				
0.5	693.15	654.36	623.00	
	675.61	638.99	609.42	
	646.66	613.36	586.57	
	603.55	574.62	551.51	
				P = 9 BAR
0.3	647.37	605.77	570.00	
	631.37	592.38	559.20	
	604.65	569.67	539.90	P = 6 BAR
	564.18	534.54	509.37	
				P = 3 BAR
0.1	568.32	519.86	476.47	
	555.50	510.31	469.74	
	533.34	493.63	457.38	P = 1 BAR
	498.61	466.08	436.05	
	1	2	3	
Feed CER (CO_2 to Ethanol ratio)				

Table 3.1: Thermoneutral points for DATR of ethanol

3.5 References

Ahmed S., Krumpelt M., 2001, Hydrogen from hydrocarbon fuels for fuel cells, Int. J. Hydrogen Energy, 26, 291–301.

Biswas P., Kunzru D., 2007, Oxidative steam reforming of ethanol over Ni/CeO_2-ZrO_2 catalyst, Chem. Eng. J., 136(1), 41–49.

Blanchard J., Oudghiri-Hassani H., Abatzoglou N., Jankhah S., Gitzhofer F., 2008, Synthesis of nano carbons via ethanol dry reforming over a carbon steel catalyst, Chem. Eng. J., 143(1), 186–194.

Cai W., Zhang B., Li Y., Xu Y., Shen W., 2007, Hydrogen production by oxidative steam reforming of ethanol over Ir/CeO_2 catalyst, Catal. Commun., 8(11), 1588–1594.

Cai W.J., Wang F.G., VanVeen A.C., Provendier H., Mirodatos C., Shen W.J., 2008, Auto thermal reforming of ethanol for hydrogen production over an Rh/CeO_2 catalyst, Catal. Today, 138(3), 152–156.

Chaffee A.L., Knowles G.P., Liang Z., Zhang J., Xiao P., Webley P.A., 2007, CO_2 capture by adsorption: materials and process development, Int. J. Greenhouse. Gas Control, 1-1, 8th International Conference on Greenhouse Gas Control Technologies – GHGT-8, 11-18.

Chen H.Q., Yu H., Tang Y., Pan M.Q., Yang G.X., Peng F., Wang H.J., Yang J., 2009, Hydrogen production via auto thermal reforming of ethanol over noble metal catalysts supported on oxides, J. Nat. Gas Chem., 18(2), 191–198.

Comas J., Laborde M., Amadeo N., 2004, Thermodynamic analysis of hydrogen production from ethanol using CaO as a CO_2 sorbent, J. Power Sources, 138(1), 61–67.

DaSilva A.L., De C., Malfatti F., Muller I.L., 2009, Thermodynamic analysis of ethanol steam reforming using gibbs energy minimization method: a detailed

study of the conditions of carbon deposition, Int. J. Hydrogen Energy, 34(10), 4321–4330.

De Oliveira-Vigier K., Abatzoglou N., 2005, Dry-reforming of ethanol in the presence of a 316 stainless steel catalyst, Can. J. Chem. Eng., 83(6), 978–984.

DeLima S.M., DaCruz I.O., Jacobs G., Davis B.H., Mattos L.V., Noronha F.B., 2008, Steam reforming, partial oxidation and oxidative steam reforming of ethanol over Pt/$CeZrO_2$ catalyst, J. Catal., 257(2), 356–368.

Deluga G.A., Salge J.R., Schmidt L.D., Verykios X.E., 2004, Renewable hydrogen from ethanol by autothermal reforming, Science, 303(5660), 993–997.

DeSouza A.C.C., Luz-Silveira J., Sosa M.I., 2006, Physical–chemical and thermodynamic analyses of ethanol steam reforming for hydrogen production, J. Fuel Cell Sci. Technol., 3(3), 346–350.

Figueroa J.D., Fout T., Plasynski S., McIlvried H., Srivastava R.D., 2008, Advances in CO_2 capture technology—the U.S. Department of Energy's Carbon Sequestration Program, Int. J. Greenhouse Gas Control, 2(1), 9–20.

Fishtik I., Alexander A., Datta R., Geana D., 2000, A thermodynamic analysis of hydrogen production by steam reforming of ethanol via response reactions, Int. J. Hydrogen Energy, 25(1), 31–45.

Garcia E.Y., Laborde M.A., 1991, Hydrogen production by the steam reforming of ethanol thermodynamic analysis, Int. J.Hydrogen Energy, 16(5), 307–312.

Goransson K., Soderlind U., He J., Zhang W., 2010, Review of syngas production via biomass DFBGs, Renewable Sustainable Energy Rev., Accepted Article in press, doi:10.1016/j.rser.2010.09.032.

Haryanto A., Fernando S., Murali N., Adhikari S., 2005, Current status of hydrogen production techniques by steam reforming of ethanol: a review, Energy Fuels, 19(5), 2098–2106.

HSC Chemistry [software], Version 5.1, 2002, Pori: Outokumpu Research Oy,.

Jankhah S., Abatzoglou N., 2008, Thermal and catalytic dry reforming and cracking of ethanol for hydrogen and carbon nanofilaments production, Int. J. Hydrogen Energy, 33(18), 4769–4779.

Kale G.R., Kulkarni B.D., 2010, Thermodynamic analysis of dry autothermal reforming of glycerol, Fuel Process. Technol., 91, 520–530.

Kale G.R., Kulkarni B.D., Joshi A.R., 2010, Thermodynamic study of combining chemical looping combustion and combined reforming of propane, Fuel, 89, 3141–3146.

Liu S., Zhang K., Fang L., Li Y., 2008, Thermodynamic analysis of hydrogen production from oxidative steam reforming of ethanol, Energy Fuels, 22(2), 1365–1370.

Markova D., Bazbauers G., Valters K., Arias R.A., Weuffen C., Rochlitz, L., 2009, Optimization of bio-ethanol autothermal reforming and carbon monoxide removal processes, J. Power Sources, 193(1) (Special Issue)), 9–16.

Mathure P.V., Ganguly S., Patwardhan A.V., Saha R.K., 2007, Steam reforming of ethanol using a commercial nickel-based catalyst, Ind. Eng. Chem. Res., 46, 8471–8479.

Ni M., Leung D.Y.C., Leung M.K.H., 2007, A reviews on reforming bio-ethanol for hydrogen production, Int. J. Hydrogen Energy, 32(15), 3238–3247.

Sahoo D.R., Vajpai S., Patel S., Pant K.K., 2007, Kinetic modeling of steam reforming of ethanol for the production of hydrogen over Co/Al_2O_3 catalyst, Chem. Eng. J., 125(3), 139–147.

Sasaki K., Fujii T., Niibori Y., Ito T., Hashida T., 2008, Numerical simulation of supercritical CO_2 injection into sub surface rock masses, Energy Convers. Manag., 49(1), 54–61.

Smith C.H., Leahey D.M., Miller L.E., Ellzey J.L., 2010, Conversion of wet ethanol to syngas via filtration combustion: an experimental and computational investigation, Proc. Combust. Inst., Accepted Article in press, doi:10.1016/j.proci.2010.06.006.

Vaidya P.D., Rodrigues A.E., 2006, Insight in to steam reforming of ethanol to produce hydrogen for fuel cells, Chem. Eng. J., 117(1), 39–49.

Vaidya P.D., Rodrigues A.E., 2006, Kinetics of steam reforming of ethanol over a Ru/Al_2O_3 catalyst, Ind. Eng. Chem. Res., 45(19), 6614–6618.

Vasudeva K., Mitra N., Umasankar P., Dhingra S.C., 1996, Steam reforming of ethanol for hydrogen production: thermodynamic analysis, Int. J. Hydrogen Energy, 21(1), 13–18.

Wang W.J., Wang Y.Q., 2009, Dry reforming of ethanol for hydrogen production: thermodynamic investigation, Int. J. Hydrogen Energy, 34(13), 5382–5389.

Wilhelm D.J., Simbeck D.R., Karp A.D., Dickenson R.L., 2001, Syngas production for gas-to-liquids applications: technologies, issues and outlook, Fuel Process Technol., 71(1), 139–148.

Xie X., Economides M.J., 2009, The impact of carbon geological sequestration, J. Nat. Gas. Sci. Eng., 1(3), 103–111.

Youn M.H., Seo J.G., Kim P., Kim J.J., Lee H.I., Song I.K., 2006, Hydrogen production by auto-thermal reforming of ethanol over Ni/-gamma-Al_2O_3

catalysts: effect of second metal addition, J. Power Sources, 162(2), 1270–1274.

Zhang W., 2010, Automotive fuels from biomass via gasification, Gasification: Fundamentals and application, Fuel Process. Technol., 91(8), 866–876.

Chapter 4

Application of DATR in gasoline fuel processors

CHAPTER 4: Application of DATR in gasoline fuel processors

Abstract

The chapter explores the thermodynamics of an alternate syngas generation process – dry autothermal reforming and its comparison to autothermal reforming process of isooctane for use in gasoline fuel processors for SOFC. A thermodynamic analysis of iso-octane as feed hydrocarbon for dry autothermal reforming and autothermal reforming processes for feed OCIR (oxygen to carbon in isooctane ratio) from 0.5 – 0.7 at 1 bar pressure under analogous thermoneutral operating conditions was done using Gibbs free energy minimization algorithm in HSC Chemistry. The trends in thermoneutral points (TNP), important product gas compositions at TNPs and fuel processor energy requirements were compared and analyzed. Dry autothermal reforming was identified as a less energy consuming alternative to autothermal reforming as the syngas can be produced with lower energy requirements at thermoneutral temperatures, making it a promising candidate for use in gasoline fuel processors to power the solid oxide fuel cells.

CHAPTER 4: Application of DATR in gasoline fuel processors

4.1 Fuel processors and Gasoline

Hydrogen energy and fuel cells are considered to be the future energy sources. Syngas production using hydrocarbon reforming has been a popular research area for more than three decades. Various hydrocarbon fuels have been evaluated for their capacity to fulfill the requirements of fuel processor system. Natural gas, LPG and gasoline are commercially available fuels that have an established infrastructure for production and distribution worldwide. Liquid fuels like gasoline have high energy density and are the most favorable choice for fuel processors (FP) as reported in literature. Brian et. al. (2007) have reported the development of compact sized powerful onboard fuel processor operating on fuels like gasoline and having hydrogen efficiencies above 77% for vehicular use. Studies related to start up strategies and performance of gasoline fuel processors have also been published (Semelsberger and Borup, 2005; Ahmed et. al., 2006). Minutillo et. al. (2005) have formulated a numerical model of a partial oxidation based reforming system and tested it with the experimental data of a plasma-assisted reformer for different fuels including gasoline for onboard hydrogen production. Sobacchi et. al. (2002) have reported the experimentation studies of a combined reforming system of gasoline-like fuels that includes both auto-thermal catalytic and non-equilibrium plasma units. Thomas et al. (2000) have discussed the economic option amongst hydrogen storage and onboard gasoline reforming for fuel cell vehicles. Boehme et al. (2008) have discussed a one-dimensional, single channel monolith model of a 4kW gasoline autothermal reformer that can successfully predict the dynamics of the fuel processor. Otsuka et al. (2002) have reported catalytic thermal decomposition of gasoline ranged alkanes to pure hydrogen and carbon for use in SOFC. Bobrova et al. (2007) have presented the study of hydrogen generation by selective catalytic oxidation of gasoline mixture containing 191 hydrocarbon species in a nearly adiabatic reactor using monolith catalysts. Research has

also been done with relation to activity of catalyst and their performance (Kaila and Krause, 2006; Kaila et. al, 2008; Qi et. al., 2007). The USDOE's 2006 no-go decision for onboard fuel processing programs has not stalled research interests in this area and scientists are constantly researching newer techniques. Rollier et. al. (2008a, 2008b) have reported work on cold plasma gasoline reforming as a better option than conventional catalytic gasoline reforming in an on-board fuel processor. Some researchers (Rabe et al., 2009) have reported the problems related to catalyst deactivation and subsequent coking due to sulfur presence in gasoline. These pose hindrance for gasoline use in research studies. Hence, iso-octane (2, 2, 4-trimethyl pentane), pure compound resembling gasoline, is used in research studies instead of gasoline. The potential of gasoline/iso-octane for hydrogen production using established process technologies like partial oxidation, steam reforming and autothermal reforming have been studied in detail by researchers.

A typical gasoline based power system consists of an ATR fuel processor and PEMFC fuel cell. These (PEMFC type) fuel cells require very low CO in feed gas, which makes WGS (Water Gas Shift) reactors compulsory in fuel processors. WGS reaction is reversible and slow, making the WGS reactor size huge and bulky. Electrochemically both H_2 and CO are fuels for SOFC of the same caliber. There are some problems for CO electrochemical oxidation due to its slower rate than H_2 oxidation in SOFC. However research in this area is in progress and that may solve it in near future. Some publications have indicated that the CO is converted to H_2 by in situ WGS reaction. External WGS reactor require a huge amount of steam (for higher Steam/CO ratio ~4) to convert CO to hydrogen. In situ WGS in the SOFC will require only stoichiometric amount of steam (S/CO =1) as the in situ generated hydrogen is quickly utilized by the SOFC that acts similar to hydrogen separation membrane reactor shifting the WGS equilibrium to completely convert to H_2.

The SOFC type fuel cells were earlier considered ideal for stationary applications only, but present research to make them smaller in size (micro-SOFCs) has given PEMFC tough competition. They are also undergoing miniaturization and venturing in automobile applications. SOFC has the potential to replace PEMFC in small scale applications too. Although earlier studies have used only H_2 as fuel in SOFC, some recent studies have reported that CO can also be used as fuel for SOFC. Burnette et al. (2008) have suggested that SOFC can operate successfully using hydrogen depleted syngas as feed. Homel et al. (2010) have explored the possibility of using CO as a primary fuel in SOFC of both tubular and planar geometries and reported that CO is a viable primary fuel for SOFCs. Ye et al. (2010) have reported that optimized anode composition of SOFC could make it run successfully on syngas for 1050hrs. Lawrence et al. (2006) have successfully operated the SOFC using the syngas generated by a dry catalytic partial oxidation diesel reformer. Cheekatamarla et al. (2008) have reported the successful operation of an anode catalytic modified SOFC using the syngas without coking and yielding stable power output. Colpan et al. (2007) have reported the thermodynamic modeling of direct internal reforming solid oxide fuel cells operating with syngas produced by gasification and model validation using literature data. Eduardo et al. (2005) have reported the development of an integrated model (electrochemical-thermal) to analyze the performance of SOFC with respect to different syngas feed compositions.

In such conditions, the possibility of SOFC using CO and H_2 both as equivalent fuels in near future cannot be ruled out and the fuel processor may be limited to only ATR for syngas generation. The WGS section may not be required. This can reduce the WGS requirements in ATR gasoline fuel processors. However, steam is still required for gasoline FP, which is energy intensive. In these circumstances, energy inputs of ATR will play a vital role for defining efficiency of the fuel processor system. Syngas can also be

generated by dry autothermal reforming (DATR) process and operating the DATR/ATR at thermoneutral points, the energy required for heating the feed CO_2 is much less than required for producing feed steam for the fuel processor. The important product gas distribution at thermoneutral points (TNP) in DATR and ATR processes as well as energy requirements of the processes for use in gasoline fuel processor system have been compared in this chapter.

Dry autothermal reforming (DATR) is a combination of dry reforming and partial oxidation and it uses CO_2 instead of steam in feed to produce syngas from hydrocarbons. However, till date DATR is not considered for fuel processor application and hence is studied in this chapter. The CO_2 availability as dry ice is very well known. New technologies like chemical looping combustion (CLC) produce pure CO_2 stream that can be compressed and used in this application.

4.2 Methodology

A thermodynamic study of ATR and DATR of iso-octane was done using Gibbs free energy minimization algorithm in HSC Chemistry 5.1 software package using 1 mole of iso-octane as feed for OCIR (feed oxygen to carbon in iso-octane ratio) of 0.5, 0.6 and 0.7 at 1 bar pressure. For ATR, the SCIR (feed steam to carbon in iso-octane ratio) was varied from 1 to 3 and for DATR the CCIR (feed CO_2 to carbon in iso-octane ratio) was varied from 1 to 3. Only realistic process conditions were chosen for this study. The process enthalpy, thermoneutral points and important product gas distribution at TNP for both processes including syngas, CO, water and carbon obtained at TNPs are analyzed and discussed. HSC Chemistry software requires quantities of input species (iso-octane, H_2O or CO_2, O_2, N_2 (all in gaseous phase)), desired output species, temperature and pressure conditions. The desired output

species fed to the program were H_2, CO, CO_2, CH_4 (all in gaseous phase), H_2O (gas & liquid phase), iso-octane (gaseous phase) and C (solid phase). Complete conversion of iso-octane and oxygen was observed in all cases. No other product species or inerts have been considered in this study. The energy balance calculations for feed gases have been performed manually using standard data.

4.3 Results and Discussion

4.3.1 Process enthalpy

Reaction enthalpy is always a deciding factor in chemical processes. Figure. 4.1a and 4.1b show the variation of enthalpy of ATR and DATR of isooctane processes with a change in OCIR, SCIR and CCIR along the process temperature. It was observed that the process exothermicity increased with increase in OCIR at constant SCIR (for ATR) and also at constant CCIR (for DATR).

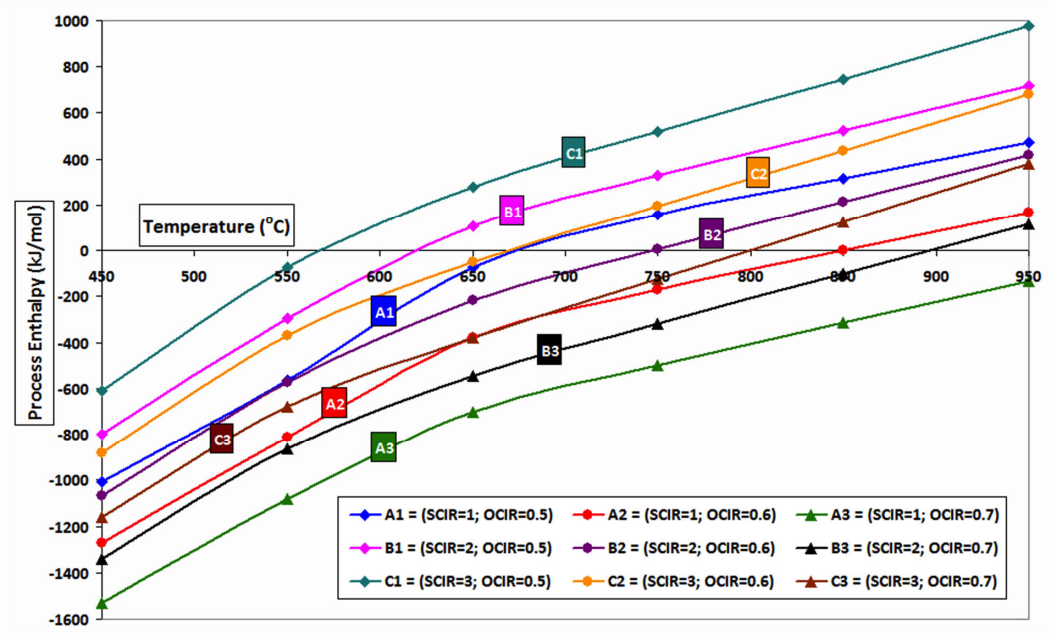

Figure 4.1a: Process enthalpy for ATR of Iso-octane

Thermoneutral temperature for ATR and DATR of iso-octane (°C)			
ATR	**SCIR=1**	**SCIR=2**	**SCIR=3**
OCIR=0.5	673.66	614.82	565.92
OCIR=0.6	849.52	748.00	669.70
OCIR=0.7	1024.45	896.13	799.70
DATR	**CCIR=1**	**CCIR=2**	**CCIR=3**
OCIR=0.5	637.51	592.01	559.63
OCIR=0.6	716.74	609.35	578.35
OCIR=0.7	900.43	735.68	632.22

Table 4.1: Thermo neutral points for ATR and DATR

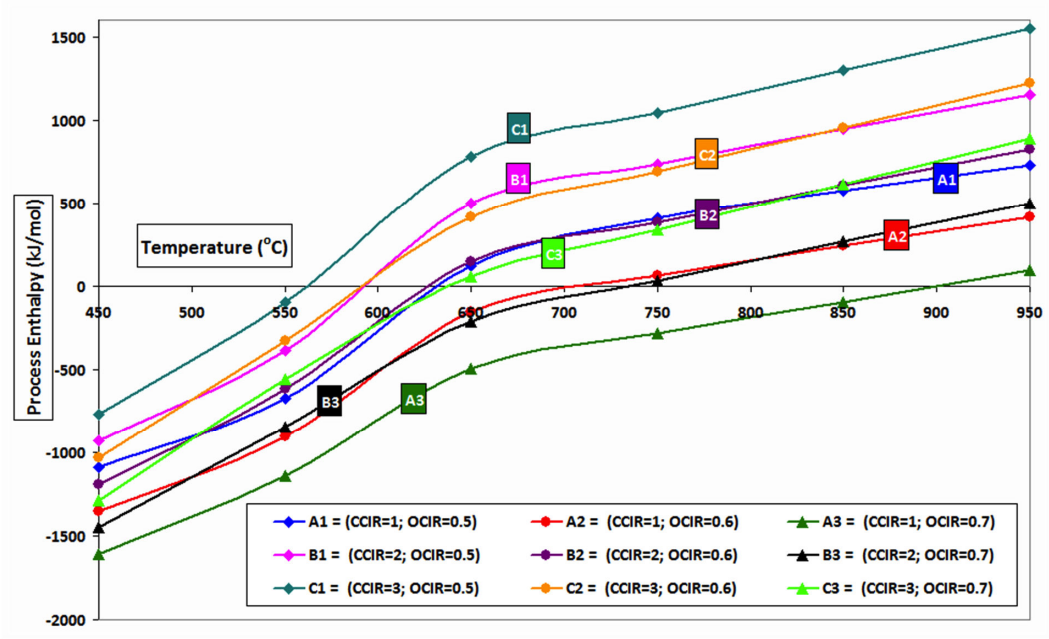

Figure 4.1b: Process enthalpy for DATR of Iso-octane

It was also observed that the reaction endothermicity increased with increase in SCIR (for ATR) from 1 to 3, at constant OCIR, and also showed a decrease in thermo neutral temperatures. A similar trend was observed in case of DATR of isooctane for analogous increase in CCIR from 1 to 3 at constant

OCIR. The ATR reaction enthalpy per mole of isooctane fed at 700°C for an increase in SCIR from 1 to 3, increased from 62.8 to 400 kJ (for OCIR=0.5), increased from -263 to 74.5 kJ (for OCIR=0.6) and increased from -594 to -251 kJ (for OCIR=0.7). The ATR reaction enthalpy per mole isooctane fed at 700°C for an increase in OCIR from 0.5 to 0.7, decreased for constant SCIR as shown in figure 1a, The DATR reaction enthalpy per mole of isooctane fed at 700 ºC for an increase in CCIR from 1 to 3, increased from 314 to 915 kJ (for OCIR=0.5), increased from -33 to 556 kJ (for OCIR=0.6) and increases from -383 to 197 kJ (for OCIR=0.7). The DATR reaction enthalpy per mole of isooctane fed at 700°C for an increase in OCIR from 0.5 to 0.7, decreased for constant CCIR as shown in figure 1b. Similar trend in reaction enthalpy of ATR and DATR was noted for all the temperatures considered.

4.3.2 Thermo neutral points

Thermo neutral operation of ATR and DATR of isooctane requires no external energy for cooling or heating, which makes it valuable from energy consumption point of view. The intersection of reaction enthalpy curves with temperature axis shows the thermo neutral temperatures (figures 4.1a and 4.1b). The thermo neutral temperatures for the study conditions are shown in table 4.1. Figure 4.2 shows the variation of thermo neutral points along OCIR for various SCIR (for ATR) and CCIR (for DATR). It was observed that the thermo neutral temperatures increased with increase in OCIR at constant SCIR (for ATR) and at constant CCIR (for DATR). The ATR thermo neutral temperature for an increase in OCIR from 0.5 to 0.7 increased for constant SCIR as shown in figure 2. The DATR thermo neutral temperature for an increase in OCIR from 0.5 to 0.7 increased for constant CCIR as shown in figure 4.2. But the thermoneutral temperatures decreased with increase in SCIR (for ATR) and also decreased with increase in CCIR (for DATR) for

constant OCIR. For an increase in SCIR from 1 to 3, the ATR thermo neutral temperature decreased from 673.66 °C to 565.92 °C (for OCIR = 0.5), decreased from 849.52 °C to 669.70 °C (for OCIR = 0.6) and decreases from 1024.45 °C to 799.70 °C (for OCIR = 0.7). The DATR thermo neutral temperature for an increase in CCIR from 1 to 3 decreased from 637.51 °C to 559.63 °C (for OCIR = 0.5), decreased from 716.74 °C to 578.35 °C (for OCIR = 0.6) and decreased from 900.43 °C to 632.22 °C (for OCIR = 0.7). Lower OCIR and higher SCIR (for ATR) gave lower thermo neutral point (temperatures) and vice versa. A similar trend was observed in case of DATR of isooctane for analogous cases. The thermo neutral temperatures for ATR ranged from a minimum of 565.92 °C (for OCIR=0.5, SCIR=3) to a maximum of 1024.45 °C (for OCIR=0.7, SCIR=1), while the thermo neutral temperatures for DATR ranged from a minimum of 559.63 °C (for OCIR=0.5, CCIR=3) to a maximum of 900.43 °C (for OCIR=0.7, CCIR=1).

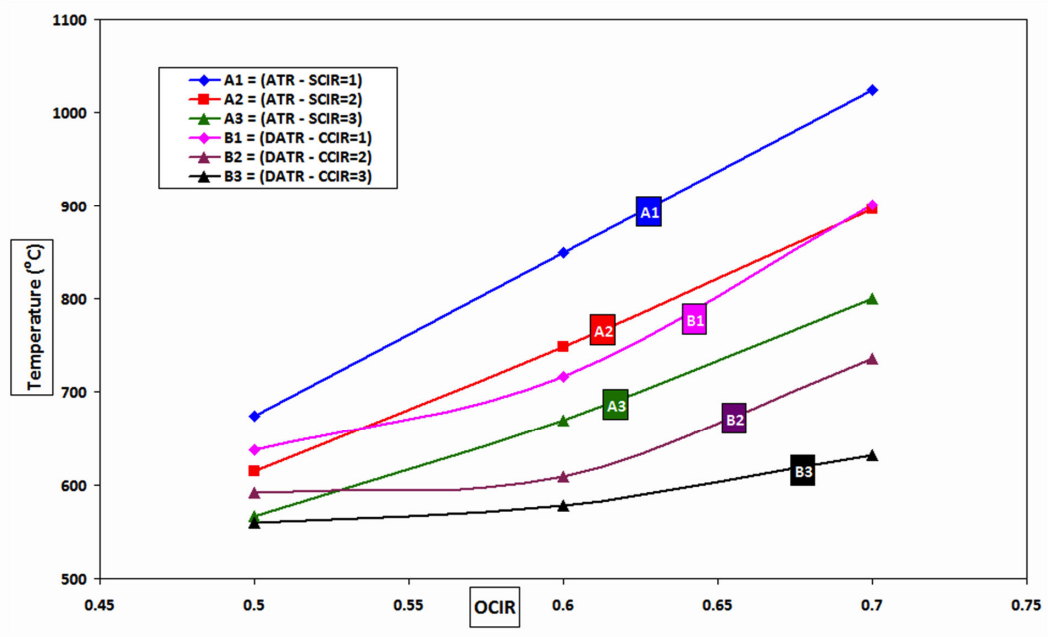

Figure 4.2: Thermoneutral temperatures for ATR and DATR of isooctane

The DATR TNPs were lower than the corresponding ATR TNPs at similar OCIR. The temperature difference between consecutive TNPs for ATR of isooctane for an increase in OCIR from 0.5 to 0.7 decreased gradually as SCIR increased from 1 to 3. The temperature difference between TNPs (for OCIR=0.5 & 0.6) for ATR of isooctane for an increase in SCIR from 1 to 3 decreased from 175.86 °C (for SCIR=1) to 133.18 °C (for SCIR=2) to 103.78 °C (for SCIR=3) and (for OCIR=0.6 & 0.7) it decreased from 174.93 °C (for SCIR=1) to 148.13 °C (for SCIR=2) to 130 °C (for SCIR=3). The temperature difference between TNPs for DATR of isooctane for an increase in OCIR from 0.5 to 0.7 at constant CCIR decreased gradually as CCIR increased from 1 to 2, but slightly increased for CCIR increase from 2 to 3 (for OCIR 0.5 & 0.6 only). The temperature difference between TNPs (for OCIR=0.5 & 0.6) for DATR of isooctane for an increase in CCIR from 1 to 3 decreased from 79.23 °C (for CCIR=1) to 17.33 °C (for CCIR=2) but increased slightly to 18.67°C (for CCIR=3) and (for OCIR=0.6 & 0.7) it decreased from 183.7 °C (for CCIR=1) to 126.33°C (for CCIR=2) to 53.87°C (for CCIR=3). The temperature difference between TNPs for ATR of iso-octane for an increase in SCIR from 1 to 3 increased gradually as OCIR increased from 0.5 to 0.7. The temperature difference between TNPs (for SCIR=1 & 2) for ATR of isooctane for an increase in OCIR from 0.5 to 0.7 increased from 58.84 °C (for OCIR=0.5) to 101.52°C (for OCIR=0.6) to 128.32°C (for OCIR=0.7) and (for SCIR=2 & 3) it increased from 48.9 °C (for OCIR=0.5) to 78.3 °C (for OCIR=0.6) to 96.43 °C (for OCIR=0.7). The temperature difference between TNPs for DATR of iso-octane for an increase in CCIR from 1 to 3 increased gradually as OCIR was increased from 0.5 to 0.7 except for the case of temperature difference between TNP of CCIR=2 and CCIR=3 at OCIR=0.5 and OCIR=0.6 when temperature difference was almost same. The temperature difference between TNPs (for CCIR=1 & 2) for DATR of isooctane for an increase in OCIR from 0.5 to 0.7 increased from 45.5 °C (for OCIR=0.5) to 107.39 °C (for OCIR=0.6) to 164.76°C (for OCIR=0.7) and (for

CCIR=2 & 3) it decreased slightly from 32.38 °C (for OCIR=0.5) to 31°C (for OCIR=0.6) but again increased to 103.46 °C (for OCIR=0.7). It was noted that the temperature difference between TNPs for SCIR=1 & 2 was more than the temperature difference between TNPs for SCIR=2 & 3 for all cases of OCIR for ATR of isooctane. A similar trend was observed in case of DATR of isooctane too.

4.3.3 Total hydrogen

Total hydrogen is the moles of syngas obtained from a particular fuel. Total hydrogen potential is a good parameter to evaluate the quality of fuels for fuel processor applications. The amount of total hydrogen obtained for ATR and DATR of isooctane at thermo neutral points (TNP) at various SCIR and CCIR for OCIR increase from 0.5 to 0.7 is plotted in figure 4.3. It was found that the total hydrogen yield decreased for SCIR increase at constant OCIR (for ATR) and also decreased for CCIR increase at constant OCIR (for DATR). Also, it is observed that the total hydrogen production decreased with increase in OCIR for ATR but increased first and then decreased for DATR (for CCIR 1 and 2). The total hydrogen yield for ATR of isooctane at TNP was same as that obtained in DATR process for some cases. The moles of total hydrogen produced at TNP, for ATR, for SCIR increase from 1 to 3, decreased from 16.31 to 15.13 (7.23%, for OCIR = 0.5), negligibly decreased from 15.37 to 15.35 (0.13%, for OCIR = 0.6) and negligibly increased from 13.80 to 13.81 (0.0724%, for OCIR = 0.7), while for DATR, the moles of total hydrogen produced at TNP, for CCIR increase from 1 to 3, decreased from 13.88 to 9.71 (30.04%, for OCIR = 0.5), 15.32 to 12.35 (19.38%, for OCIR = 0.6) and 13.80 to 13.69 (0.797%, for OCIR = 0.7). The moles of total hydrogen produced at TNP, for ATR, for OCIR increase from 0.5 to 0.7 decreased at constant SCIR as shown in figure 4.3, while for DATR, for OCIR increase from

0.5 to 0.7, the moles of total hydrogen produced at TNP, initially increased and then decreased for CCIR = 1, 2 and increased continuously for CCIR = 3. The maximum total hydrogen yield for ATR of isooctane at TNP was found to be 16.31 moles (for SCIR = 1, OCIR = 0.5) while the maximum total hydrogen yield for DATR at TNP was 15.32 moles (CCIR = 1, OCIR = 0.6). The minimum total hydrogen yield for ATR at TNP was 13.80 moles (SCIR = 1, OCIR = 0.7) and 9.71 moles (CCIR = 3, OCIR = 0.5) for DATR. The minimum total hydrogen yield at TNP of isooctane was 15.39% less than the maximum for ATR and 36.61% less for DATR. Lower OCIR and lower SCIR increased the total hydrogen yield in ATR while medium OCIR and lower CCIR increased the total hydrogen yield in DATR.

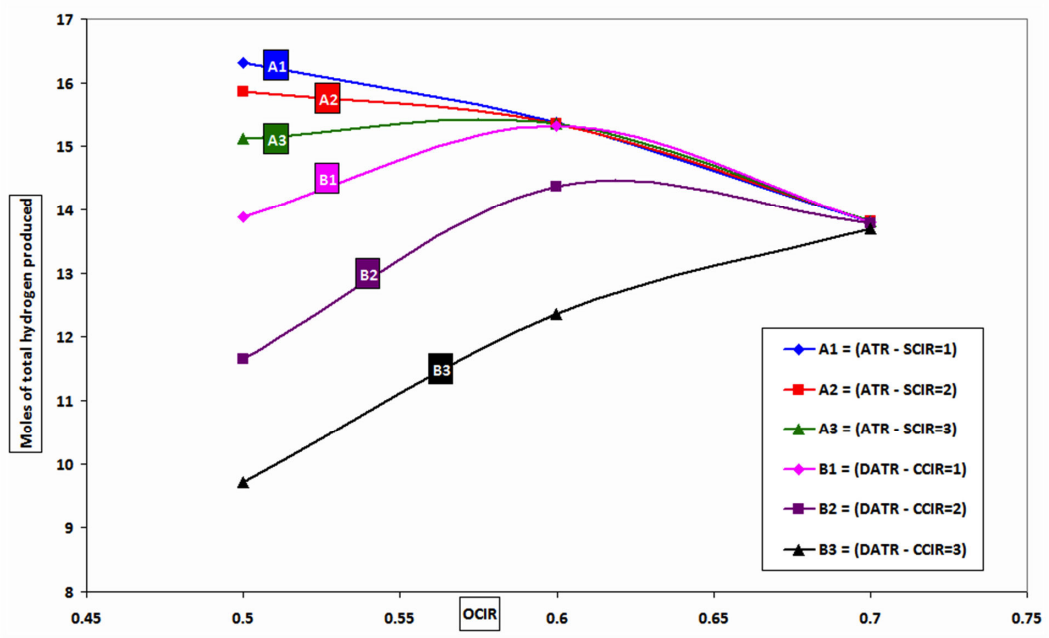

Figure 4.3: Total Hydrogen for ATR and DATR of isooctane

4.3.4 CO yield

Carbon monoxide is a poison for PEMFC. However, it is a fuel for the SOFC and hence is very much desired. The number of moles of carbon monoxide produced at TNP for ATR and DATR of isooctane, for OCIR of 0.5, 0.6 and 0.7 were calculated for SCIR and CCIR of 1, 2 and 3 respectively. These observations are plotted in figure 4.4. With increase in OCIR at constant CCIR (for DATR), the CO yield generally increased, except for CCIR =1, where it increased and then decreased slightly. For DATR, at constant OCIR, the CO yield generally decreased with increase in CCIR. The same trend was observed in ATR, for the corresponding SCIR increase but without any exceptions. The moles of CO produced at TNP for ATR for SCIR increase from 1 to 3 decreased from 4.51 to 1.43 (68.3%, for OCIR = 0.5), 5.07 to 2.15 (57.6%, for OCIR 0.6) and 5.19 to 2.61 (49.71%, for OCIR = 0.7) while for DATR, the moles of CO produced at TNP, decreased from 7.86 to 5.8 (26.2%, for OCIR = 0.5), 9.30 to 7.97 (14.3%, for OCIR = 0.6) but then increased from 9.21 to 9.54 (3.5%, for OCIR = 0.7), then decreased to 9.42 (1.25% , for OCIR = 0.7) for CCIR increase from 1 to 3. The moles of CO produced at TNP, for ATR, for OCIR increase from 0.5 to 0.7, increased for constant SCIR as shown in figure 4.4, while for DATR, for OCIR increase from 0.5 to 0.7, the moles of CO produced at TNP, initially increased and then decreased for CCIR = 1 whereas for CCIR = 2, 3 it increased as shown in figure 4.4. The maximum CO yield for ATR of isooctane at TNP was found to be 5.19 moles (for SCIR = 1, OCIR = 0.7) while the maximum CO yield for DATR of isooctane at TNP was 9.54 moles (CCIR = 2, OCIR = 0.7). The minimum CO yield for ATR at TNP was 1.43 moles (SCIR = 3, OCIR = 0.5) and 5.80 moles (CCIR = 3, OCIR = 0.5) for DATR. The minimum CO yield at TNP of isooctane was 72.44% less than the maximum for ATR and 39.2% less for DATR.

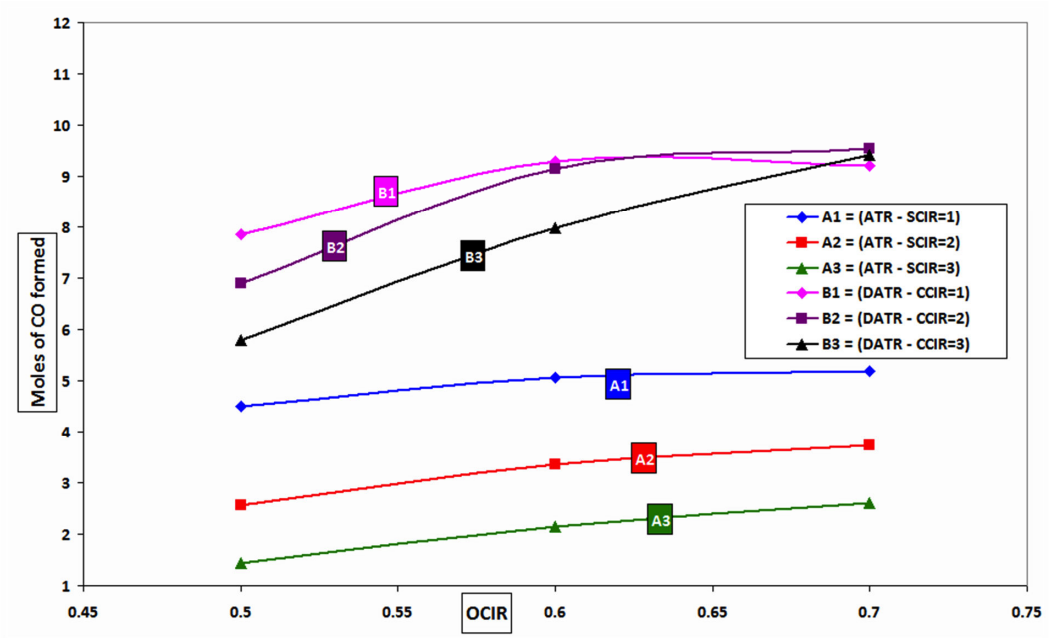

Figure 4.4: CO formation for ATR and DATR of isooctane

4.3.5 Water formation

Water formation is the loss of hydrogen moles but is sometimes required for internal WGS in the SOFC; hence monitoring the water formation in reforming process is an important issue. The H_2O moles in the product gas of ATR and DATR was calculated at TNPs at various SCIR and CCIR conditions for OCIR increase from 0.5 to 0.7 and was plotted in figure 4.5. It was observed that the water in the product stream increased with SCIR (for ATR) and CCIR (for DATR) increase from 1 to 3 for constant OCIR. Also, it is observed that water formation increased with increase in OCIR from 0.5 to 0.7 at constant SCIR (for ATR) and first decreased negligibly for increase in OCIR from 0.5 to 0.6 but again increased with OCIR increase from 0.6 to 0.7 at constant CCIR (for DATR). The moles of water formed at TNP for ATR, for SCIR increase from 1 to 3, increased from 4.86 to 18.3 moles (for OCIR = 0.5), from 6.67 to 19.80

moles (for OCIR = 0.6) and 8.39 to 21.8 (for OCIR = 0.7), while for DATR, for CCIR increase from 1 to 3, the moles of water generated increased from 2.45 to 4.61 moles (88.2% for OCIR = 0.5), from 2.94 to 4.20 moles (42.8% for OCIR = 0.6) and from 4.41 to 4.67 moles (5.89% for OCIR = 0.7) . The water generated at TNP for ATR, for OCIR increase from 0.5 to 0.7, increased for constant SCIR as shown in figure 5. For DATR, the amount of water formed, for an OCIR increase from 0.5 to 0.7, increased continuously for CCIR = 1, but increased initially and later decreased for CCIR = 2 and 3 as shown in figure 4.5.

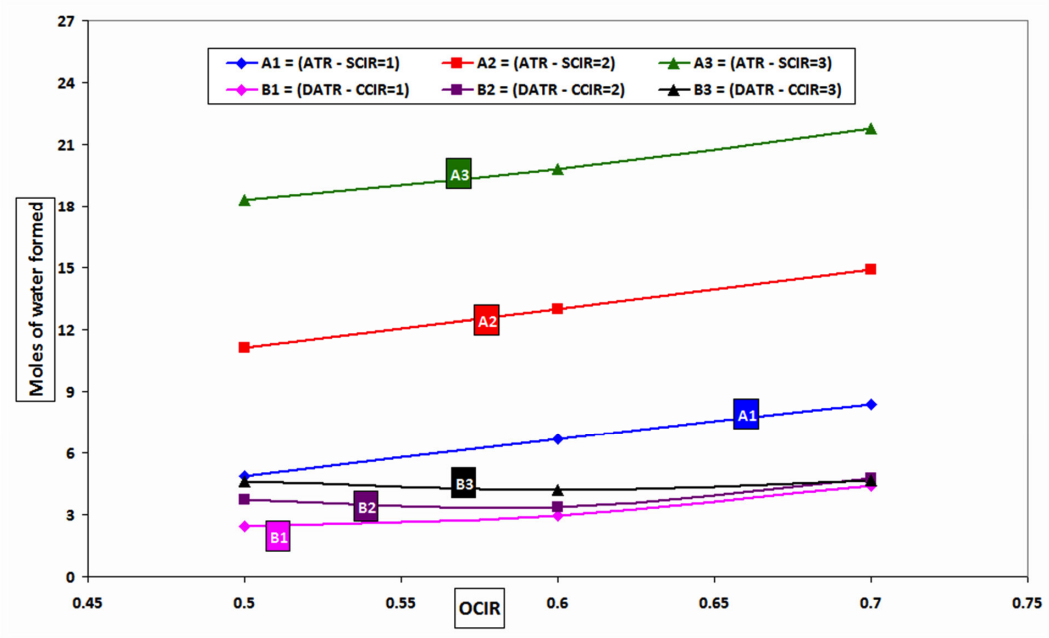

Figure 4.5: Water formation for ATR and DATR of isooctane

The maximum water in the product stream of ATR at TNP was found to be 21.8 moles (for SCIR = 3, OCIR = 0.7) and 4.75 moles (for CCIR = 2, OCIR = 0.7) for DATR. The minimum water observed in the product stream of ATR of isooctane at TNP was 4.86 moles (SCIR = 1, OCIR = 0.5) while the minimum

of 2.45 moles (for CCIR = 1, OCIR = 0.5) of water was formed for DATR. The minimum water formation at TNP of isooctane was 77.70% less than the maximum for ATR and 48.42% less than the maximum for DATR. Since water is a feed component of ATR, higher OCIR and higher SCIR increased the water in the product stream of ATR, while lower OCIR and lower CCIR decreased the water formation in DATR.

4.3.6 Carbon formation

Carbon formation or coking is undesired in fuel processors as it deactivates the catalyst and increases pressure drop of reactors. Figure 4.6 shows the carbon deposition in ATR and DATR of isooctane at thermo neutral point temperatures for OCIR of 0.5, 0.6 and 0.7 at SCIR and CCIR of 1, 2 and 3. The moles of carbon formed were higher in DATR process as compared to ATR of isooctane at TNP. No carbon formation was seen in ATR of isooctane at TNP while a small amount of carbon formation was observed in the product stream of DATR of isooctane at some thermo neutral points. The moles of carbon produced at TNP for ATR remained zero for SCIR increase from 1 to 3 (for OCIR = 0.5, 0.6 and 0.7), while for DATR, the moles of carbon produced at TNP, for CCIR increase from 1 to 3, increased from 1.03 to 3.16 (for OCIR = 0.5), 0 to 1.11 (for OCIR = 0.6) and remained zero (for OCIR = 0.7). The moles of carbon produced at TNP, for ATR, for OCIR increase from 0.5 to 0.7, remained zero (for SCIR= 1, 2 and 3) while for DATR, for OCIR increase from 0.5 to 0.7, the moles of carbon produced at TNP, decreased to 0 for constant CCIR as shown in fig 4.6. The maximum carbon yield for DATR of isooctane at TNP was 3.16 moles (for CCIR = 3, OCIR = 0.5), while the minimum carbon yield for DATR at TNP was zero (for CCIR = 3, OCIR = 0.7; CCIR=1, OCIR=0.6 and 0.7; and CCIR=2, OCIR=0.7). The carbon yield for ATR of isooctane at TNP was found to be zero (for all SCIR and OCIR values).

Higher OCIR and lower CCIR conditions decreased the carbon formation in DATR.

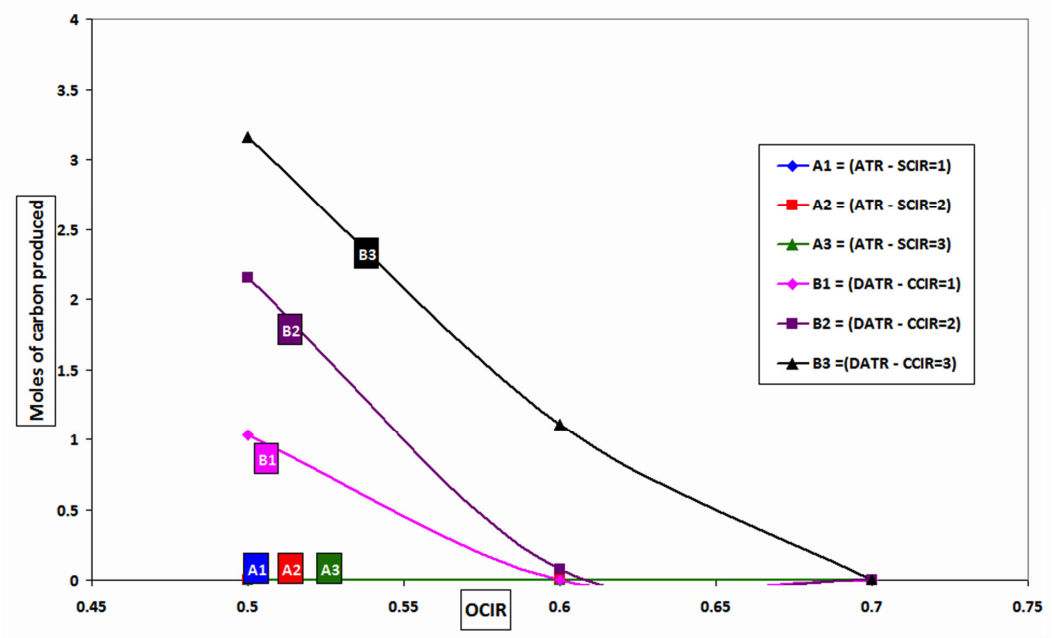

Figure 4.6: Carbon formation for ATR and DATR of isooctane

4.3.7 Process energy calculations

Thermo neutral operation of ATR and DATR of isooctane requires no external energy. But energy is required for heating the feed to the reaction temperature. Since the SOFC operates at high temperatures, the hot gases from the fuel processor can be directly fed to the SOFC. Energy calculations were done to compare the energy requirements of the gasoline fuel processor using ATR and DATR processes. The common feed components like iso-octane (1 mol) and air or oxygen (for OCIR cases) for ATR and DATR were the same; hence they were not considered in the comparison. The energy required for heating the feed components like CO_2 (for DATR) and H_2O (for

ATR) to thermoneutral temperatures were calculated, for producing 1 mole syngas. The following cases were considered:

a) Heating feed CO_2 in DATR (for CCIR 1, 2 and 3) to thermoneutral temperature.

b) Heating feed H_2O in ATR (for SCIR 1, 2 and 3) to thermoneutral temperature.

c) Case a) plus Heat required for extra steam to make S/CO=1.1 of DATR product gas.

Some publications have reported that the CO in feed of SOFC undergoes internal WGS to produce hydrogen that actually contributes to energy generation. ATR product gas has water to make S/CO=1, so there is no need to add more steam, but the S/CO ratio of DATR product gas is less than 1, so additional steam is required to makeup the steam requirement. Energy requirements for producing 1 mole syngas for the three scenarios were plotted in figure 4.7. It was observed that the total energy increased with increase in OCIR at constant SCIR (for ATR) and also at constant CCIR (for DATR). It was also noted that the total process energy increases with increase in SCIR (for ATR) from 1 to 3, at constant OCIR. A similar trend was observed for DATR of isooctane for analogous increase in CCIR from 1 to 3 at constant OCIR.

The total energy required for ATR per mole of total hydrogen produced, for an increase in SCIR from 1 to 3, increased from 33.15 to 100.38 kJ (for OCIR=0.5), increased from 38.99 to 105.41 kJ (for OCIR=0.6) and increased from 47.88 to 126.51 kJ (for OCIR=0.7). The total energy required per mole of total hydrogen produced for ATR, for an increase in OCIR from 0.5 to 0.7, increased for constant SCIR as shown in figure 4.7. For DATR, the total energy required per mol of total hydrogen, for an increase in CCIR from 1 to

3, increased from 16.48 to 60.56 kJ (for OCIR=0.5), increased from 17.15 to 49.51 kJ (for OCIR=0.6) and increased from 24.92 to 49.64 kJ (for OCIR=0.7). Also, the total energy required per mole of total hydrogen, for an increase in OCIR from 0.5 to 0.7, increased for CCIR = 1, decreased and then increased for CCIR = 2, and decreased for CCIR = 3 as shown in figure in 4.7.

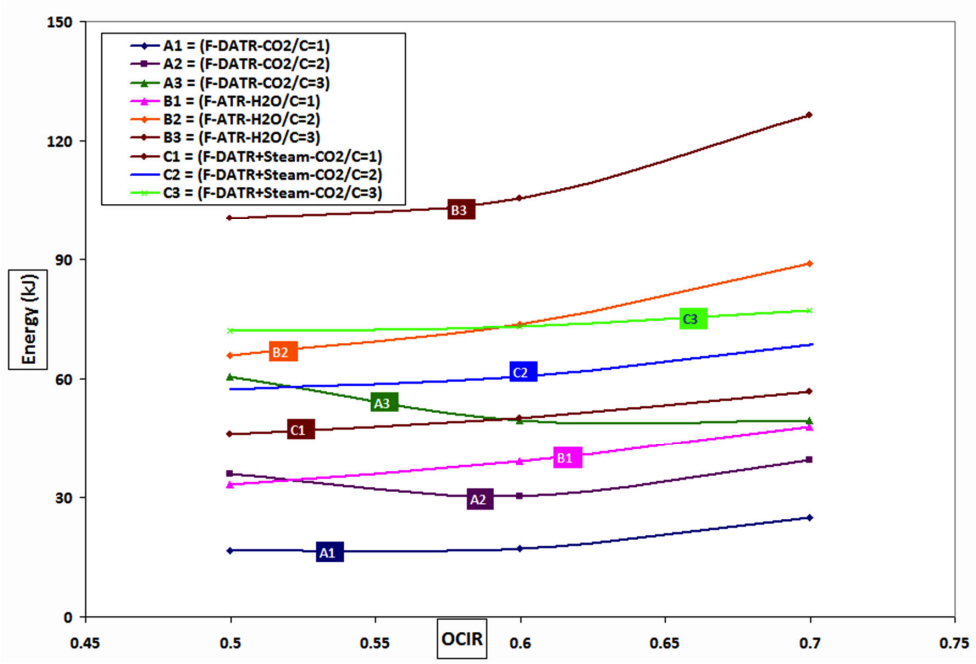

Figure 4.7: Energy comparison per mole syngas

Addition of steam (heated to respective thermoneutral temperature) to the DATR product stream to increase the product stream S/CO ratio to 1.1 (the 0.1 more than required 1.0 is for design calculations), showed increased energy requirement than the DATR process. However it was observed that the total energy required per mol of total hydrogen for DATR at S/CO=1.1 was still less as compared to that in ATR process for the ATR cases of SCIR 2 and 3 (ATR of isooctane is usually operated at higher S/C ratios) consumed more

energy than others. For DATR process with additional steam, the total energy required per mol of total hydrogen, for an increase in CCIR from 1 to 3, increased from 46.00 to 72.05 kJ (for OCIR=0.5), increased from 50.15 to 73.11 kJ (for OCIR=0.6) and increased from 56.88 to 77.04 kJ (for OCIR=0.7). Also, the total energy required per mole of total hydrogen, for an increase in OCIR from 0.5 to 0.7, increased for constant CCIR as shown in figure 4.7. It was observed that the energy requirements for DATR process were the lowest in all cases.

4.4 Conclusion

Auto thermal reforming of isooctane and dry autothermal reforming of isooctane process comparison was done at thermo neutral temperatures to analyze the total hydrogen production and energy requirements for selecting the best process. The process comparison was based on parameters like syngas obtained, carbon formation and total energy required for heating the process feed (neglecting the common feed components). Although the isooctane conversion was same for ATR as well as DATR, the amount of syngas produced varied a lot for different SCIR (for ATR) and CCIR (for DATR). At SCIR and CCIR 1 (for OCIR = 0.6 and 0.7), at SCIR and CCIR 2 (for OCIR = 0.7) and at SCIR and CCIR 3 (for OCIR = 0.7) the moles of total hydrogen produced were almost same at thermoneutral points. Carbon formation in DATR was almost zero at CCIR 1 (OCIR =0.6 & 0.7), CCIR 2 & 3 (OCIR =0.7). Hence these points can be chosen as suitable operating conditions. A quick comparison for the energy requirements of the processes showed that the process energy required per mol of total hydrogen was considerably less for DATR as compared to the ATR process and large amount of extra heat was needed for ATR of isooctane to produce same moles of total hydrogen. Hence DATR process can be used at thermoneutral points for syngas generation as feed to the SOFC to give considerable energy

savings. Experimentation is required to compare the results obtained in this study. Further study of using DATR of isooctane to generate syngas at thermoneutral temperatures and spraying water in the product stream to cool it to room temperature in stagewise WGS reactors to make the process suitable for PEMFC can also be explored.

4.5 References

Ahmed S., Ahluwalia R., Lee S.H.D., Lottes S., 2006, A gasoline fuel processor designed to study quick-start performance, Journal of Power Sources, 154(1), 214-222.

Ashcroft A.T., Cheetham A.K., Green M.L.H., Vernon P.D.F., 1991, Partial oxidation of methane to synthesis gas using carbon dioxide, Nature (London, UK), 352(6332), 225-226.

Bowers B.J., Zhao J.L., Ruffo M., Khan R., Dattatraya D., Dushman N., 2007, Onboard fuel processor for PEM fuel cell vehicles, International Journal of Hydrogen Energy, 32(10-11), 1437-1442.

Bobrova L., Zolotarsky I., Sadykov V., Sobyanin V., 2007, Hydrogen rich gas production from gasoline in a short contact time catalytic reactor, International Journal of Hydrogen Energy, 32(16), 3698-3704.

Boehme T.R., Onder C.H., Guzzella L., 2008, Dynamic model of an auto-thermal gasoline fuel processor, International Journal of Hydrogen Energy, 33(21), 6150-6164.

Burnette D.D., Kremer G.G., Bayless D.J., 2008, The use of hydrogen depleted coal syngas in solid oxide fuel cells, Journal of Power Sources, 182(1), 329-333.

Cheekatamarla P.K., Finnerty C.M., Cai J., 2008, Internal reforming of hydrocarbon fuels in tubular solid oxide fuel cells, International Journal of Hydrogen Energy, 33(7), 1853-1858.

Colpan C.O., Dincer I., Hamdullahpur F., 2007, Thermodynamic modeling of direct internal reforming solid oxide fuel cells operating with syngas, International Journal of Hydrogen Energy, 32(7), 787-795.

Horng R., Huang H., Lai M., Wen C., Chiu W., 2008, Characteristics of hydrogen production by a plasma-catalyst hybrid converter with energy saving schemes under atmospheric pressure, International Journal of Hydrogen Energy, 33(14), 3719-3727.

Homel M., Gur T.M., Koh J.H., Virkar A.V., 2010, Carbon monoxide fueled solid oxide fuel cell, Journal of Power Sources, 195(19), 6367-6372.

HSC Chemistry [software], version 5.1., 2002, Pori: Outokumpu Research Oy,.

Kaila R.K., Krause A.O.I., 2006, Autothermal reforming of simulated gasoline and diesel fuels, International Journal of Hydrogen Energy, 31(13), 1934-1941.

Kaila R.K., Gutiérrez A., Slioor R., Kemell M., Leskela M., Krause A.O.I., 2008, Zirconia-supported bimetallic RhPt catalysts: characterization and testing in autothermal reforming of simulated gasoline, Applied Catalysis B, 84(1-2), 223-232.

Kale G.R., Kulkarni B.D., 2010, Thermodynamic analysis of dry autothermal reforming of glycerol, Fuel Processing Technology, 91, 520-530.

Lawrence J., Boltze M., 2006, Auxiliary power unit based on a solid oxide fuel cell and fuelled with diesel, Journal of Power Sources, 154(2), 479-488.

Minutillo M., 2005, On-board fuel processor modeling for hydrogen-enriched gasoline fuelled engine, International Journal of Hydrogen Energy, 30(13-14), 1483-1490.

Otsuka K., Shigeta Y., Takenaka S., 2002, Production of hydrogen from gasoline range alkanes with reduced CO_2 emission, International Journal of Hydrogen Energy, 27(1), 11-18.

Pacheco E.H., Mann M.D., Hutton P.N., Singh D., Martin K.E., 2005, A cell level model for a solid oxide fuel cell operated with syngas from a gasification process, International Journal of Hydrogen Energy, 30(11), 1221-1233.

Puolakka K.J., Krause A.O.I., 2004, CO_2 reforming of n-heptane on a Ni/Al_2O_3 catalyst, Studies in Surface Science and Catalysis, 153, 329-332.

Puolakka K.J., Juutilainen S., Krause A.O.I., 2006, Combined CO_2 reforming and partial oxidation of n-heptane on noble metal zirconia catalysts, Catalysis Today, 115(1-4), 217-221.

Perry R.H., Green D.W., 1997, Chemical engineers' handbook, 7th ed. USA: McGraw-Hill.

Qi A., Wang S., Ni C., Wu D., 2007, Autothermal reforming of gasoline on Rh-based monolithic catalysts, International Journal of Hydrogen Energy, 32(8), 981-991.

Rollier J.D., Petitpas G., Gonzalez-Aguilar J., Darmon A., Fulcheri L., Metkemeijer R., 2008a, Thermodynamics and kinetics analysis of gasoline reforming assisted by arc discharge, Energy and Fuels, 22(3), 1888-1893.

Rollier J.D., Gonzalez-Aguilar J., Petitpas G., Darmon A., Fulcheri L., Metkemeijer R., (2008b), Experimental study on gasoline reforming assisted by nonthermal arc discharge, Energy and Fuels, 22(1), 556-560.

Rabe S., Vogel F., Truong T.B., Shimazu T., Wakasugi T., Aoki H., 2009, Catalytic reforming of gasoline to hydrogen: kinetic investigation of deactivation processes, International Journal of Hydrogen Energy, 34(19), 8023-8033.

Semelsberger T.A., Borup R.L., 2005, Fuel effects on start-up energy and efficiency for automotive PEM fuel cell systems, International Journal of Hydrogen Energy, 30(4), 425-435.

Smith W.R., 1996, Computer software reviews, HSC Chemistry for Windows, 2.0, Journal of Chemical Information and Computer Sciences, 36(1), 151-152.

Sobacchi M.G., Saveliev A.V., Fridman A.A., Kennedy L.A., Ahmed S., Krause T., 2002, Experimental assessment of a combined plasma/catalytic system for hydrogen production via partial oxidation of hydrocarbon fuels, International Journal of Hydrogen Energy, 27(6), 635-642.

Thomas C.E., James B.D., Lomax Jr F.D., Kuhn Jr, I.F., 2000, Fuel options for the fuel cell vehicle: hydrogen, methanol or gasoline, International Journal of Hydrogen Energy, 25(6), 551-567.

Turpeinen E., Raudaskoski R., Pongracz E., Keiski R.L., 2008, Thermodynamic analysis of conversion of alternative hydrocarbon-based feed stocks to hydrogen, International Journal of Hydrogen Energy, 33(22), 6635-6643.

Ye X.F., Wang S.R., Zhou J., Zeng F.R., Nie H.W., Wen T.L., 2010, Assessment of the performance of Ni-yttria-stabilized zirconia anodes in anode-supported solid oxide fuel cells operating on H_2/CO syngas fuels, Journal of Power Sources, 195(21), 7264-7267.

Chapter 5

Dry autothermal gasification of lignite coal

CHAPTER 5: Dry autothermal gasification of lignite coal

Abstract

Dry autothermal gasification is an important process for research in coal gasification to reduce the steam generation energy in the gasification system. A comparison study of dry autothermal gasification with steam gasification & mixture of CO_2 and steam gasification system is done in this chapter. A thermodynamic study involving the effect of temperature, pressure and feed CO_2 & steam ratios in gasification of lignite coal was studied. The product generation trends of syngas and methane with carbon (in coal) conversion was studied in detail. The carbon (in lignite coal) was converted completely at a lower temperature than pure carbon in the combined gasification. Some applications of the gasifier product gas were also studied. Dry autothermal gasification with steam (combined gasification) offers great advantages to produce syngas of exact ratio in one step for use in petrochemical manufacture and fuel cell systems. The complete carbon (in coal) conversion occurred beyond the thermoneutral gasification temperature in the study. The combined gasification process was a useful way for CO_2 utilization reducing the net CO_2 emission to the atmosphere.

CHAPTER 5: Dry autothermal gasification of lignite coal

5.1 Coal as fuel

Coal is a natural resource available in many countries worldwide. It is a carbon source used mainly for energy generation. Some other coal based value added products include syngas (H_2 + CO). Syngas can be utilized in many ways - for electric power generation in gas engine or gas turbine, for Fischer–Tropsch (FT) synthesis of liquid fuels, for production of gaseous products such as synthetic natural gas and also as fuel in fuel cells. Coal (steam) gasification is a popular technology to produce syngas from coal. Some researchers are also working on underground coal gasification (UCG) which is a potential clean coal technology to convert coal gas in situ into syngas using dry air (Prabhu et al., 2012).

Traditionally coal gasification is done using steam and air in coal gasifiers. Neogi et al. (1986) have experimentally studied coal gasification in a fluidized bed reactor using steam as the fluidizing medium and simulated the dynamic behavior and steady state performance of the gasifier to a mathematical model. Bayarsaikhan et al. (2006) have experimentally studied the steam gasification of a Victorian brown coal in an atmospheric bubbling fluidized-bed reactor with continuous feeding of the coal. Sekine et al. (2006) have studied the reactivity and structural change of coal char during steam gasification. Peng et al. (1995) have studied the reactivities of in-situ and ex-situ coal chars of bituminous coal, subbituminous coal and lignite in steam gasification

and found that the reactivities of the resulting insitu chars were up to six times higher than that of the corresponding exsitu chars. Foong et al. (1980) have studied the coal gasification in a spouted bed reactor to produce syngas using mixtures of steam and air and compared the results to commercial moving and fluidized bed systems. Chatterjee et al. (1995) have studied the gasification of high ash India coal in a laboratory scale, atmospheric fluidized bed gasifier using steam and air as fluidizing media and compared the predicted and experimental data to show similar trends.

Coal gasification can also be done using CO_2. Muhammad et al. (2011) have reported a detailed review of coal gasification in CO_2 atmosphere and its kinetics since 1948. Hecth et al. (2011) have studied the effect of CO_2 gasification reaction on oxy-combustion of pulverized coal char and reported new calculations that give new insight into the complexity of the effects from the CO_2 gasification reaction. Wei-Biao and Qing-Hua (2011) have found a general relationship between the kinetic parameters for the gasification of coal chars with CO_2 and coal type. Marcourt et al. (1983) have experimentally studied the coal gasification at pressure by mixtures of carbon dioxide and oxygen and reported that experimental results could be satisfactorily explained by means of a model based on thermodynamic equilibria. Coal is also gasified with biomass (Kumabe et al., 2007) and wood (Aigner et al., 2011).

Oxygen is already present in the coal matrix. Use of air in coal gasification results in nitrogen dilution of the gasifier product gas which reduces the value of the syngas produced. Hence gasification without external air/oxygen input is beneficial to applications that use syngas. Thermodynamic studies are also popular in coal gasification area. Eftekhari et al. (2012) have used a chemical equilibrium model to analyze the effect of process parameters on product composition and use it for an exergy analysis of underground coal gasification. Dufaux et al. (1990) have investigated the gasifier involving underground coal gasification using mathematical models based on the simultaneous resolution of the different thermodynamic equilibria of the gasification reactions. Yi and Wojciech (2012) have done thermodynamic analyses for solar thermal steam and dry gasification of anthracite, bituminous, lignite and peat coals. Giuffrida et al. (2011) have analyzed the thermodynamic performance of IGCC power plants based on an air-blown gasifier. Prins et al. (2007) have studied the effect of fuel composition on the thermodynamic efficiency of gasifiers and gasification systems using a chemical equilibrium model to describe the gasifier. Wang et al. (2006) have conducted a thermodynamic equilibrium analysis of hydrogen production by coal based on Coal/CaO/H_2O gasification system.

Most of the gasification thermodynamic studies have reported the use of Gibbs free energy minimization algorithm (Liu et al., 2006; Letellier et al., 2010; Haryanto et al., 2009) or Gibbs free energy routine of aspen plus for

biomass gasification (Cohce et al., 2010). HSC Chemistry software has also been used by some researchers in thermodynamic studies related to coal gasification (Diaz-Somoano et al., 2003), biomass gasification (Konttinen et al., 2012; Detournay et al., 2011). Shabbar and Janajreh (2012) have performed the thermodynamics analysis of gasification process using the Gibbs energy minimization approach through Lagrange multiplier method to study the three different methods of gasification using air, air-steam and solar-steam to convert bituminous (RTC) coal into syngas.

Use of excess steam and excess CO_2 in gasification processes is common to enhance the chemical reactivity in gasification (Bell et al., 2011). Steam generation is a very energy consuming task as water has high latent heat of vaporization. CO_2 does not require phase change but the CO_2 molecule is very inert and its chemical reactivity in gasification is low. Combined gasification offers an advantageous middle path to reduce the disadvantages of pure steam or CO_2 gasification. The syngas produced by steam gasification has very high hydrogen content while that produced by CO_2 gasification has significant amount of CO. The high hydrogen containing syngas cannot be generally used in FT synthesis. The syngas required for syngas based applications e.g. FT synthesis requires adjustment of syngas ratio (preferably between 1-3). This adjustment is usually done by coupling water gas shift (WGS) reactor (sometimes reactors in stages) to the gasifier. The following reaction occurs in the WGS reactor:

$$CO + H_2O = CO_2 + H_2 \qquad \text{----------(A.1)}$$

These water gas shift reactors operate at low temperatures than the gasifier e.g. High temperature shift reactor operates around 400-500ºC. These are catalytic reactors requiring selective WGS catalyst for operation. The WGS reaction using commercial Fe based catalyst requires high steam input to make the ratio of feed $H_2O/CO = 4.5$). This additional steam requirement is a huge energy consuming process. F. Kiso and M Matsuo (2011) have studied the factors to improve the thermal efficiency of fuel production and electricity generation by dry coal feed gasification and have suggested that the primary cause of thermal efficiency loss is the use of steam in the water-gas shift reactor. Moreover the sulphur compounds in coal can poison the WGS catalyst. The WGS reaction is also very slow and requires huge reactors.

Combined gasification of coal using steam and CO_2 in appropriate ratio can produce syngas of the desired syngas ratio in one step. Although several such studies on coal gasification have been published in literature, coal gasification using both steam and CO_2 simultaneously has not yet been studied extensively although such study for biomass is recently reported (Renganathan et al., 2012). This study aims to study the feasibility aspects of coal gasification using steam and CO_2 simultaneously and understand the trends in product generation and their utility to some specific applications.

CHAPTER 5: Dry autothermal gasification of lignite coal

Different coal types have been used in various research studies. Lignite coal gasification studies have also been reported in literature (Adanez et al., 1985; Ashman et al., 2005; Smolinski et al., 2011; Bhattacharya, 2006). Tremel et al. (2012) have studied the pyrolysis and gasification behavior at operation conditions relevant to industrial scale entrained flow gasifiers and have reported high level of conversion of Rhenish lignite coal at atmospheric pressure. Karimipour et al. (2012) have experimentally studied the effect of coal feed rate, coal particle size, and steam/O_2 ratio, and their interactions on the quality of syngas produced from fluidized bed gasification of lignite coal. Lignite coal is reported for its high activity in gasification (Liu et al., 2009; Burger, 2010; Crnomarkovic et al., 2007) and hence was selected for this study.

Coal gasification is affected by the inorganic matter content of the coal char (Kopsel et al., 1990; Squires et al., 1986; Fernandez-Morales et al., 1985; Yu et al., 2006). Coal gasification is also slightly affected the particle size of coal (Hanson et al., 2002; Ye et al., 1998). Thus, barring the extreme mass transfer and kinetic limitations, thermodynamic study of gasification can be of universal use to predict the conversions and product distributions.

Coal gasification involves many chemical reactions. The gasification reactions mentioned in earlier literature are given below:

$C + CO_2 = 2CO$ ----------(A.2)

$C + H_2O = H_2 + CO$ ----------(A.3)

$C + 2H_2 = CH_4$ ----------(A.4)

$2C + 2H_2O = CH_4 + CO_2$ ----------(A.5)

$C + 2H_2O = 2H_2 + CO_2$ ----------(A.6)

$CH_4 + H_2O = CO + 3H_2$ ----------(A.7)

$2CO = CO_2 + C$ ----------(A.8)

$CO + H_2O = H_2 + CO_2$ ----------(A.1)

The coal gasification products reported in literature are H_2, CO, CO_2, CH_4, C_2H_6, C_3H_6, C_3H_8, H_2O, and C. The coal gasification reactions and their products have been discussed in literature earlier (Brar et al., 2012; Belghit et al., 2009; Molina et al., 1998; Everson et al., 2006; Carrazza et al., 1985; Li et al., 2012).

5.2 Methodology

It is assumed that the exit products of the coal gasifier are in thermodynamic equilibrium. HSC Chemistry software has been used in gasification studies. Although coal composition varies a lot, its main constituents are carbon (C), hydrogen and oxygen with negligible amount of sulfur and nitrogen. The dry ash free base compositions of lignite coal taken were 73.73 % C, 4.04 % H, 20.21 % O, 1.01 % S, and 1.01 % N by weight which were nearly same as

(Dennis et. al., 2010 & Nandi et. al., 2006). For 1 mole of carbon, 0.3288 moles of hydrogen, 0.1027 moles of oxygen, 0.0059 moles nitrogen and 0.00514 moles sulfur (present in lignite coal) have been used as basis for all calculations in the temperature range of 500 – 1200 ºC for the entire process study.

Coal gasification involves species such as C(s), CO_2 (g), H_2 (g), CO (g), H_2O (g), CH_4 (g), H_2S (g), SO_2 (g), N_2 (g) and H_2O (l) which are usually found in the gasification are considered in this study. Generally it is assumed that no hydrocarbons other than methane are present in any appreciable quantity in the outlet of gasifier at high gasifier temperature as seen earlier (Liu et al., 2009). Hence no other hydrocarbon gases such as C_2H_6, C_2H_4 and C_2H_2 & also no other by-products were considered in the calculations similar to the report by some researchers (Fushimi et. al., 2003). The input species to the gasifier were carbon (solid), oxygen, hydrogen, sulfur, nitrogen, water and CO_2 (in gaseous phase) reacting to give the products. The material balances are done by Equilibrium Composition module of HSC Chemistry and these results were used to calculate reaction enthalpy by Reaction Equation module of HSC Chemistry software. The results may be slightly different using different software due to the difference of thermodynamic databases. Steam and CO_2 are used as gasifying agents in this study. The gasifying agent to carbon ratio (GaCR) ranging from 1 to 3 was selected as boundary for this study. Combined gasification of coal using CO_2 and H_2O is considered in this

study and hence the intermediate steps for increase in CO_2 with simultaneous decrease in steam for each ratio was also considered in the calculations. These feed conditions for CO_2 and steam input per mole coal input are shown in table 5.1. The equilibrium compositions of the coal gasifier were used to calculate the reaction enthalpy required in the process. The effect of variation of these feed compositions and temperature on the products and gasifier enthalpy are discussed in detail in the next section.

Feed Conditions	Input moles of Coal			Input moles of CO_2	Input moles of H_2O	Gasifying agent to carbon ratio (GaCR) $((H_2O+CO_2)/C)$
	C	H_2	O_2			
A1	1	0.3288	0.1027	0	1	1
A2	1	0.3288	0.1027	0.25	0.75	1
A3	1	0.3288	0.1027	0.5	0.5	1
A4	1	0.3288	0.1027	0.75	0.25	1
A5	1	0.3288	0.1027	1	0	1
B1	1	0.3288	0.1027	0	2	2
B2	1	0.3288	0.1027	0.5	1.5	2
B3	1	0.3288	0.1027	1	1	2
B4	1	0.3288	0.1027	1.5	0.5	2
B5	1	0.3288	0.1027	2	0	2
C1	1	0.3288	0.1027	0	3	3
C2	1	0.3288	0.1027	1	2	3
C3	1	0.3288	0.1027	1.5	1.5	3
C4	1	0.3288	0.1027	2	1	3
C5	1	0.3288	0.1027	3	0	3

Table 5.1: Gasification conditions

5.3 Results and discussion

5.3.1 Effect of pressure

Pressure is an important process parameter. The effect of pressure on combined gasification of coal was studied for 1, 10 and 20 bar. Initially the effect of pressure on carbon conversion and syngas yield in the gasifier was studied at 600°C only. Figure 5.1 shows the carbon (in lignite coal) conversion for the 15 feed input conditions (A1 to C5) at 600°C. It was observed that the carbon conversion decreased with increase in pressure for all cases. It was also observed that at constant pressure, the carbon conversion decreased with increase in feed CO_2 moles (and simultaneous decrease in feed H_2O moles) at constant GaCR for all pressures. It was also seen that the carbon conversion increased as the feed steam to carbon ratio increased from 1 to 3 for all pressures in combined gasification with steam & CO_2 for cases (A2, B2 and C2). Similar observation was also noted for cases (A3, B3 and C3) and cases (A4, B4 and C4). Figure 5.2 shows the syngas yield at 600°C for the different feed conditions. It was observed that the syngas yield decreased with increase in pressure for all cases. It was also observed that at constant pressure, the syngas yield decreased with increase in feed CO_2 moles (and simultaneous decrease in feed H_2O moles) at constant GaCR for all pressures. It was also seen that the syngas yield increased as the respective feed GaCR increased from 1 to 3 for all pressures in combined gasification with steam & CO_2 for cases (A2, B2 and C2), cases (A3, B3 and C3) and cases (A4, B4 and C4). It is reported that increase in gasification pressure

decreases the H_2 (Molina et. al, 1998) and CO yield; while increase in the methane yield due to methanation reaction occurs at higher pressures (Krzysztof et al., 2011). Considering the negative effect of pressure on carbon conversion and syngas yield in the gasifier, it was noted that the maximum carbon conversion and maximum syngas yield can be obtained at low pressure (1 bar). This is purely a thermodynamic analysis result and any conflict arising due to kinetic or other limitations are not considered in this study. Hence this pressure was selected for this coal gasification study.

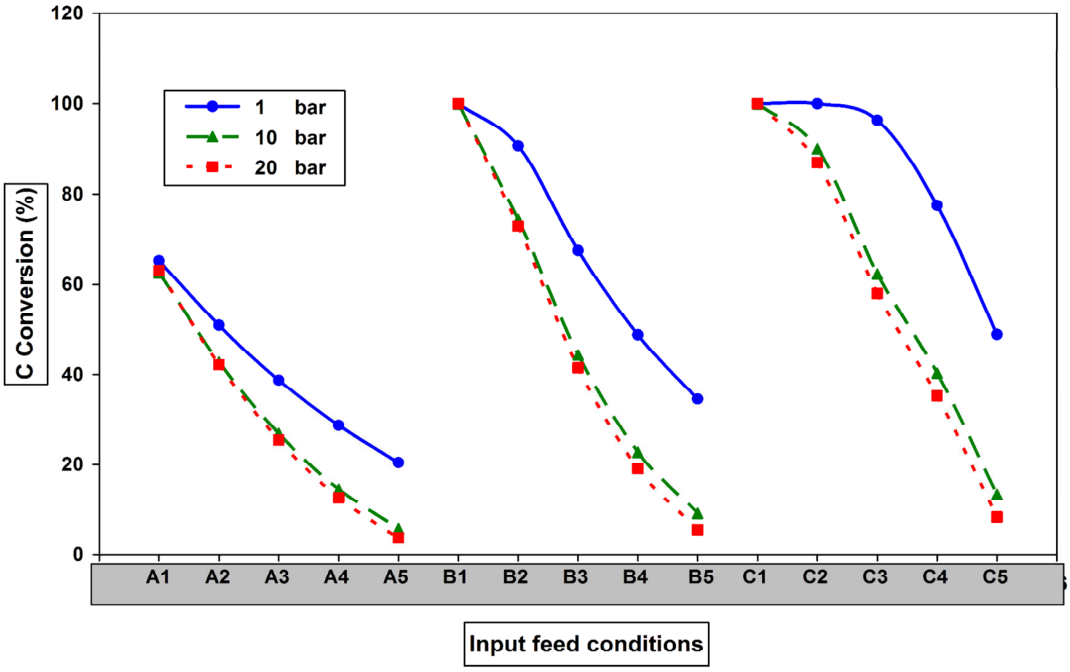

Figure 5.1: Carbon conversion at different pressures

5.3.2 Syngas yield

Syngas potential of a process is calculated by the sum of moles of hydrogen and carbon monoxide obtainable in the process. Syngas is the most desired product of the coal gasifier. As seen in figure 5.3, the syngas moles generally

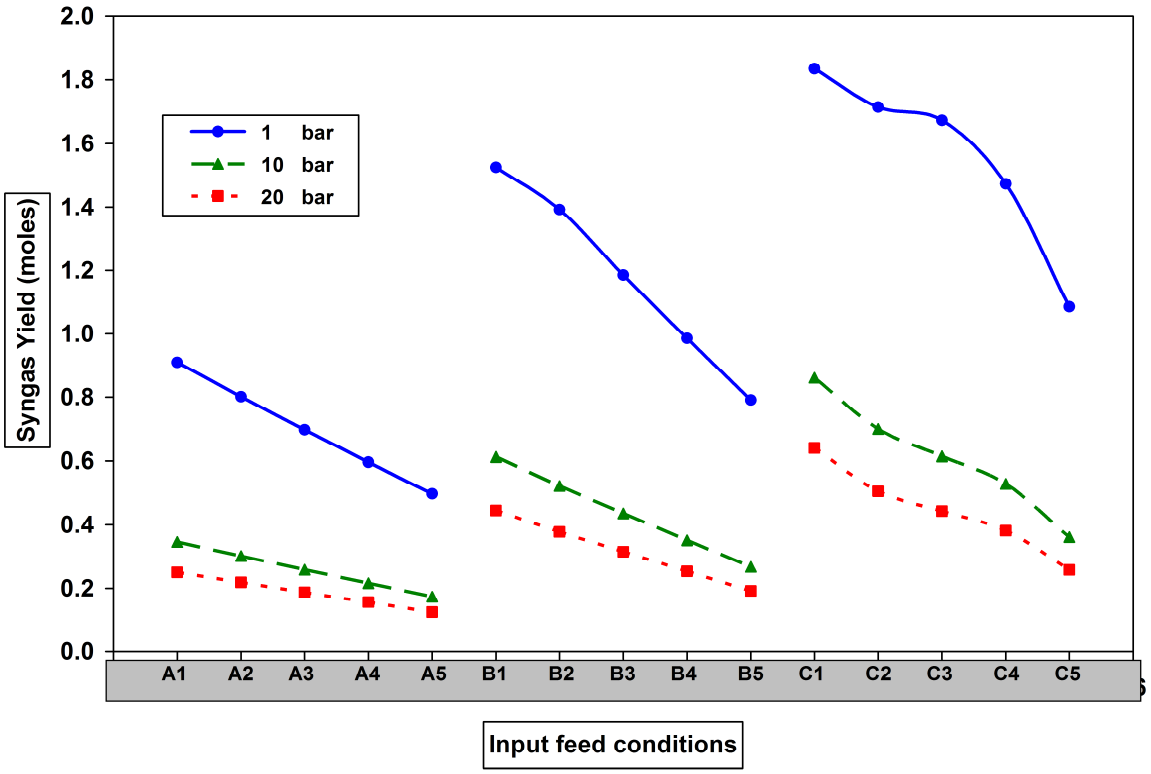

Figure 5.2: Syngas yield at 600°C for the different feed conditions

increased for all cases of A, B and C then became nearly constant at higher temperature ~800°C in combined gasification with steam & CO_2 with increase in temperature from 500 to 1200°C and at constant GaCR, e.g. the syngas yield increased from 0.218 to 2.118 moles for case A4, the syngas moles

increased from 0.597 to 2.118 moles for case B2 and increased from 0.522 to 2.118 moles for case C4. The syngas moles generally decreased with increase in feed CO_2 moles (with simultaneous decrease in feed H_2O moles) at constant GaCR and constant temperature then became nearly constant at higher temperature. For e.g. it decreased from 0.539 to 0.366 moles for case A (i.e. A2 to A4); from 0.928 to 0.588 moles for case B (i.e. B2 to B4) and from 1.230 to 0.892 moles for case C (i.e. C2 to C4) at 550°C.

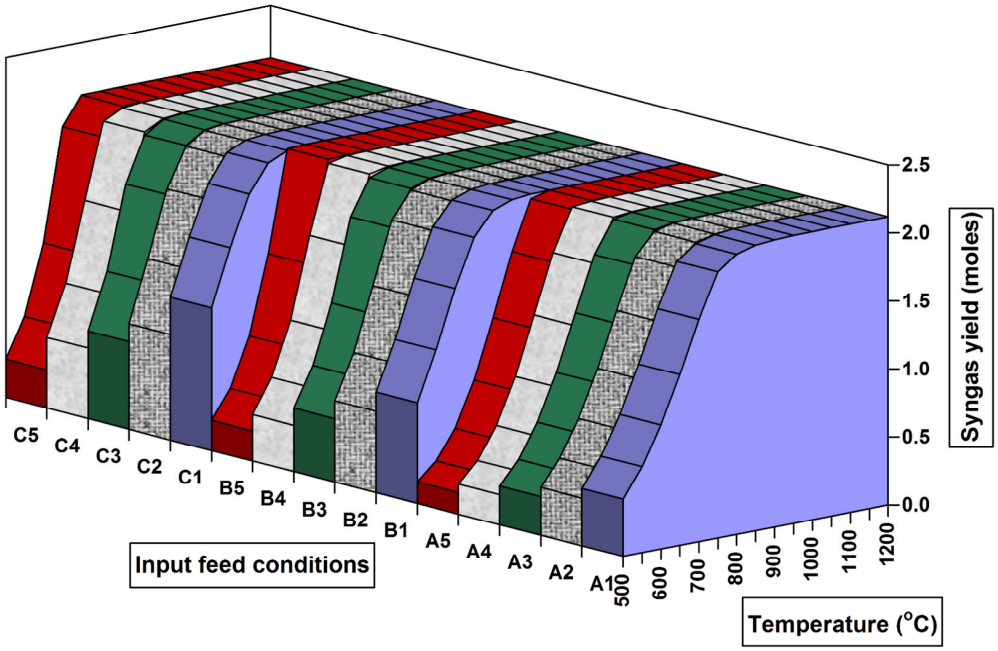

Figure 5.3: Syngas yield in combined coal gasification

It was also observed that the syngas moles in the combined gasification cases (A2, B2 and C2) increased with increase in steam to carbon ratio at constant temperature then became almost constant at higher temperature (above 850°C), i.e. it increased from 0.539 to 1.230 moles at 550°C. Similar

observation was noted for combined gasification cases (A4, B4 and C4), i.e. the syngas yield increased from 0.9307 to 2.0288 moles at 650°C. The syngas yield also increased for equimolar input moles of H_2O and CO_2 with increase in GaCR from 1 to 3 (cases A3, B3 and C3) at constant temperature i.e. it increased from 0.451 to 1.058 moles at 550°C. The maximum of for all combined 2.118 moles of syngas were obtained in gasification with steam & CO_2 conditions (above ~1000°C for all cases A, B and C), while minimum moles of syngas obtained were 0.157 moles at 500°C for case A5 in combined gasification of lignite coal.

5.3.3 Methane Formation

Methane is an imminent product of combined gasification of coal. Methane formation is undesirable due to the loss of hydrogen and carbon moles. As seen from figure 5.4, methane formation generally decreased with increase in temperature from 500-1200°C at constant GaCR for all cases A, B and C in combined gasification. Almost zero moles of methane were obtained for all GaCR conditions in combined gasification of lignite coal at higher temperatures. e.g. methane formation decreased from 0.143 to 0.00 moles for case C3 with increase in gasification temperature. The methane yield generally decreased with increase in feed CO_2 moles (with simultaneous decrease in feed H_2O moles) at constant GaCR condition and constant temperature. For e.g. CH_4 yield decreased from 0.133 to 0.036 moles for case

A (i.e. A2 to A4); from 0.213 to 0.041 moles for case B (i.e. B2 to B4) and decreased from 0.237 to 0.074 for case C (i.e. C2 to C4) at 500°C. In combined gasification cases, with increase in GaCR from 1 to 3, the methane yield increased upto certain temperature i.e. 700°C but it decreased at higher temperatures, e.g. at 500°C, the methane yield increased from 0.133 (A2) to 0.237 (C2) moles, but it decreased from 0.042 to 0.007 moles (A2, B2 and C2) at 700°C. Similar trend was obtained case (A4, B4 and C4), for example the methane yield increased from 0.036 to 0.074 moles at 500°C but at 700°C, it decreased from 0.012 to 0.004 moles with increase in GaCR from 1 to 3. The methane yield for equimolar input moles of H_2O and CO_2 (cases A3, B3 and C3) at constant temperature increased at lower temperatures up to 600°C but it decreased at high temperatures, i.e. at 500°C, the methane yield increased from 0.076 to 0.143 moles (from A3 to C3) while at 700°C, it decreased from 0.025 to 0.006 moles. The maximum methane yield was found to be 0.345 moles for case B1 at 500°C, while the minimum methane yield was observed to be 0.00 at all cases above ~950°C. Generally methane formation increases at higher pressures (Krzysztof et. al., 2011) and hence methane formation was found insignificant in this study at 1 bar pressure.

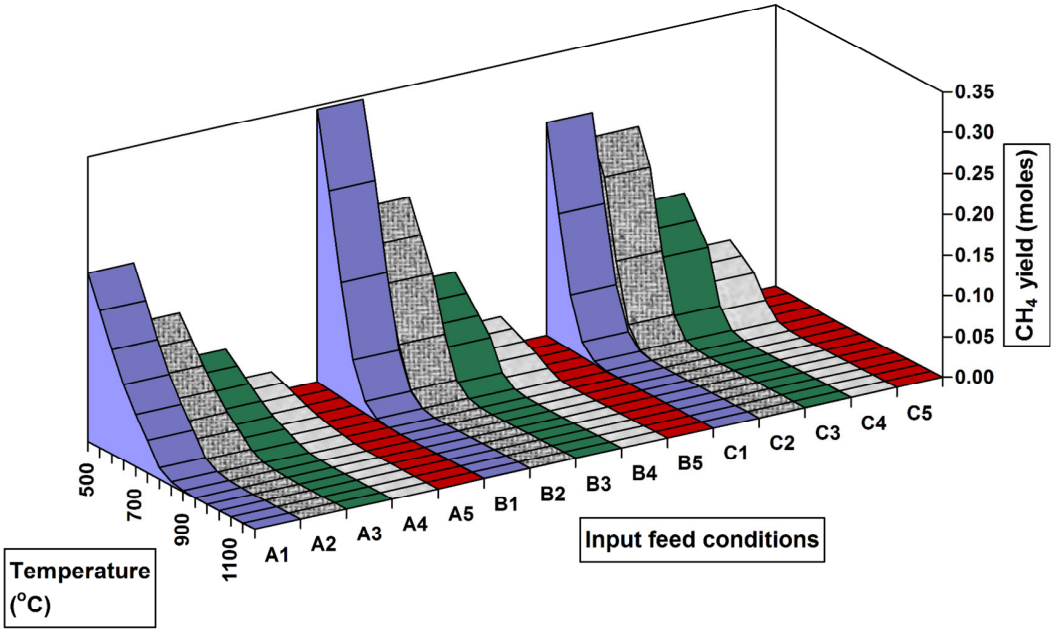

Figure 5.4: CH_4 formation in combined coal gasification

5.3.4 Carbon (in coal) conversion (%)

Coal conversion is directly linked to the carbon conversion in the combined gasification process. Table 5.2 shows the carbon conversion in gasifier within the temperature range 500-1200°C for all GaCR cases (A, B and C) at 1 bar pressure. It was observed that the carbon (in coal) conversion increased with increase in process temperature. For example, the carbon conversion increased by ~40% for pure steam case A1 with increase in temperature from 550ºC to 1000ºC similar to earlier reported data (Liu et al., 2004). As seen

from table 5.2, the carbon conversion generally increased to its maximum with increase in temperature from 500-1200°C at constant GaCR for all cases of A, B and C in combined gasification e.g. it increased from 12 to 100 % for case A4. It was also observed that the carbon conversion generally decreased with increase in feed CO_2 moles (with simultaneous decrease in feed H_2O moles) for constant GaCR case and constant temperature, for e.g. it decreased from 43 % to 18 % (A2 to A4); from 75% to 30 % (B2 to B4) and from 95% to 51 % (C2 to C4) at 550°C. From the table, it was also seen that the 100% carbon conversion temperature decreased with increase in GaCR from 1 to 3. The carbon conversion for the combined gasification cases (A2, B2 and C2) increased with increase in feed steam to carbon ratio at constant temperature before reaching its maximum (100%), e.g. it increased from 43% (A2) to 95% (C2) at 550°C, while the carbon conversion in combined gasification cases (A4, B4 and C4) increased with increase in feed CO_2 to carbon ratio at constant temperature, for example, it increased from 18% (A4) to 51 % (C4) at 550°C. The carbon conversion also increased for equimolar input moles of H_2O and CO_2 with increase in GaCR from 1 to 3 (cases A3, B3 and C3) at constant temperature, i.e. it increased from 29 to 71% (from A3 to C3) at 550°C.

This observation was compared to the carbon conversion in combined gasification using pure carbon (Kale et al., 2013). Table 5.3 shows the carbon conversion (%) within the temperature range 500-1200°C for all input feed

conditions of GaCR at 1 bar pressure for pure carbon. As seen from table 5.2 and 5.3, the 100% carbon conversion were observed at lower temperatures in almost all cases of lignite coal than pure carbon as feed to the gasifier. This comparison on the basis of thermodynamic analysis shows the higher reactivity of lignite coal than pure carbon in gasification which may be due to the presence of hydrogen and oxygen in the coal structure.

Temperature (°C) Conditions	500	550	600	650	700	750	800	850	900	950	1000	1050	1100	1150	1200
A1	56	59	65	75	89	100	100	100	100	100	100	100	100	100	100
A2	38	43	51	64	80	96	100	100	100	100	100	100	100	100	100
A3	23	29	39	53	72	90	100	100	100	100	100	100	100	100	100
A4	12	18	29	44	64	85	100	100	100	100	100	100	100	100	100
A5	4	10	20	36	58	81	98	100	100	100	100	100	100	100	100
B1	100	100	100	100	100	100	100	100	100	100	100	100	100	100	100
B2	67	75	91	100	100	100	100	100	100	100	100	100	100	100	100
B3	39	50	67	94	100	100	100	100	100	100	100	100	100	100	100
B4	19	30	49	77	100	100	100	100	100	100	100	100	100	100	100
B5	6	17	34	63	100	100	100	100	100	100	100	100	100	100	100
C1	100	100	100	100	100	100	100	100	100	100	100	100	100	100	100
C2	80	95	100	100	100	100	100	100	100	100	100	100	100	100	100
C3	55	71	96	100	100	100	100	100	100	100	100	100	100	100	100
C4	35	51	78	100	100	100	100	100	100	100	100	100	100	100	100
C5	9	23	49	90	100	100	100	100	100	100	100	100	100	100	100

Table 5.2: 100% carbon conversion temperatures for Lignite coal

Temperature (°C) / Conditions	500	550	600	650	700	750	800	850	900	950	1000	1050	1100	1150	1200
A1	46	48	53	62	73	84	91	96	98	99	100	100	100	100	100
A2	29	33	40	100	100	100	100	100	100	100	100	100	100	100	100
A3	51	64	78	88	94	97	98	99	100	100	100	100	100	100	100
A4	8	13	21	33	50	68	82	91	95	98	99	99	100	100	100
A5	3	7	15	27	45	64	80	90	95	97	99	99	100	100	100
B1	91	96	100	100	100	100	100	100	100	100	100	100	100	100	100
B2	57	66	80	100	100	100	100	100	100	100	100	100	100	100	100
B3	32	42	58	82	100	100	100	100	100	100	100	100	100	100	100
B4	16	25	41	67	100	100	100	100	100	100	100	100	100	100	100
B5	6	15	29	54	90	100	100	100	100	100	100	100	100	100	100
C1	100	100	100	100	100	100	100	100	100	100	100	100	100	100	100
C2	72	86	100	100	100	100	100	100	100	100	100	100	100	100	100
C3	49	63	87	100	100	100	100	100	100	100	100	100	100	100	100
C4	31	45	69	100	100	100	100	100	100	100	100	100	100	100	100
C5	10	22	44	82	100	100	100	100	100	100	100	100	100	100	100

Table 5.3: 100% carbon conversion in pure carbon gasification

5.3.5 Net CO_2 Emission / CO_2 utilization

CO_2 emissions are important points for chemical processes. Combined gasification uses CO_2 as feed but the gasifier product gas also contains CO_2. Hence a balance of CO_2 utilization and emission was estimated using the net CO_2 emission terminology and is plotted in figure 5.5. The net CO_2 emission (moles) = CO_2 moles (in output) – CO_2 moles (in input). Negative net CO_2 emission implies CO_2 utilization. As seen in figure 5.5, the net CO_2 emission decreased with increase in temperature from 500-1200°C at constant GaCR for all cases A, B and C. e.g. it decreased from 0.357 to -0.127 moles for case B2. The net CO_2 emission generally decreased with increase in feed CO_2 moles (with simultaneous decrease in feed H_2O moles) at constant GaCR and constant temperature for all combined gasification cases. For e.g. it

decreased from -0.086 to -0.468 moles for case A (A2 to A4); from 0.094 to -0.557 moles for case B (B2 to B4) and from 0.087 to -0.412 moles for case C (C2 to C4) at 750°C. The net CO_2 emission for the combined gasification cases (A2, B2 and C2) increased with increase in feed steam to carbon ratio at lower temperature upto 700°C after which a mixed trend was observed in these cases, e.g. the net CO_2 emission increased from 0.016 to 0.146 moles cases (A2 to C2) at 700°C. The net CO_2 emission also showed a mixed trend for combined gasification cases (A4, B4 and C4) and equimolar input moles of H_2O and CO_2 i.e. case (A3, B3 and C3) with increase in GaCR from 1 to 3. The maximum net CO_2 emission was found to be 0.686 moles for case 1 at 550°C, while the minimum observed was -1.026 moles for case C5 at 1200°C.

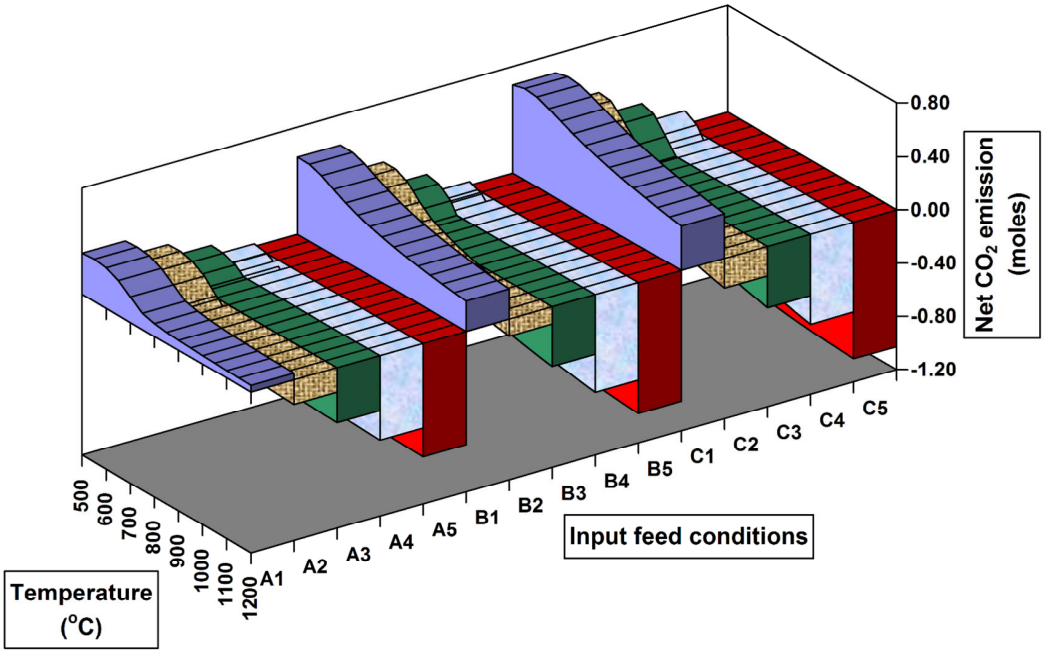

Figure 5.5: Net CO_2 emission in combined coal gasification

5.3.6 Gasification enthalpy and thermoneutral points

Process enthalpy is always a crucial parameter in gasification processes. Gasification without oxygen input is an endothermic process. However the lignite coal contains insitu oxygen in its chemical matrix. This oxygen helps to generate exothermicity in the absence of external oxygen or air. The effect of gasification temperature on gasification process enthalpy was studied at all feed conditions. The intersection of gasification enthalpy curves with temperature axis shows the thermoneutral temperatures (TNP). Thermoneutral operation requires no external energy for cooling or heating, which makes it valuable from energy consumption point of view. TNPs were observed for all GaCR cases (1-3) except case C1. Figure 5.6 shows the variation of gasification enthalpy for coal gasification at constant GaCR with the thermoneutral line (zero enthalpy line). As seen from the figure 5.6, the reaction endothermicity first increased and then became almost constant with increase in temperature from 500-1200°C at constant GaCR for all cases A, B and C. e.g. it increased from -35.885 to 88.932 kJ for case A2. It was also observed that the gasification enthalpy generally decreased upto certain temperature but increased at higher temperature with increase in CO_2 moles (with simultaneous decrease in feed H_2O moles) at constant GaCR case and constant temperature. For e.g. the enthalpy decreased from -35.885 to -42.952 kJ at 500°C, while it increased from 89.114 to 104.322 kJ at 900 °C for case A (A2 to A4). The gasification enthalpy for equimolar input moles of H_2O and CO_2 showed a mixed trend with increase in GaCR from 1 to 3 (cases A3,

B3 and C3). The minimum gasification enthalpy observed was -45.961 kJ for case A5 at 500°C, while the maximum gasification enthalpy observed was 117.152 kJ for case C5 at 800°C.

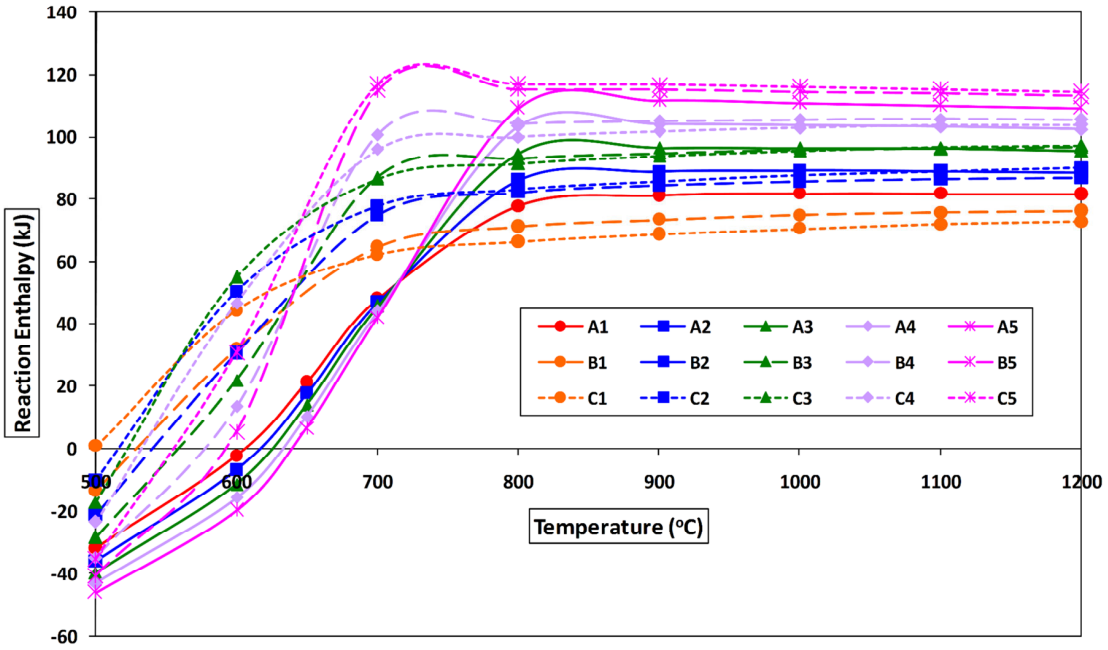

Figure 5.6: Thermoneutral temperatures in combined coal gasifier

Table 5.4 shows the product gas yields at thermoneutral conditions while table 5.5 shows the comparison of TNP temperature (°C) and 100% carbon conversion temperature (°C) obtained for different input cases of lignite coal. It was seen that the 100% carbon conversion temperature was always higher than the thermoneutral point temperature. Hence it was seen that additional external energy was required to convert 100% carbon in coal.

Cases	TNP (°C)	Equilibrium product gas compositions									
		H_2O (g) moles	CO_2 (g) moles	H_2(g) moles	CO(g) moles	CH_4(g) moles	Syngas moles	Syngas Ratio	H_2O(g) Conv.(%)	CO_2(g) Conv.(%)	C moles
A1	605.28	0.3649	0.3038	0.7100	0.2329	0.1244	0.9429	3.0485	63.51	----	0.3389
A2	615.27	0.3286	0.4095	0.5925	0.3079	0.0763	0.9004	1.9243	56.19	- 63.80	0.4564
A3	624.37	0.2744	0.5221	0.4646	0.3868	0.0424	0.8514	1.2011	45.12	-4.420	0.5487
A4	632.06	0.2052	0.6408	0.3294	0.4687	0.0196	0.7981	0.7028	17.92	23.52	0.6210
A5	638.85	0.1232	0.7648	0.1885	0.5526	0.0060	0.7411	0.3411	----	14.56	0.6766
B1	534.11	0.9111	0.5793	0.8428	0.1359	0.2849	0.9787	6.2016	54.45	-----	0.0000
B2	551.10	0.7648	0.8572	0.7109	0.2262	0.1740	0.9371	3.1428	49.01	-71.44	0.2426
B3	567.00	0.6018	1.1374	0.5540	0.3288	0.0839	0.8828	1.6849	39.82	- 13.74	0.4499
B4	580.66	0.3990	1.4303	0.3644	0.4459	0.0301	0.8103	0.8172	20.20	4.650	0.5937
B5	592.40	0.1654	1.7332	0.1496	0.5737	0.0044	0.7233	0.2608	-----	13.34	0.6888
C1	-----	-----	-----	-----	-----	-----	-----	-----	-----	-----	-----
C2	520.13	1.1496	1.4237	0.7317	0.2085	0.2212	0.9402	3.5094	42.52	- 42.37	0.1466
C3	533.64	0.9495	1.7351	0.6188	0.2858	0.1277	0.9046	2.1652	36.70	- 15.67	0.3515
C4	545.80	0.7187	2.0558	0.4783	0.3751	0.0634	0.8534	1.2751	28.13	- 2.790	0.5057
C5	566.67	0.1879	2.7165	0.1290	0.5846	0.0034	0.7136	0.2207	-----	9.450	0.6955

Table 5.4: Equilibrium gasifier gas composition at thermoneutral temperatures

GaCR	Cases	TNP Temperature (°C)	100 % Carbon conversion Temperature
1	A1	605.28	≥ 750
	A2	615.57	≥ 800
	A3	624.37	≥ 800
	A4	632.06	≥ 800
	A5	638.85	≥ 800
2	B1	534.11	≥ 500
	B2	551.10	≥ 650
	B3	567.00	≥ 700
	B4	580.66	≥ 700
	B5	592.40	≥ 700
3	C1	-----	-----
	C2	520.13	≥ 600
	C3	533.64	≥ 650
	C4	545.80	≥ 650
	C5	566.67	≥ 700

Table 5.5: Comparison between thermoneutral temperature (°C) and 100% carbon conversion temperature (°C) for Lignite coal

5.3.7 Syngas ratio

Syngas ratio is an important factor for petrochemical manufacture by FT. The syngas ratio of the product gas obtained in the combined gasification process was plotted in figure 5.7. As seen from the figure, the syngas ratio generally decreased with increase in temperature from 500-1200°C at constant GaCR for all cases A, B and C, e.g. it decreased from 1.733 to 0.224 for the case

B4. It was also observed that the syngas ratio generally decreased with increase in feed CO_2 moles (with simultaneous decrease in feed H_2O moles) at constant GaCR and constant temperature for all cases. For e.g. At 600°C, the syngas ratio decreased from 2.192 to 0.907 for case A (A2 to A4); from 2.014 to 0.694 for case B (B2 to B4) and from 1.957 to 0.791 for case C (C2 to C4). It was seen that the syngas ratio obtained in combined coal gasification process had a lower value in the range (1-5) which is useful for petrochemical manufacture by FT synthesis. Thus combined gasification can generate syngas of lower ratio in one step without the need of external water gas shift reactors.

5.3.8 Applications

a. Syngas for petrochemical manufacture

The syngas ratio in the range of 1–3 (desirable for use in petrochemical manufacture) is easily obtained in this process in one step. Fischer–Tropsch processes to synthesize hydrocarbon fuels usually require syngas with a H_2/CO ratio close to 2 (Caldwell, 1980; Dry, 2002). This coal gasification product gas can be processed through gas-solid separators to remove any coke/solids and can be compressed to a suitable pressure for use in petrochemical manufacture by FT synthesis (Dry, 1989 ;Van Dyk et al., 2006; Demirdas et al., 2007).

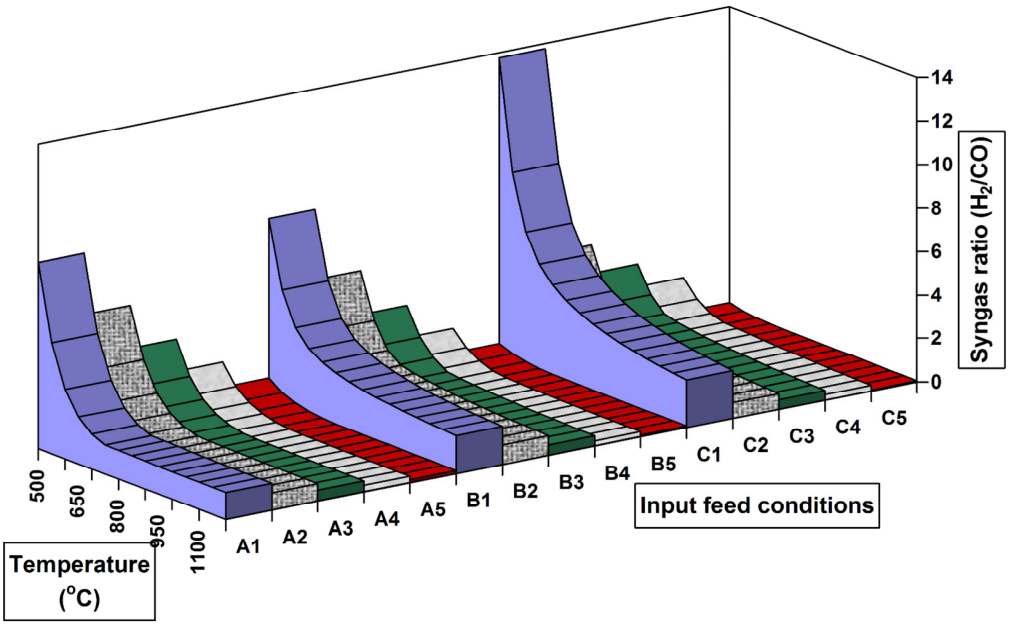

Figure 5.7: Syngas ratio of product gas

Table 5.6 shows the temperature range in which syngas ratio 1-3 is obtained in the combined gasification process at different feed conditions. It was seen that the syngas ratio 1 was obtained at relatively higher temperatures than syngas ratio 2 and syngas ratio 3 for the same feed condition. The desirable syngas ratio (1-3) was definitely obtained in the A2, A3, B2, B3 and C2, C3 feed conditions. It was also observed that the temperatures for obtaining a particular syngas ratio decreased as the input feed CO_2 increased in the combined gasification. The combined gasification considered in this study does not use oxygen (air) in the input. Hence the syngas generated is free of nitrogen dilution. Table 5.7 shows the syngas concentration in the product gas

at different syngas ratios (1-3). It was seen that some gasification conditions yield a very high syngas concentration for the desirable syngas ratio (e.g. 80.60% for syngas ratio 1 at A2). Some of the conditions [case, syngas conc., syngas ratio] for obtaining high syngas concentration in the gasifier product gas for desirable syngas ratio were as follows: [A2, 80.60 %, 1], [A1, 72.05%, 2], [B1, 63.52%, 2], [B1, 60.17%, 3] and [B2, 63.52%, 1]. Most of the high syngas concentration was obtained for GaCR 1 and 2. It was also seen that for a particular feed condition, the syngas conc. in the product gas decreased as the desirable syngas ratio of 1 increased to 2 and 3. It was also seen that the syngas conc. in the product gas decreased as the feed CO_2 increased for the desired syngas ratio at constant GaCR.

b. Production of Synthetic natural gas (SNG)

The syngas ratio above 3 is also obtained in the gasifier. This product gas can be used for the manufacture of synthetic natural gas as the production of SNG via thermo-chemical process uses the stoichiometric ratio of the reactants H_2/CO of at least three or more (Kopyscinski et al., 2010).

Cases	Temperature Range (°C)		
	Syngas Ratio		
	1	2	3
A1	----	650-700	600-650
A2	700-750	600-650	550-600
A3	600-650	550-600	500-550
A4	550-600	500-550	----
A5	500-550	----	----
B1	----	950-1000	650-700
B2	1000	600	550-600
B3	600-650	500-550	500-550
B4	550-600	----	----
B5	----	----	----
C1	----	----	850-900
C2	900	550-600	500-550
C3	650-700	500-550	500-550
C4	550-600	----	----
C5	----	----	----

Table 5.6: Temperature range (in °C) for syngas ratio 1-3

c. Syngas for Fuel cells - SOFC & PEMFC

The syngas produced in the gasification of lignite coal can be used as fuel in fuel cells. Solid oxide fuel cells (SOFC) can easily operate with CO contaminated hydrogen gas. The hot product gas from the combined coal gasifier can be passed through suitable gas-solid separators and directly fed to the SOFC type fuel cells. It is assumed by some researchers that the CO

undergoes insitu water gas shift reaction (reaction A.1) with water present in the product gas to produce hydrogen, which is used in the SOFC.

$$CO + H_2O = CO_2 + H_2 \qquad \text{---------- (A.1)}$$

As seen from reaction (A.1), the product gas containing equimolar or higher H_2O/CO ratio can be easily used as feed to the SOFC. However, Polymer Electrolyte membrane fuel cells (PEMFC) generally cannot tolerate CO more than 1% in the product gas. Hence the syngas needs to be processed through water gas shift reactors to reduce the CO content by converting it to hydrogen (reaction A.1) and further CO reduction is achieved by preferential oxidation reactors. But WGS catalysts require H_2O/CO ratio > 4.5 to convert the CO to hydrogen. Table 5.8 shows the temperatures of the combined gasifier to produce syngas that can be used in SOFC and PEMFC. As seen from the table, the syngas having H_2O/CO ratio above 1.1 (& less than 4.5) can be used in SOFC, while the syngas having H_2O/CO ratio > 4.5 can be used for both SOFC and PEMFC (after external WGS reaction). From this table, it was observed that the syngas having H_2O/CO greater than 4.5 is obtained at lower temperatures as compare to syngas of H_2O/CO ratio $1.1 \leq (H_2O/CO) \leq 4.5$. It was also observed that cases B1, C1 and C2 have a very large temperature range of syngas of H_2O/CO ratio between 1.1 and 4.5, while the syngas of $H_2O/CO > 4.5$ was obtained within the temperature range of ~500-600°C for all GaCR feed conditions. Table 5.8 also shows the concentration of syngas in the gasifier product gas having H_2O/CO ratio $1.1 \leq (H_2O/CO) \leq 4.5$ & greater

than 4.5. It was observed the syngas concentration range was wide for syngas having H_2/CO in 1.1 - 4.5 value. It was also observed that the syngas concentration in the gasifier product gas decreased with increase in feed CO_2 for desired H_2O/CO ratio in both the cases i.e., 1.1≤ (H_2O/CO) ≤ 4.5 & H_2O/CO > 4.5 at constant GaCR.

Cases	Syngas concentration (%) in gasifier product gas		
	Syngas Ratio		
	1	2	3
A1	----	72.05	59.26
A2	80.60	54.91	41.35
A3	50.38	36.48	24.97
A4	31.49	20.42	----
A5	15.82	----	----
B1	----	63.52	60.17
B2	63.52	46.85	40.37
B3	48.91	23.49	23.49
B4	29.24	----	----
B5	----	----	----
C1	----	----	48.87
C2	48.86	36.57	26.45
C3	47.66	22.91	22.91
C4	30.34	----	----
C5	----	----	----

Table 5.7: Syngas concentration (%) of syngas ratio (1-3) gasifier gas

In dry gasification case 5, the syngas concentration was much less as compared to the steam gasification case 1 in all GaCR cases. e.g. for case A1

the syngas concentration for 1.1 ≤ (H_2O/CO) ≤ 4.5 is in the range between 39.66-65.97 % while in case A5, the syngas concentration was in the range 11.57-20.08%. Higher syngas concentration was obtained in cases A1, A2, B1, B2 for 1.1 ≤ (H_2O/CO) ≤ 4.5 ratio. The highest syngas concentration was obtained for case A1 (39.66-65.97%) for 1.1 ≤ (H_2O/CO) ≤ 4.5 ratio condition, while the lowest syngas concentration was observed in case C5 (8.30-16.07 %) for 1.1 ≤ (H_2O/CO) ≤ 4.5 ratio condition. Similar observations were also noted for H_2O/CO > 4.5 conditions.

Cases	1.1 ≤ (H_2O/CO) ≤ 4.5		H_2O/CO > 4.5	
	Syngas Concentration (%)	Temperature range (°C)	Syngas Concentration (%)	Temperature range (°C)
A1	39.66-65.97	550-650	28.25-39.66	500-550
A2	34.88-61.99	550-650	24.08-34.88	500-550
A3	30.04-42.93	550-600	19.91-30.04	500-550
A4	25.10-37.87	550-600	15.74-25.10	500-550
A5	11.57-20.08	500-550	----	----
B1	50.20-63.52	600-1200	27.91-50.20	500-600
B2	33.89-57.73	550-650	23.20-33.89	500-550
B3	28.44-41.33	550-600	18.54-28.44	500-550
B4	13.88-35.59	500-600	----	----
B5	9.22-17.20	500-550	----	----
C1	48.49-48.87	700-1200	27.63-47.37	500-650
C2	31.62-48.87	550-1200	21.25-31.62	500-550
C3	27.81-40.70	550-600	18.01-27.81	500-550
C4	23.97-36.72	550-600	14.77-23.96	500-550
C5	8.30-16.07	500-550	----	----

Table 5.8: Temperature range (°C) and syngas concentration (%) for H_2O/CO ratio of gasifier product gas

d. Power generation

Syngas is used for power generation in turbines. The syngas is combusted in hot air and these hot product gases expand through the turbine, doing work, and exit at nearly atmospheric pressure at a temperature of 500-640 °C. The work extracted during the expansion is used to turn the turbine which drives the generator that produces electricity (Fan et al., 2008). The hot exit gas from the turbine still has significant amounts of energy which is used to raise steam to drive a steam-turbine and another generator. This combination of gas and steam cycle is termed as 'combined cycle gas turbine' (CCGT) plant. The combined energy for combustion of H_2, CO and CH_4 of the gasifier product gas obtained (for 1 mole of carbon in coal basis) is calculated in the figure 5.8. The combustion energy is huge as seen from the figure at various gasification conditions. As seen in figure 5.8, the total heat of combustion increased with increase in temperature from 500-1200°C at constant GaCR for all the cases A, B and C, e.g. it increased from -133.380 to -600.324 kJ/mole for the case B4. The total heat of combustion showed a mixed trend with increase in feed CO_2 moles (with simultaneous decrease in feed H_2O moles) but at higher temperature it was almost constant at constant GaCR and constant temperature for all the cases. For equimolar input moles of H_2O and CO_2 with increase in GaCR from 1 to 3 (cases A3, B3 and C3) at constant temperature, the total heat of combustion increased upto 900°C and then become almost constant. The minimum total heat of combustion of gasifier product gas was

observed to be -54.56 kJ/mol (case A5) at 500°C, while the maximum total heat of combustion was noted to be -604.173 kJ/mol (case C1) at 800°C.

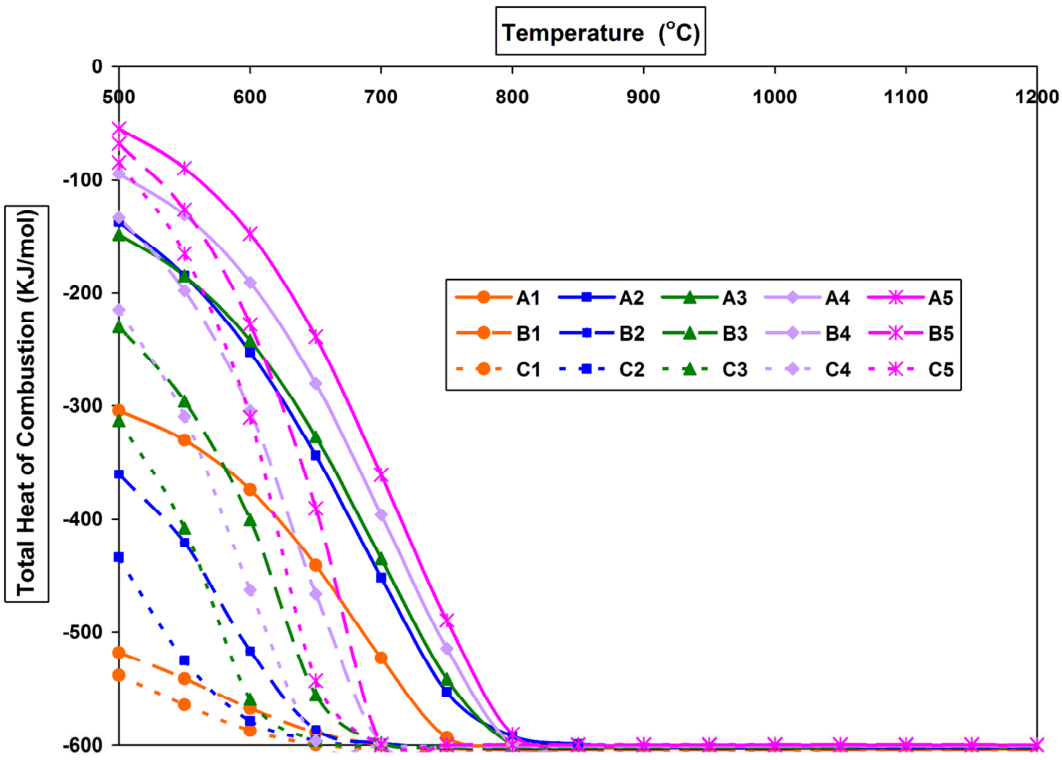

Figure 5.8: Total heat of combustion of gasifier product gas

5.4 Conclusion

A thermodynamic study of dry autothermal gasification of lignite coal gasification using both CO_2 and steam simultaneously was conducted to understand the effect of temperature, pressure and feed CO_2 and steam ratio on the product composition, carbon (in coal) conversion), syngas ratio of the product gas and process enthalpy in the gasifier. The combined gasification process was a useful way for CO_2 utilization reducing the net CO_2 emission to the atmosphere. The concentration of syngas in the gasifier product gas was

very high due to the absence of air use in the process. Combined gasification can help to reduce the energy consumption of steam generation in the pure steam gasification process while it can also help to accelerate the slow CO_2 gasification reaction by using steam. The applications of the gasifier product gas were also studied. The syngas ratio of the gasifier product gas had a low ratio (1-3) which can be used in FT processes for the manufacture of value added products and also SNG. The syngas was also suitable as feed to the fuel cells - SOFC and PEMFC and the absence of nitrogen dilution can help to increase the efficiency of the fuel cells. Although thermoneutral operation of the combined gasifier is possible, this temperature is low and insufficient for complete carbon (in coal) conversion but can produce syngas free of nitrogen. External energy is required to operate the combined gasifier to achieve maximum carbon (in coal) conversion.

5.5 References

Adanez J., Miranda J., Gavilan J., 1985, Kinetics of a lignite-char gasification by CO_2, Fuel, 64, 801–804.

Aigner I., Pfeifer C., Hofbauer H., 2011, Co-gasification of coal and wood in a dual fluidized bed gasifier, Fuel, 90, 2404–2412.

Ashman P.J., Mullinger P.J., 2005, Research issues in combustion and gasification of lignite, Fuel, 84, 1195–1205.

Bayarsaikhan B., Sonoyama N., Hosokai S., Shimada T., Hayashi J., Li C.Z., 2006, Inhibition of steam gasification of char by volatiles in a fluidized bed under continuous feeding of a brown coal, Fuel, 85, 340–349.

Belghit A., Gordillo E.D., Issami S.E., 2009, Coal steam-gasification model in chemical regime to produce hydrogen in a gas–solid moving bed reactor using nuclear heat, Int. J. Hydrogen Energy, 34, 6114–6119.

Bell D.A., Towler B.F., Fan M., 2011, Coal gasification and its applications, Boston: William Andrew Publishing; http://dx.doi.org/10.1016/B978-0-8155-2049-8.10003-8.

Bhattacharya S.P., 2006, Gasification performance of Australian lignites in a pressurized fluidized bed gasifier process development unit under air and oxygen-enriched air blown conditions, Process Safe. Environ. Protect., 84, 453–460.

Brar J.S., Singh K., Wang J., Kumar S., 2012, Cogasification of coal and biomass: a review, Int. J. Forest Res., Article ID 363058, 10 pages.

Burger S., 2010, Lignite gasification increases cost of coal to liquids. http://www.miningweekly.com/article/lignite-gasification-increases-costs-of-coal-to-liquids-2010-10-22.

Caldwell L., 1980, Selectivity in Fischer–Tropsch synthesis: review and recommendations for further work, http://www.fischertropsch.org/DOE/DOEreports/81223596/pb81223596.pdf [accessed 07.07.10].

Carrazza J., Tysoe W.T., Heinemann H., Somorjai G.A., 1985, Gasification of graphite with steam below 900 K catalyzed by a mixture of potassium hydroxide and transition metal oxide, J. Catal., 96, 234–241.

Chatterjee P.K., Datta A.B., Kundu K.M., 1995, Fluidized bed gasification of coal, Can. J. Chem. Eng., 73, 204–210.

Cohce M.K., Dincer I., Rosen M.A., 2010, Thermodynamic analysis of hydrogen production from biomass gasification, Int. J. Hydrogen Energy, 35, 4970–4980.

Crnomarkovic N., Repic B., Mladenovic R., Neskovic O., Veljkovic M., 2007, Experimental investigation of role of steam in entrained flow coal gasification, Fuel, 86, 194–202.

Demirbas A., Science S., Turkey T., 2007, Converting biomass derived synthetic gas to fuels via Fisher–Tropsch synthesis, Energy Sources Part A, 29, 1507–1512.

Dennis J.S., Scott S.A., 2010, In situ gasification of a lignite coal and CO_2 separation using chemical looping with a Cu-based oxygen carrier, Fuel, 89, 1623–1640.

Detournay M., Hemati M., Andreux R., 2011, Biomass steam gasification in fluidized bed of inert or catalytic particles: comparison between experimental results and thermodynamic equilibrium predictions, Powder Technol., 208, 558–567.

Díaz-Somoano M., Martínez-Tarazona M.R., 2003, Trace element evaporation during coal gasification based on a thermodynamic equilibrium calculation approach, Fuel, 82, 137–145.

Dry M., 1989, Commercial conversion of carbon monoxide to fuels and chemicals, J. Organomet. Chem., 372, 117–127.

Dry M., 2002, The Fischer–Tropsch process: 1950–2000, Catal. Today, 71, 227–241.

Dufaux A., Gaveau B., Letolle R., Mostade M., Noël M., Pirard J.P., 1990, Modelling of the underground coal gasification process at Thulin on the basis of thermodynamic equilibria and isotopic measurements, Fuel, 69, 624–632.

Eftekhari A.A., Van Der Kooi H., Bruining H., 2012, Exergy analysis of underground coal gasification with simultaneous storage of carbon dioxide, Energy, 45, 729–745.

Everson R.C., Neomagus H.W., Kasaini H., Njapha D., 2006, Reaction kinetics of pulverized coal-chars derived from inertinite-rich coal discards: gasification with carbon dioxide and steam, Fuel, 85, 1076–1082.

Fan L., Li F., Ramkumar S., 2008, Utilization of chemical looping strategy in coal gasification processes, Particuology, 8, 131–142.

Fernández-Morales I., López-Garzon F.J., López-Peinado A., Moreno-Castilla C., Rivera-Utrilla J., 1985, Study of heat-treated Spanish lignites: characteristics and behaviour in CO_2 and O_2 gasification reactions, Fuel, 64, 666–673.

Foong S.K., Lim C.J., Watkinson A.P., 1980, Coal gasification in a spouted bed, Can. J. Chem. Eng., 58, 84–91.

Fushimi C., Goto M., Tsutsumi A., Hayashi J., Chiba T., 2003, Steam gasification characteristics of coal with rapid heating, J. Anal. Appl. Pyrol., 70, 185–197.

Giuffrida A., Romano M.C., Lozza G., 2011, Thermodynamic analysis of air-blown gasification for IGCC applications, Appl. Energy, 88, 3949–3958.

Hanson S., Patrick J.W., Walker A., 2002, The effect of coal particle size on pyrolysis and steam gasification, Fuel, 81, 531–537.

Haryanto A., Fernando S.D., Pordesimo L.O., Adhikari S., 2009, Upgrading of syngas derived from biomass gasification: a thermodynamic analysis, Biomass Bioenergy, 33, 882–889.

Hecht E.S., Shaddix C.R., Molina A., Haynes B.S., 2011, Effect of CO_2 gasification reaction on oxy-combustion of pulverized coal char, Proc. Combust. Inst., 33, 1699–1706.

Kale G., Borkhade S., Shriwas P., 2013, Gasification coupled Chemical looping combustion of coal: a thermodynamic process design study, ISRN

Chemical Engineering, http://dx.doi.org/10.1155/2013/565471 [Article ID 565471, 11 p.].

Karimipour S., Gerspacher R., Gupta R., Spiteri R.J., 2013, Study of factors affecting syngas quality and their interactions in fluidized bed gasification of lignite coal, Fuel, 103, 308-320.

Kiso F., Matsuo M., 2011, A simulation study on the enhancement of the shift reaction by water injection into a gasifier, Energy, 36, 4032–4040.

Konttinen J., Backman R., Hupa M., Moilanen A., Kurkela E., 2013, Trace element behavior in the fluidized bed gasification of solid recovered fuels—a thermodynamic study, Fuel, 106, 621-631.

Kopsel R., Zabawski H., 1990, Catalytic effects of ash components in low rank coal gasification: 1. Gasification with carbon dioxide, Fuel, 69, 275–281.

Kopyscinski J., Schildhauer T.J., Biollaz S.M.A., 2010, Production of synthetic natural gas (SNG) from coal and dry biomass—a technology review from 1950 to 2009, Fuel, 89, 1763–1783.

Krzysztof K., Krzysztof S.C., 2011, Pollution of water during underground coal gasification of hard coal and lignite, Fuel, 90, 1927–1934.

Kumabe K., Hanaoka T., Fujimoto S., Minowa T., Sakanishi K., 2007, Co-gasification of woody biomass and coal with air and steam, Fuel, 86, 684–689.

Letellier S., Marias F., Cezac P., Serin J.P., 2010, Gasification of aqueous biomass in supercritical water: an equilibrium analysis, J. Supercrit. Fluids, 51, 353–361.

Li Z., Zhang X., Sugai Y., Wang J., Sasaki K., 2012, Properties and developments of combustion and gasification of coal and char in a CO_2-rich

and recycled flue gases atmosphere by rapid heating, Journal of Combustion, Vol.2012, Article ID 241587, 1-11.

Liu G.S., Niksa S., 2004, Coal conversion submodels for design applications at elevated pressures. Part II. Char gasification, Prog. Energy Combust., 30, 679–717.

Liu K., Song C., Subramani V., 2009, Hydrogen and syngas production and purification technologies, Wiley. http://onlinelibrary.wiley.com/book/10.1002/9780470561256.

Liu S., Wang Y., Yu L., Oakey J., 2006, Thermodynamic equilibrium study of trace element transformation during underground coal gasification, Fuel Process Technol., 87, 209–215.

Liu S.Q., Wang Y.Y., Zhao K., Yang N., 2009, Enhanced-hydrogen gas production through underground gasification of lignite, Min. Sci. Technol. (China), 19, 389–394.

Marcourt M., Paquay V., Piel, A., Jean-Paul, P., 1983, Coal gasification at pressure by mixtures of carbon dioxide and oxygen, Fuel, 62, 823–828.

Molina A., Mondragon F., 1998, Reactivity of coal gasification with steam and CO_2, Fuel, 77, 1831–1839.

Muhammad F.I., Muhammad R.U., Kusakabe K., 2011, Coal gasification in CO_2 atmosphere and its kinetics since 1948: a brief review, Energy, 36, 12–40.

Nandi S.P., Johnson J.L., 2006, Catalytic gasification of lignite chars. Institute of Gas Technology, http://web.anl.gov/PCS/acsfuel/preprint%20archive/Files/24_3_ WASHINGTON_0979_0017.pdf.

Neogi D., Chang C.C., Walawender W.P., Fan L.T., 1986, Study of coal gasification in an experimental fluidized bed reactor, AIChE, 32, 17–28.

Peng F.F., Lee I.C., Yang R.Y.K., 1995, Reactivities of in-situ and ex-situ coal chars during gasification in steam at 1000–1400°C, Fuel Process Technol., 41, 233–251.

Prabhu V., Jayanti S., 2012, Underground coal-air gasification based solid oxide fuel cell system, Appl. Energy, 94, 406–414.

Prins M.J., Ptasinski K.J., Frans T., Janssen J.J.G., 2007, From coal to biomass gasification: comparison of thermodynamic efficiency, Energy, 32, 1248–1259.

Renganathan T., Yadav M.V., Pushpavanam S., Voolapalli R.K., Cho Y.S., 2012, CO_2 utilization for gasification of carbonaceous feedstocks: a thermodynamic analysis, Chem. Eng. Sci., 83, 159–170.

Sekine Y., Ishikawa K., Kikuchi E., Matsukata M., Akimoto A., 2006, Reactivity and structural change of coal char during steam gasification, Fuel, 85, 122–126.

Shabbar S., Janajreh I., 2013, Thermodynamic equilibrium analysis of coal gasification using Gibbs energy minimization method, Energy Convers. Manage., 65, 755-763.

Smolinski A., Howaniec N., Stanczyk K., 2011, A comparative experimental study of biomass, lignite and hard coal steam gasification, Renew Energy, 36, 1836–1842.

Squires R.G., Laurendeau N.M., Koenig P.C., 1986, Effect of potassium carbonate on char gasification by carbon dioxide, J. Catal., 100, 228–239.

Tremel A., Haselsteiner T., Kunze C., Spliethoff H., 2012, Experimental investigation of high temperature and high pressure coal gasification, Appl. Energy, 92, 279–285.

Van Dyk J.C., Keyser M.J., Coertzen M., 2006, Syngas production from South African coal sources using Sasol–Lurgi gasifiers, Int. J. Coal Geol., 65, 243–253.

Wang Z., Zhou J., Wang Q., Fan J., Cen K., 2006, Thermodynamic equilibrium analysis of hydrogen production by coal based on Coal/CaO/H_2O gasification system, Int. J. Hydrogen Energy, 31, 945–952.

Fu W.B., Wang Q.H., 2001, General relationship between the kinetic parameters for the gasification of coal chars with CO_2 and coal type, Fuel Process Technol., 72, 63–77.

Ye D.P., Agnew J.B., Zhang D.K., 1998, Gasification of a South Australian low-rank coal with carbon dioxide and steam: kinetics and reactivity studies, Fuel, 77, 1209–1219.

Yi C.N., Wojciech L., 2012, Thermodynamic analyses of solar thermal gasification of coal for hybrid solar-fossil power and fuel production, Energy, 44, 720–731.

Yu J.L., Tian F.J., Chow M.C., McKenzie L.J., Li C.Z., 2006, Effect of iron on the gasification of Victorian brown coal with steam: enhancement of hydrogen production, Fuel, 85, 127–133.

Chapter 6

DATR in Chemical looping combustion systems

Abstract

Dry autothermal reforming requires CO_2 as feed. Chemical looping combustion generates a CO_2 rich stream. The thermodynamic feasibility of a new process scheme combining chemical looping combustion (CLC) and dry autothermal reforming of propane (LPG) is studied in this chapter. The study of CLC of propane with $CaSO_4$ as oxygen carrier shows thermodynamic feasibility in temperature range (400 – 792.95ºC) at 1 bar pressure. The CO_2 rich stream generated in the CLC can be used for reforming of additional propane in an autothermal way within the temperature range (400 – 1000ºC) at 1 bar pressure to generate syngas (ratio < 3.0 above 600ºC) which is extremely desirable for petrochemical manufacture. The process scheme generates a) huge thermal energy in CLC that can be used for various processes, b) pure N_2 and syngas rich streams can be used for petrochemical manufacture and c) takes care of the expensive CO_2 separation from flue gas stream and also CO_2 sequestration.

CHAPTER 6: DATR in Chemical looping combustion systems

6.1 Introduction

Dry autothermal reforming requires CO_2 as a primary reactant. Chemical looping combustion (CLC) is a new technology that generates CO_2 rich product stream which can be cooled to separate water and generate an almost pure CO_2 stream which can be sequestrated. Combining the CLC process with DATR can help utilize the CO_2 produced in the CLC process.

The thermodynamic feasibility of a new process scheme combining chemical looping combustion (CLC) coupled DATR with steam [also referred as combined reforming (CR)] is studied in this chapter, to facilitate energy production using the existing fossil fuels and reduce carbon footprint thus reducing the impacts of global warming.

6.1.1 Chemical looping combustion

CLC is an emerging area for energy generation that has several advantages like no direct mixing of fuel and air. The CLC system consists of 2 reactors, the fuel is oxidized by the oxygen carrier in fuel reactor (FR) and the reduced oxygen carrier is oxidized (regenerated) by air in the air reactor (AR). The process operates continuously and many oxygen carriers have been evaluated for long term durability of oxidation-reduction cycles. The fuel reactor product stream mainly consisting of steam and CO_2 is usually cooled to condense out water and the pure CO_2 stream is compressed, liquefied and injected deep underground into porous rock for sequestration without separation expense.

Many research groups have published CLC related studies. Lyngfelt et al. (2001) have studied the feasibility of a boiler with two interconnected fluidized bed CLC system. Johansson et al. (2006) have discussed the successful operation of natural gas based CLC system. Abad et al. (2006) reported the operation of a 300 W CLC system using Mn oxygen carrier. Cho et al. (2004)

have reported that Ni, Cu and Fe oxygen carriers showed good reactivity for CLC. Adánez et al. (2004) have studied Cu-based oxygen carriers on SiO_2 or TiO_2 and Fe-based oxygen carriers on Al_2O_3 and ZrO_2. Jin et al. (1999) have reported the development of a better oxygen carrier $NiO/NiAl_2O_4$. Mattisson et al. (2001) have experimentally studied the Fe_2O_3 oxygen carrrier in a fixed bed quartz reactor. Ishida et al. (1996) have studied the effects of reaction temperature, particle size and gas composition on NiO mixed with YSZ particles. Mattisson et al. (2003) have experimentally investigated Cu, Co, Mn, and Ni oxides supported on γ-Al_2O_3. Jin et al. (1998) have reported that synthesized CoO-NiO/YSZ has high reactivity, prevents carbon deposition and shows good repeatability. Mattisson et al. (2004) have studied the Fe_2O_3 particles supported on Al_2O_3, ZrO_2, TiO_2, or $MgAl_2O_4$ supports for CLC. Villa et al. (2003) have studied the preparation, characterization and redox properties of Ni-Al-O and Ni-Mg-Al-O mixed oxides for CH_4 CLC system. Ishida et al. (1998) have identified the conditions for completely preventing carbon formation in CLC systems. Mattisson et al. (2006) have studied the reactivity of NiO with $NiAl_2O_4$, $MgAl_2O_4$, TiO_2 and ZrO_2 in a small fluidized bed simulated CLC system. De Diego et al. (2004) have concluded that Cu based oxygen carriers prepared by mechanical mixing or by coprecipitation showed excellent chemical properties but poor mechanical properties. Cho et al. (2005) have recommended high fuel conversion conditions to avoid carbon formation.

The CLC product stream contains CO_2 and water in a particular ratio depending on the CLC fuel. For e.g. if methane, propane or isooctane are used as CLC fuels, the CLC fuel reactor reactions are:

$CH_4 + 3MeO = CO_2 + 2H_2O + 3Me$ $CO_2:H_2O=1:2$ (0.5)

$C_3H_8 + 10MeO = 3CO_2 + 4H_2O + 10Me$ $CO_2:H_2O=3:4$ (0.75)

C_8H_{18} + 25MeO = 8CO_2 + 9H_2O + 25Me CO_2:H_2O=8:9 (0.89)

Although CLC can generate a CO_2 rich stream, the processing of CO_2 i.e. to compress, liquefy and inject the CO_2 to deep underground into porous rock for sequestration is an expensive and serious issue for safety. Scientists are concerned about carbon dioxide injections triggering seismic activity or leaking out of the reservoirs and no safe explanation has emerged out yet. Secondly, the product stream of fuel reactor is hot and cooling it to separate water and CO_2 is also not very appealing.

Such CLC product streams can be reformed autothermally by using additional fuel and oxygen for conversion of CO_2 to CO, which is a useful syngas component. The quantity of the additional fuel, oxygen and the reactor operating temperature can play a major role in the CO_2 conversion to CO and hence are of prime importance.

This chapter proposes the development of a new process scheme to address these issues by thermodynamically analyzing the favorable conditions for direct feeding the hot CLC product stream to a dry autothermal reformer to produce a syngas rich stream. Pure steam reforming and dry reforming studies have been published, but dry autothermal reforming studies directly applicable to CLC product gas processing have not been published in literature yet. Such an analysis is useful to determine the operational conditions of reformer to maximize the yields of desired products and minimize the undesired product formation. Propane is the major constituent of LPG (easily available commercial fuel) and is hence chosen for this study.

6.1.2 Dry autothermal reformer

In this DATR case, the steam mixed CO_2 stream, fuel and oxygen (air) is used as feed in the DATR reactor. This DATR with steam reforming [also referred

as combined (CO_2 + H_2O) reforming] is a catalytic process that combines steam reforming (SR), dry reforming (DR) and partial oxidation (PO) reactions at thermoneutral conditions (preferably) to produce syngas rich stream. Such combined reforming has also been studied by many researchers. Michael et al. (2009) have experimentally studied the PO, SR and DR of methane on Rh/Al_2O_3 catalysts in one step process. Maestri et al. (2008) have reported microkinetic models for SR and DR of methane on Rh catalysts. Li et al. (2008) have reported optimum reformer conditions for coke elimination in autothermal steam and CO_2 reforming. York et al. (2007) have discussed the carbon deposition and deactivation in combined reforming (oxyforming). Choudhary and Mondal (2006) reported reduced $NdCoO_3$ perovskite-type mixed-oxide catalyst as highly promising material. Song et al. (2004) have studied the thermodynamic analysis and experimental testing of combined reforming of methane in a fixed-bed flow reactor. Le et al. (2004) have studied the low temperature plasma combination of SR and DR. Naqvi and Johnson (2004) have strongly emphasized the idea of producing syngas from CO_2 and steam. Tomishige et al. (2004) have experimentally studied the effect of oxygen addition to steam and dry reforming of methane. Panczyk et al. (2001) have reported the improved coking resistance of commercial catalysts modified by small additions of promoters (K, Ba, Ce, W and Mo). Qin and Lapszewicz (1994) have experimentally studied the MgO-supported noble metal catalysts for combined reforming.

6.2 Conceptual Process Design and Methodology

Figure 6.1 shows the conceptual process design for CLC coupled DATR. Huge thermal energy is generated in the CLC system that can be used for various applications. Generally, oxygen carrier is used in excess to facilitate the complete conversion of fuel to CO_2 and H_2O. It is assumed that the CLC reactors are operated such that the gas leaving the air reactor consists only of nitrogen, while the gas from the fuel reactor consists only of water and carbon

dioxide which can be used as feed for DATR to produce syngas using an additional propane and oxygen (air) to make it autothermal. In (partial / complete) absence of oxygen, the energy required for reformer can also be obtained from the CLC. Such a CLC coupled reforming process can produce energy and syngas (basic building block of petrochemical industry) taking care of CO_2 emissions and expensive CO_2 storage/sequestration problem.

HSC Chemistry software version 5.1 (2002) has been used to generate the data for the study. In the CLC fuel reactor, species such as C_3H_8 (g), CO_2 (g), H_2(g), CO(g), H_2O(g), CH_4(g), O_2(g), N_2(g) H_2O(l) and C(s) are considered. Ethane (C_2H_6) and other C2, C3 species were considered for the study in preliminary cases. Since negligible formation of these hydrocarbons was observed, it was decided to neglect them in further study. The input species are propane, water, air and CO_2 (all in gaseous phase) reacting to give the products. The material and energy balances are done by HSC Chemistry database and the results may be slightly different using different software. The results presented are within reasonable error limit. Any other inerts in feed, product–byproduct formation is not considered in this study. The steam reforming and dry reforming chemistry for hydrocarbon fuels is well established in chemical literature and hence no such details are presented in this chapter.

The products of the CLC fuel reactor will be different for different systems and operating parameters. These are mixed with the additional fuel and fed to the DATR reactor. The chemical reaction occurring inside a typical CLC fuel reactor (assumed for this study) using propane as fuel and $CaSO_4$ as oxygen carrier is represented as:

R1: $C_3H_8(g) + 2.5CaSO_4 = 2.5CaS(g) + 4H_2O(g) + 3CO_2(g)$

The thermodynamic feasibility of CLC using propane as fuel and $CaSO_4$ as oxygen carrier has been investigated as follows:

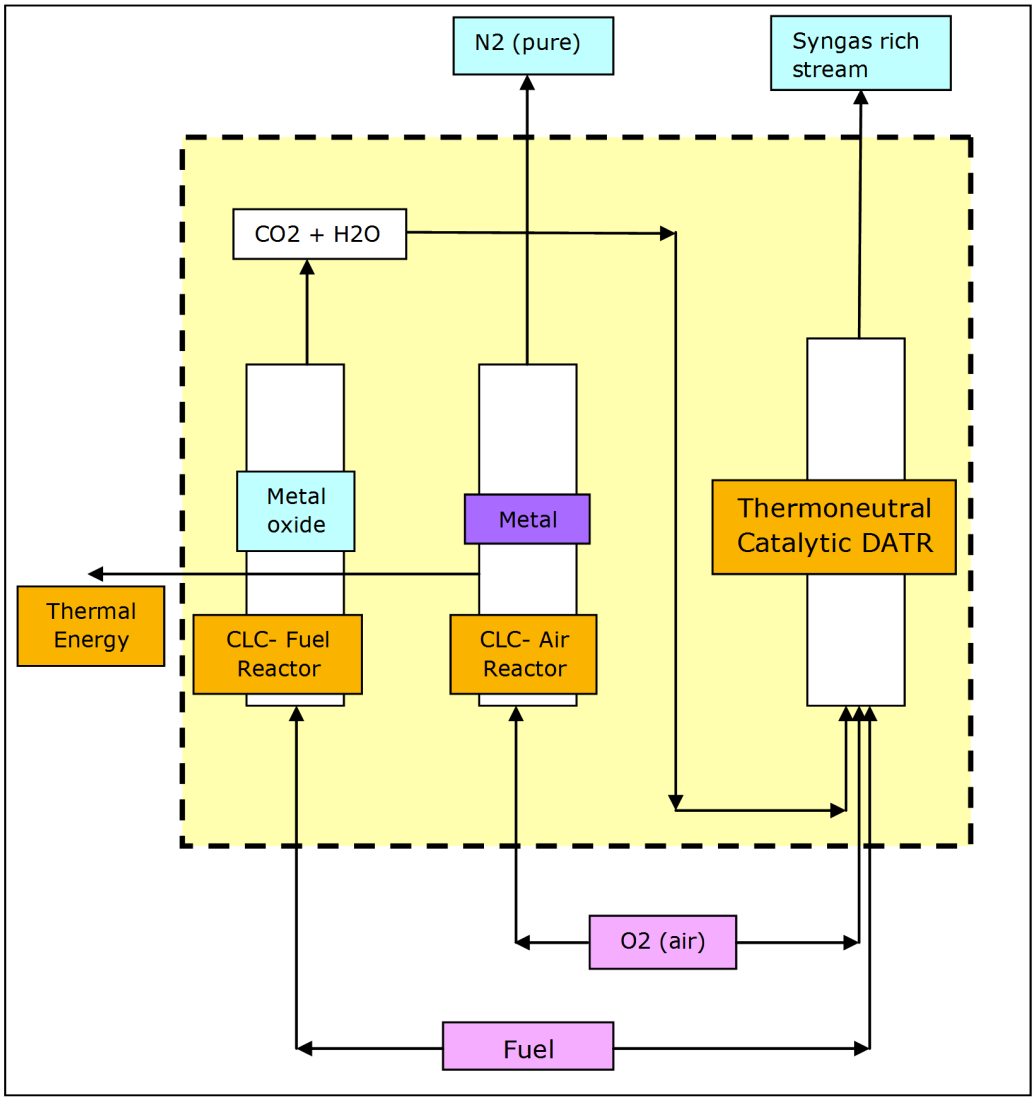

Figure 6.1: Process Diagram of CLC coupled CR

CLC Reactions for Propane fuel:

Fuel Reactor (FR) - mildly endothermic ($\Delta H_{FR} > 0$)

R1 C_3H_8 (g) + 2.5$CaSO_4$ = 2.5CaS + 4H_2O (g) + 3CO_2 (g)

ΔH = 328.95 kJ (750ºC)

Air Reactor (AR) - highly exothermic ($\Delta H_{AR} << 0$)

R2 $CaS + 2\ O_2\ (g) = CaSO_4$

$\Delta H = -950.01$ kJ (750ºC)

Net Reaction - highly exothermic ($\Delta H_{CLC} \equiv \Delta H_{FR} + \Delta H_{AR}$)

R3 $C_3H_8\ (g) + 5\ O_2\ (g) = 3CO_2\ (g) + 4H_2O\ (g)$

$\Delta H = -2046.07$ kJ (750ºC)

The possibility of calcium sulfate forming calcium oxide and sulfur dioxide via reaction (R4) is also considered.

R4 $C_3H_8\ (g) + 10CaSO_4 = 10CaO + 4H_2O\ (g) + 3CO_2\ (g) + 10SO_2\ (g)$

It is assumed that the CLC product stream contains only CO_2 and H_2O in ratio 3:4 and change in oxygen carrier does not alter this ratio as it solely depends on the fuel used. 1 mol propane along with 3 moles CO_2 and 4 moles H_2O in feed with O_2 (g) have been used for all cases. The temperature range of 450 – 950 ºC at 1 bar pressure was used. As steam to carbon ratio (S/C) and CO_2 to carbon in fuel ratio are important parameters in steam and dry reforming processes, similarly variation of feed fuel rate at constant CO_2: H_2O ratio is important factor to study the variation in product distribution of this process, as the combined (CO_2 and H_2O) stream of fixed ratio comes directly from the CLC reactor. Hence variation of input fuel in DATR reactor at constant fuel, CO_2 and H_2O inputs is an important case identified and process product-enthalpy distribution with reactant conversion trends for this case was studied. The variation of feed propane was done by gradually increasing the moles from 0.5 to 1.5 in intervals of 0.5 moles at constant CO_2 and H_2O feeds in the first case (conditions : A, B and C). In the second case, 1 mol propane, 3 mol CO_2 and 4 mol H_2O were kept constant and OCPR (oxygen to carbon in propane ratio) was increased from 0.2 to 1.0 in intervals of 0.2 (conditions:

B2, B4, B6, B8 and B10). The effect on product gas yields, reactant conversions and process enthalpy at different temperatures was analyzed and discussed.

6.3 Results and Discussion

The simple shortcut technique to assess the feasibility of CLC fuel reactor was studied and presented. The effect of temperature and feed variation in combined reforming of propane on the equilibrium product compositions is analyzed and also discussed in this section. The trend with regard to the variation of products for change in reactant propane moles was studied. A detailed analysis along with a graphical representation of the data has been provided in the preceding section.

6.3.1 Gibbs Free Energy of CLC reactions

Figure 6.2 shows the Gibbs free energy change (ΔG) for chemical reactions (R1, R2, R3 and R4) as a function of reaction temperature. The negative value of ΔG implies the feasibility of the reactions (in forward direction).

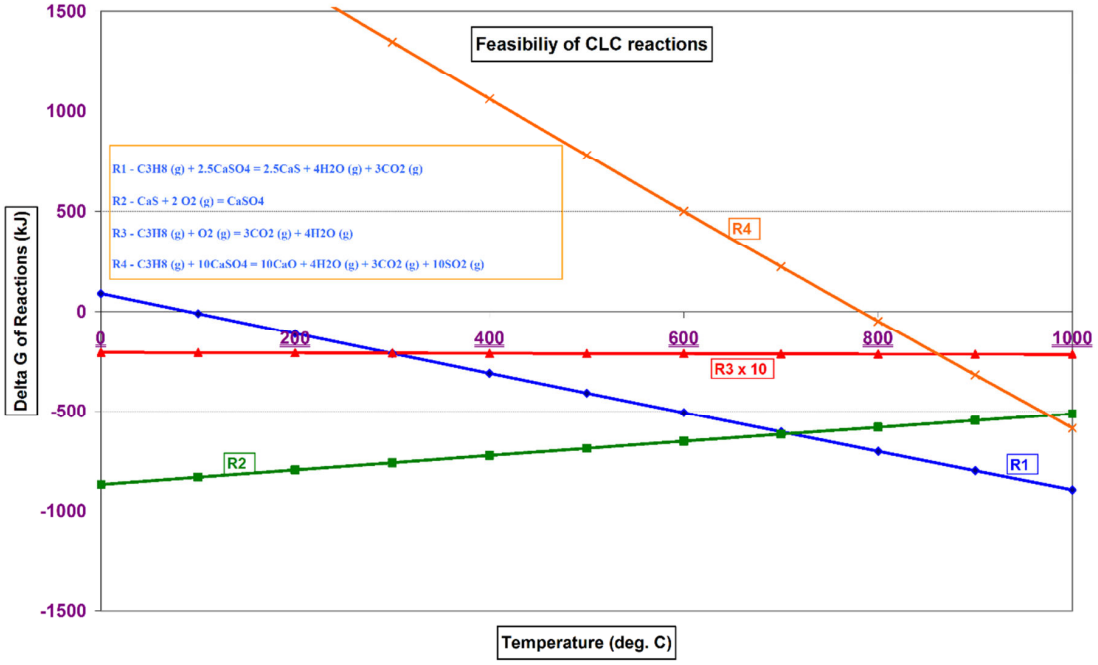

Figure 6.2: Thermodynamic Feasibility of CLC Reactions

It was seen that the feasibility of reaction R2 slightly decreased with increase in temperature. The reactions R1 (favorable) and R4 (undesirable) were found to be competing, and reactor operation below 782.95ºC was found suitable for R1 reaction to produce desired output products, while SO_2 formation seemed negligible at temperatures below 782.95ºC (figure 6.2).

6.3.2 Reaction Enthalpy of DATR reactor

Reaction enthalpy is a very important entity in chemical processes. Since the product stream of CLC reactor will usually be at higher temperature, the only external heat required for the DATR reactor will be mostly consist of the reaction enthalpy of the DATR reaction. The reaction enthalpy for combined reforming of propane without oxygen was studied for molar feed values of C3H8 varying from 0.5 to 1.5, and the results are shown in figure 6.3 (A-B-C). It is observed that the process endothermicity increases with increase in

temperature and also with increase in C_3H_8 feed rate. The reaction enthalpy for the CR process in the temperature range 450 to 950 ºC increases from 178 to 645 kJ, from 191 to 1000 kJ and from 205 to 1360 kJ for propane feed values of 0.5, 1.0 and 1.5 moles respectively. The reaction enthalpy in combined reforming of propane with oxygen addition was studied for OCPR values varying from 0.2 to 1.0 and the results are plotted in figure 6.3 (B2-B10). The point at which the enthalpy curve touches the temperature axis is the thermoneutral point. It is observed that the process endothermicity increases with increase in temperature at constant OCPR and the process endothermicity decreases with increase in OCPR at constant temperature. The reaction enthalpy values range from -1.58 kJ to 771.00 kJ (OCPR=0.2), from -196 kJ to 540 kJ (OCPR=0.4), from -390 kJ to 308 kJ (OCPR=0.6), from -587 kJ to 75.20 kJ (OCPR=0.8) and from -792 to -158 kJ (OCPR=1.0) within the temperature range 450 – 950 ºC for the process. The thermo-neutral temperatures (within 450 – 950 ºC range considered in this study) were observed for OCPR values of 0.4, 0.6 and 0.8 and located at 537.55ºC, 626.73ºC and 873.13ºC respectively.

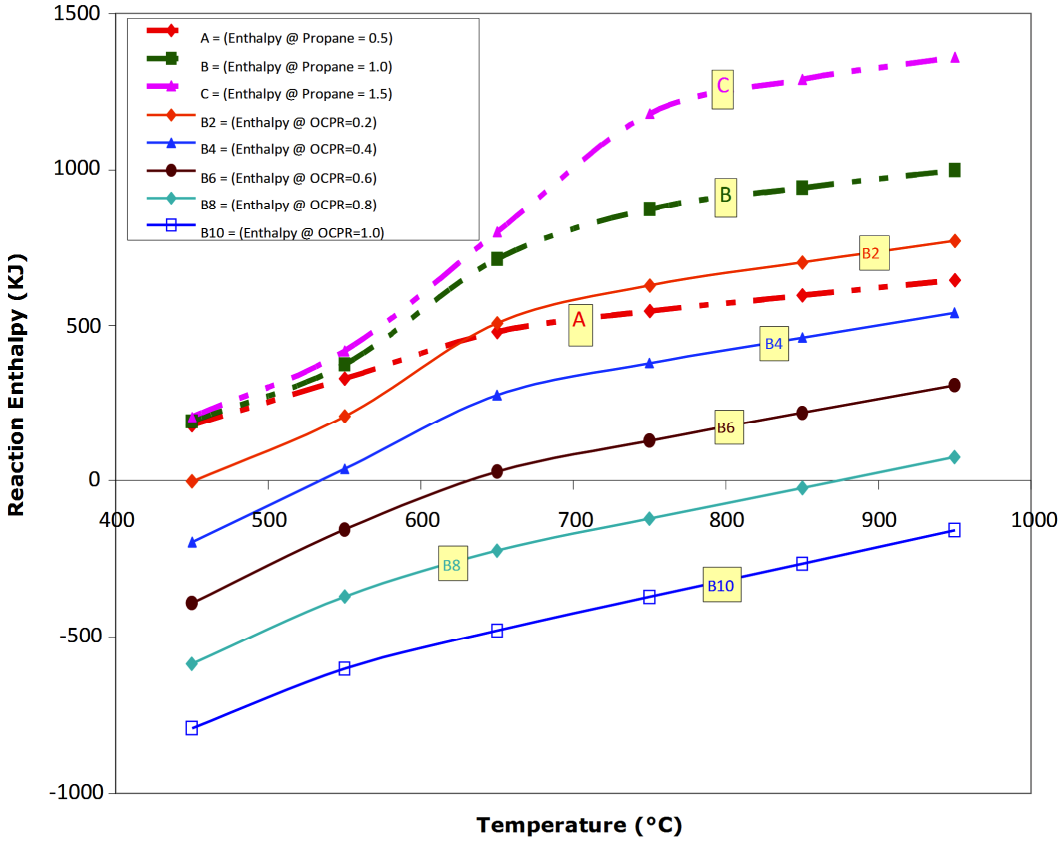

Figure 6.3: Enthalpy of combined reforming

6.3.3 Hydrogen yield

Hydrogen is a valuable product of reforming processes as it has many applications including use in fuel cells and syngas production. The H_2 yield for combined reforming of propane without oxygen input was studied and the results obtained are shown in figure 6.4 (A-B-C). It was observed that the H_2 yield generally increases, reaches a maximum value and then decreases with increase in CR temperature and the H_2 yield is directly proportional to the moles of C_3H_8 in feed. The maximum hydrogen yield for increase in C_3H_8 feed from 0.5 to 1.5 moles was found to be 3.14, 5.79 and 8.48 moles at temperatures 667.5°C, 748°C and 827°C respectively. However, it was also found that the hydrogen yield per mole propane feed declined from 6.28 (0.5

mol propane) to 5.79 (1 mol propane) and 5.65 (1.5 mol propane). The H_2 yield for combined reforming of propane (constant 1 mol) with gradual increase in oxygen feed is also shown in figure 6.4 (B2-B10). In this case too, it was observed that the H_2 yield initially increased, reached a maximum value and then decreased with increase in DATR temperature and the lower OCPR feed gave higher hydrogen yield (T > 600ºC). The maximum hydrogen yields for increase in OCPR from 0.2 to 1.0 were found to be 5.25, 4.71, 4.16, 3.56 and 2.9 moles at temperatures of 706.5°C, 670.5°C, 636.5°C, 606.5 and 576°C respectively. The hydrogen yields at thermo-neutral temperatures for OCPR values of 0.4, 0.6 and 0.8 were 3.19, 4.15 and 2.82 moles respectively. It is observed that as the OCPR increases, the thermo-neutral temperatures increase, but the H_2 yield first increases and then decreases.

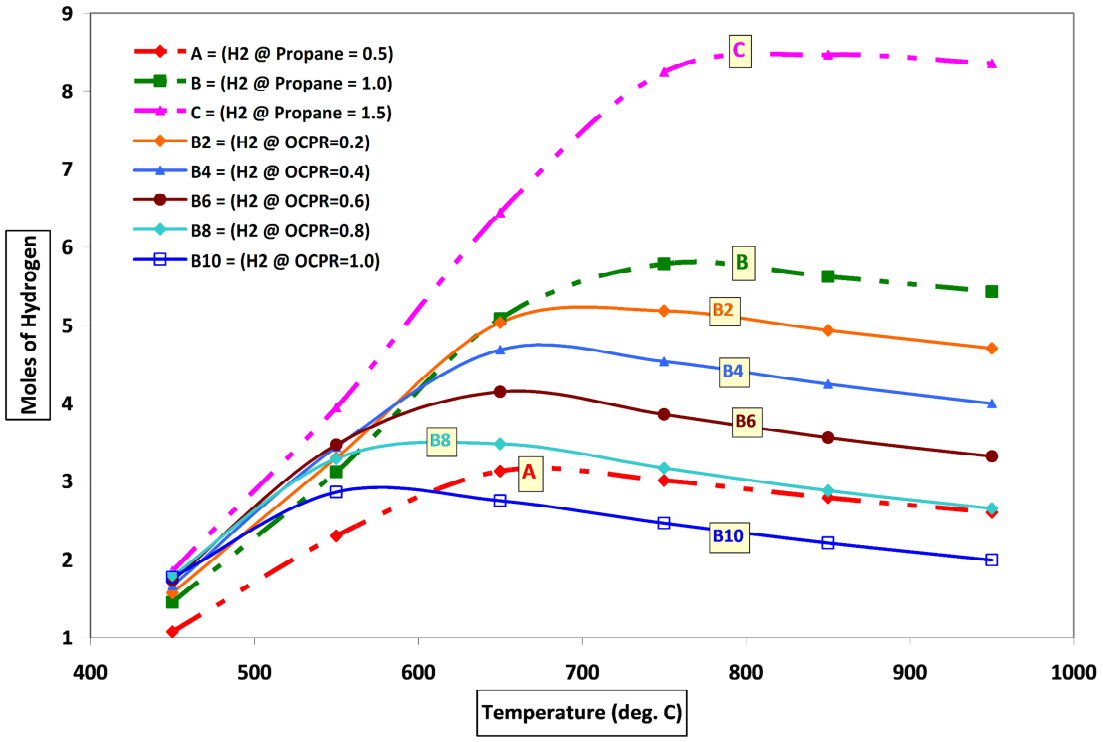

Figure 6.4: Hydrogen yield in combined reforming of propane

6.3.4 Carbon Monoxide yield

The CO yield for combined reforming of propane without oxygen feed for variation in feed of C_3H_8 moles from 0.5 to 1.5 is shown in figure 6.5 (A-B-C). It was observed that the CO yield generally increases with increase in DATR process temperature and it is directly proportional to the feed moles of C_3H_8 at higher temperatures. It was seen that the CO yield was similar for all C_3H_8 molar feed values at lower temperature (<550ºC), but later increased with higher C_3H_8 molar feed values and then increased very slowly at higher temperatures. The maximum CO yields for increase in C_3H_8 feed moles from 0.5 to 1.0 and 1.5 were found to be 2.40 moles, 4.56 moles, 6.63 moles respectively at 950°C, while the corresponding minimum CO yields were found to be 0.133 moles, 0.134 moles, 0.135 moles respectively at 450°C. The CO yield for combined reforming of propane with oxygen is shown in figure 6.5 (B2-B10). It was observed that the CO yield increased with increase in CR temperature, but it decreased with increase in OCPR at constant temperature. Higher CO yield was favored by lower OCPR and higher temperatures.

The maximum CO yields for increase in OCPR were found to be 4.09 moles (for OCPR = 0.2), 3.85 moles (for OCPR = 0.4), 3.08 moles (for OCPR = 0.6), 2.55 moles (for OCPR = 0.8) and 2.00 moles (for OCPR = 1.0) at 950°C, while the minimum CO yields were found to be 0.167 (for OCPR 0.2), 0.183 (for OCPR = 0.4), 0.231 (for OCPR = 0.6), 0.256 (for OCPR = 0.8) and 0.24 (for OCPR = 1.0) at 450°C. The CO yields at thermo-neutral temperatures for OCPR values of 0.4, 0.6 and 0.8 were found to be 0.98, 1.97 and 2.38 moles. Thus as the OCPR increased, the thermo-neutral temperature and the CO yield both increased.

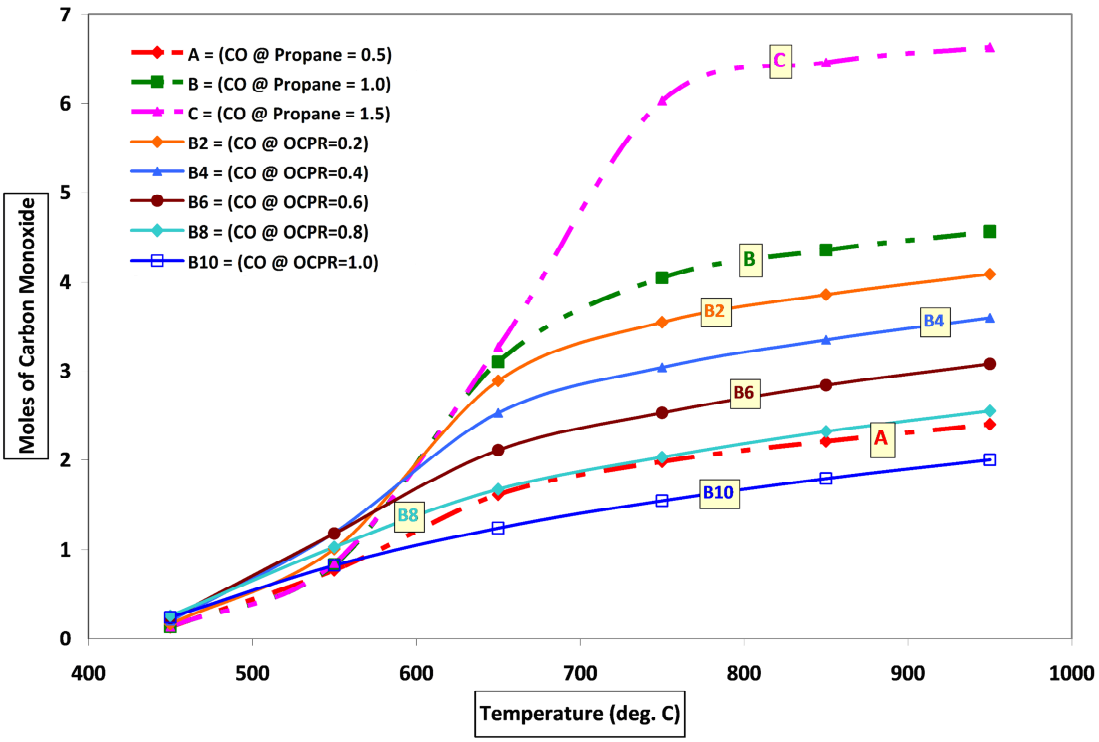

Figure 6.5: Carbon monoxide yield in combined reforming

6.3.5 CO_2 Conversion

The main objective of combined reforming process is to utilize CO_2 to produce valuable products such as hydrogen / syngas and sometimes also carbon as CNF (carbon nanofilaments) formation has been reported by some researchers in CO_2 reforming. The estimation of CO_2 conversion at various temperatures and feed variations is therefore important. The CO_2 conversion (%) obtained in combined reforming of propane without oxygen input was studied for variation in molar feed values of C_3H_8 from 0.5 to 1.5 and the results were plotted in figure 6.6 (A-B-C). It was observed that the CO_2 conversion initially decreased with increase in DATR temperature (till 550 ºC) but then increased with temperature for all feed molar values of C_3H_8. It is evident from the graph that higher CO_2 conversion is favored by higher C_3H_8 molar values and higher temperatures. The maximum CO_2 conversions obtained for C_3H_8 feed moles of 0.5, 1 and 1.5 were found to be 30.00, 52.00

and 71.07 respectively at 950°C. The CO_2 conversion for combined reforming of propane with oxygen addition was studied for OCPR increase from 0.2 to 1.0 and the results obtained were plotted in figure 6.6 (B2-B10). The CO_2 conversion initially decreased for OCPR 0.2 and 0.4 but later increased for OCPR 0.6, 0.8 and 1.0, with increase in DATR temperature. It is seen from the graph that higher CO_2 conversions are favored by higher temperatures and lower OCPR. The negative value of CO_2 conversion depicts more CO_2 emission from the process.

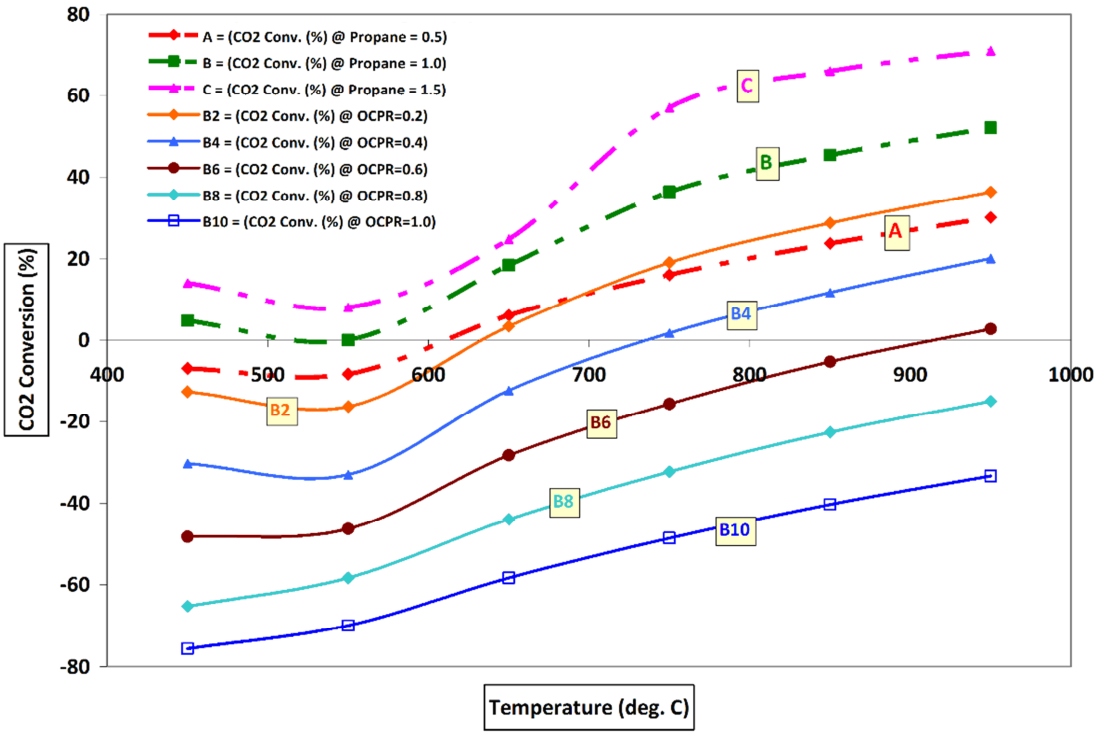

Figure 6.6: CO_2 conversion in combined reforming of propane

The minimum CO_2 conversion for oxygen addition to the CR process was found to be -75.67% at OCPR 1.0 and 450°C, while the maximum CO_2 conversion was found to be 36.33 at 0.2 OCPR and 950°C. The CO_2 conversion at thermo-neutral temperatures for OCPR values of 0.4, 0.6 and 0.8 were found to be -33.82%, -32.21% and -20.81% suggesting that thermoneutral operation of the process at these points may not contribute to

CO_2 sequestration. It was observed that as the OCPR increased the thermo-neutral temperature and the CO_2 conversion both increased.

6.3.6 CH_4 formation

Methane formation is assumed in all reforming process calculations as it is a very stable hydrocarbon and is mostly present in products of reforming processes. The CH_4 yield in combined reforming of propane without oxygen with varying the propane moles in feed (from 0.5 to 1.5 moles) was studied and the results obtained were plotted in figure 6.7 (A-B-C). It was observed that the CH_4 yield generally decreased with increase in CR temperature and finally became zero for all cases. It was also seen that the lower CH_4 yield was favored by lower propane feeds and higher temperatures. The methane yield decreased from 1.72 moles (450ºC) to zero moles (950ºC); from 1.20 moles (450ºC) to zero moles (850ºC) and from 0.74 moles to zero moles (750ºC) for the propane feed moles of 1.5, 1.0 and 0.5 moles respectively. The CH_4 yield for variation in OCPR at constant propane, CO_2 and water inputs to the CR reactor was studied and the results are shown in figure 6.7 (B2-B10). It was observed that the methane formation was favored at lower temperatures and lower OCPR. The methane yields for all OCPR values finally decreased to zero value at higher temperatures. The maximum CH_4 yields were found to be 1.07 (OCPR = 0.2), 0.98 (OCPR = 0.4), 0.90 (OCPR = 0.6), 0.79 (OCPR = 0.8), 0.49 (OCPR = 1.0) at 450ºC. It was also observed that as the OCPR increased, the temperatures for getting zero methane yields decreased. The CH_4 yields at thermo-neutral temperatures for OCPR values of 0.4, 0.6 and 0.8 were found to be 0.71, 0.07 and 0.00 moles. Thus it was observed that as the OCPR increased, the thermo-neutral temperature increased and the CH_4 yield decreased.

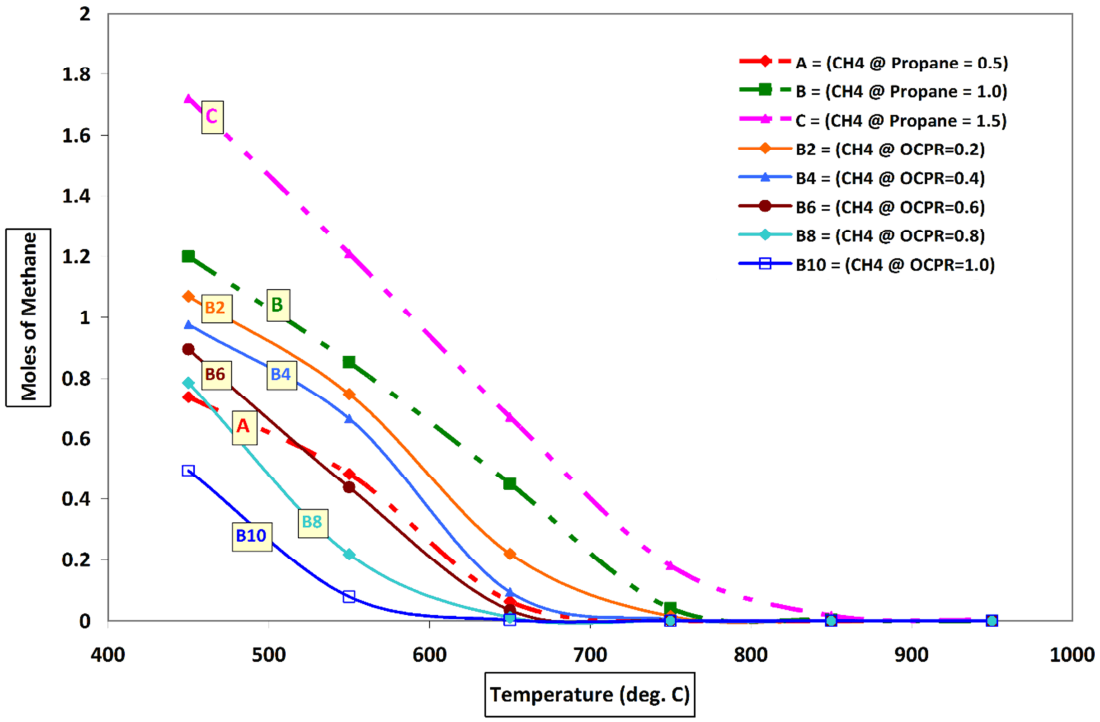

Figure 6.7: Methane yield in combined reforming of propane

6.3.7 Syngas (H_2+CO) yield

The syngas (H_2+CO) yield is the most important component of this thermodynamic study. Syngas is the most useful product of reforming processes and has multiple applications. The syngas yield in combined reforming of propane without oxygen addition was studied for variation in molar feed values of C3H8 from 0.5 to 1.5 and the results obtained were shown in figure 6.8 (A-B-C). It was observed that the syngas yield increased with increase in CR temperature till a certain temperature and then remained almost constant. The syngas yield increased with increase in propane feed. It was seen that the syngas yield increases from 1.21(450ºC) to 4.99 (750ºC), increases from 1.59 (450ºC) to 9.99 (850ºC) and increases from 2.00 to 14.99 (950ºC) for propane feeds of 0.5, 1.0 and 1.5 moles respectively. The results of the syngas yield in combined reforming of propane for increase in oxygen input are shown in figure 6.8 (B2-B10). The syngas yield generally showed decline with increase in OCPR. It was seen from the graph that higher syngas

yield was favoured by higher temperatures and lower OCPR. The maximum syngas yields were found to be 8.80 (OCPR = 0.2, T > 850ºC), 7.60 (OCPR =0.4, T > 750ºC), 6.40 (OCPR = 0.6, T > 750ºC), 5.20 (OCPR = 0.8, T > 750ºC) and 4.00 (OCPR = 1.0, T > 650ºC). The syngas moles obtained in the temperature range of 450 – 950 ºC ranged from 1.75 to 8.80, 1.87 to 7.60, 1.97 to 6.40, 2.06 to 5.20 and 2.02 to 4.00 for OCPR increase from 0.2 to 1.0 showing a decrease in range with increase in temperature and OCPR. The syngas yields at thermo-neutral temperatures for OCPR values of 0.4, 0.6 and 0.8 were found to be 4.17, 6.11 and 5.20 moles respectively. It was seen that as the OCPR increased, the thermo-neutral temperature increased and the syngas yield first increased and then decreased.

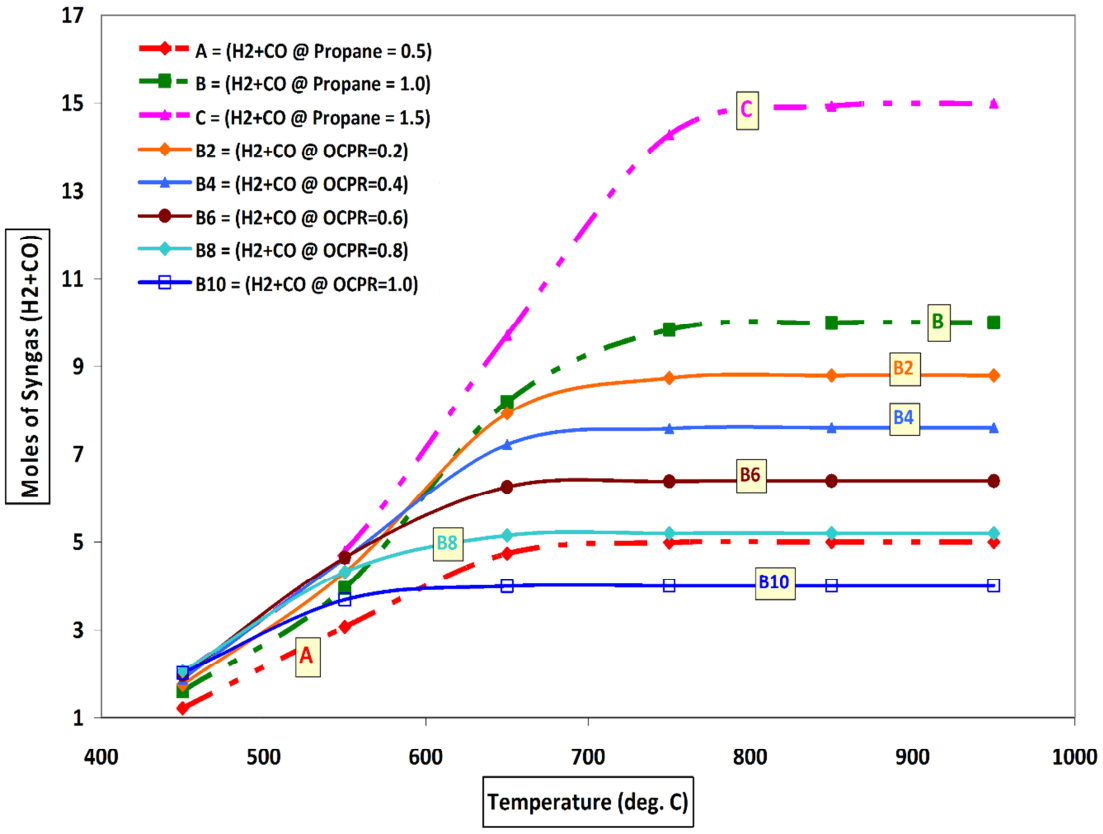

Figure 6.8: Syngas yield in combined reforming of propane

6.3.8 Syngas ratio (H_2/CO)

Syngas ratio is an important factor for petrochemical manufacture by FT synthesis and the desirable syngas ratio range is 1 to 3. The variation of product syngas ratio in combined reforming of propane for increase in molar feed of C_3H_8 from 0.5 to 1.5 without oxygen input was studied and the results obtained were plotted in figure 6.9 (A-B-C). It was observed that the syngas ratio decreased with increase in CR temperature for all cases. The initial decrease in the syngas ratio was very steep between 450 – 550ºC, i.e. 8.12 to 2.99, 10.90 to 3.75 and 13.78 to 1.26 but later the decrease was slow to final values of 1.08, 1.19 and 1.26 at 950ºC for propane feeds of 0.5, 1.0 and 1.5 moles respectively. It was also seen that higher propane in feed showed higher syngas ratio values. Thus lower syngas ratio was favored by lower C_3H_8 feed and at high temperatures. The variation of product syngas ratio in combined reforming of propane with increase in oxygen to feed was studied and the results were plotted in figure 6.9 (B2-B10). It is observed that the syngas ratio decreased rapidly at lower temperatures (450 – 550ºC) and then slowly decreased at higher temperatures. Thus a lower syngas ratio was favoured by higher temperatures and higher OCPR. The syngas ratios in the range of 4.00 to 1.00 are obtained in the temperature range 550 – 950ºC. The maximum syngas ratio values observed at 450ºC showed a decrease with increase in OCPR, i.e. 9.46 (OCPR=0.2), 8.39 (OCPR=0.4), 7.53 (OCPR=0.6) till 7.03 (OCPR=0.8) before increasing to 7.45 (OCPR=1.0). The syngas ratio values obtained at thermo-neutral temperatures for OCPR values of 0.4, 0.6 and 0.8 were found to be 3.25, 2.11 and 1.19 respectively. It was observed that as the OCPR increased, the thermo-neutral temperature increased and the syngas ratio decreased.

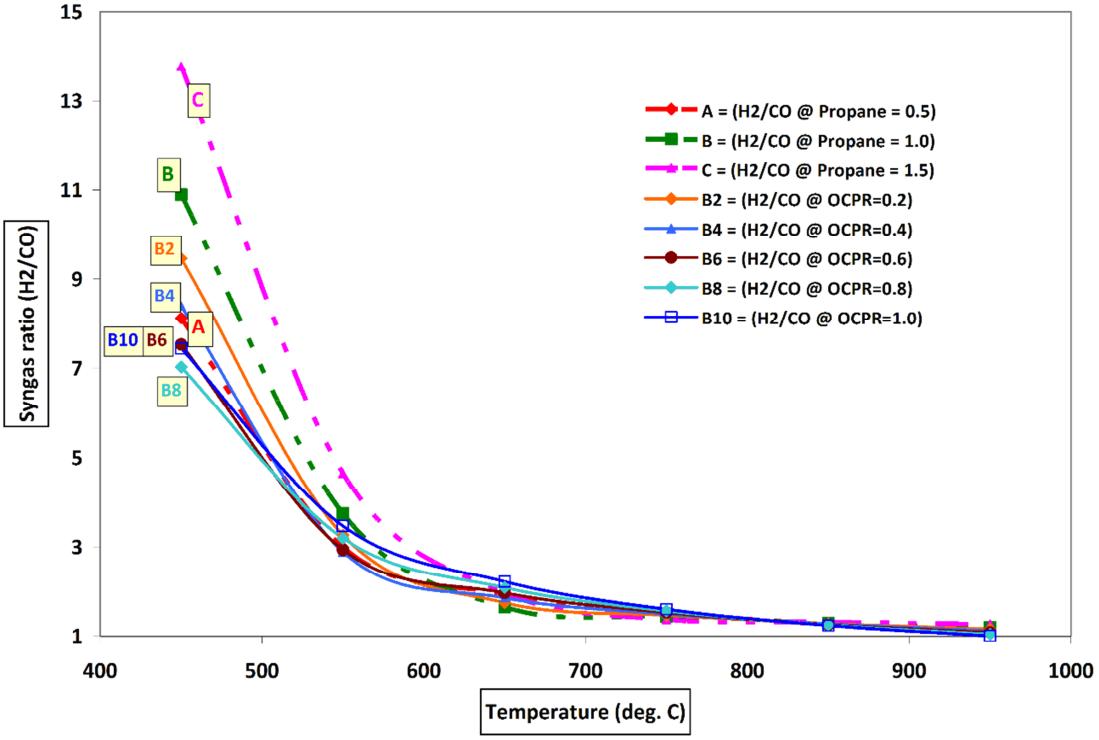

Figure 6.9: Syngas ratio in combined reforming of propane

6.3.9 Carbon formation

Usually carbon is also an undesired product of reforming processes; however carbon formation in the form of CNF (carbon nanofilament) has been proved valuable in some dry reforming studies. Hence estimation of carbon yield for variations in feed and temperature was also studied. The results obtained for variation of carbon yield at different propane feeds in DATR is shown in figure 6.10 (A-B-C). It was observed that higher propane feed resulted in higher carbon formation and the carbon formation decreased to zero at higher temperatures. The carbon yield decreased from 0.42 (450ºC) to zero (550 – 950ºC), 1.81 (450ºC) to zero (650 – 950ºC) and 3.07 (450ºC) to zero (750ºC – 950ºC) for propane feed values of 0.5, 1.0 and 1.5 moles respectively. The carbon yield in combined reforming of propane with increase in oxygen addition was studied and the results were plotted in figure 6.10 (B2-B10). It

was seen that lower carbon yield was favored by higher temperatures and higher OCPR.

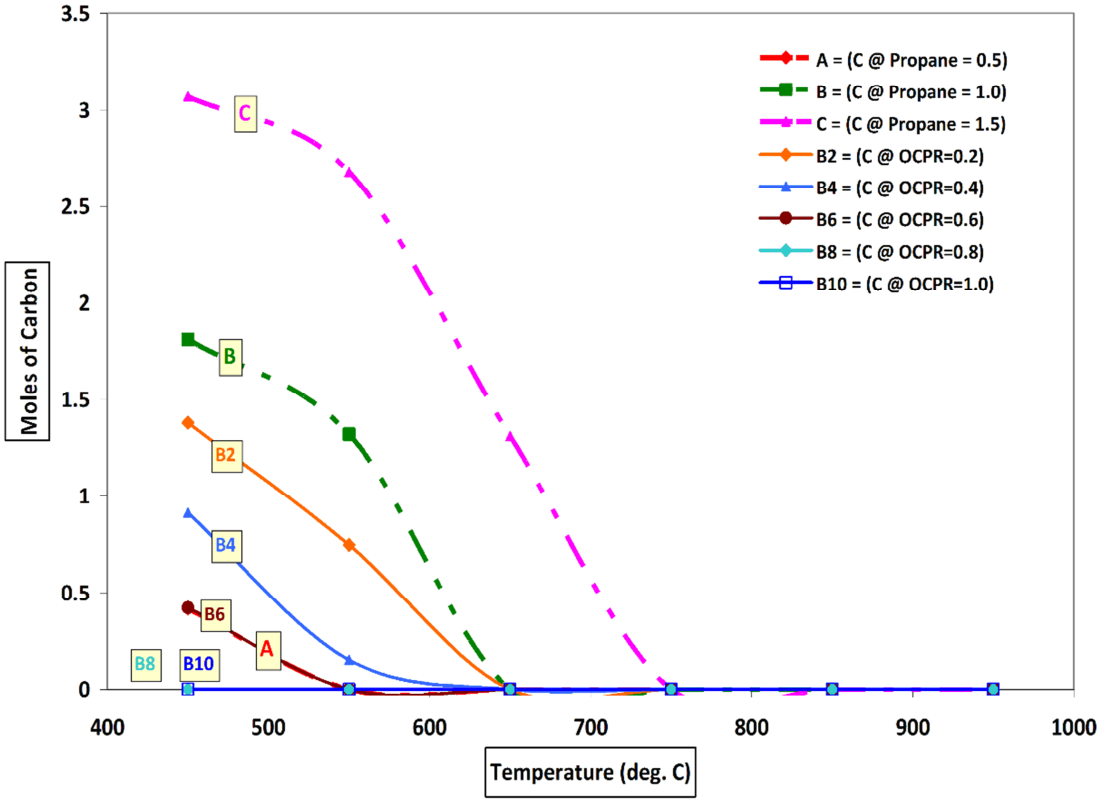

Figure 6.10: Carbon formation in combined reforming of propane

The carbon yields obtained at various OCPRs decreased from 1.38 (450ºC) to zero (650 – 950ºC), 0.91 (450ºC) to zero (650 – 950ºC) and 0.42 (450ºC) to zero (550 – 950ºC) for OCPR values of 0.2, 0.4 and 0.6 respectively. No carbon formation in the temperature range of 450 – 950ºC was observed at OCPR values of 0.8 and 1.0. The carbon yields obtained at thermo-neutral temperatures for OCPR values of 0.4, 0.6 and 0.8 were found to be 0.29, 0.00 and 0.00. It was seen that as the OCPR increased, the thermo-neutral temperature increased and the carbon formation decreased.

6.3.10 H_2O conversion

Water is one of the feed components to the DATR reactor. In the DATR, maximizing CO_2 conversion is essential, but water conversion can also lead to maximize syngas yield. Water formation is also imminent in reforming processes. Hence process conditions for maximizing water conversion and minimizing water formation in such processes are also important study points. The H_2O conversion in DATR of propane was studied for molar feed values of C_3H_8 varying from 0.5 to 1.5, without oxygen and the results were plotted in figure 6.11 (A-B-C). It was observed that the water conversion initially increased, reached a maximum value and then decreased with increase in CR temperature and higher propane feed required higher CR temperatures yielding higher water conversion at those temperatures. Some negative water conversion data points are also observed at lower CR temperature indicating more water formation in the CR process at those points, however positive water conversion is observed above 525ºC for all cases. The H_2O conversion for combined reforming of propane with oxygen addition at various OCPR values was plotted in figure 6.11 (B2-B10). The H_2O conversion plot showed the similar variation as seen in case without oxygen addition but with much lower conversion values for all OCPR cases. It was seen from the graph that higher H_2O conversions are favored at middle temperatures (500 – 700ºC) and lower OCPR conditions. The water conversion values obtained at thermo-neutral temperatures for OCPR values of 0.4, 0.6 and 0.8 were found to be 15.28, 7.25 and -29.39. Hence it was observed that as the OCPR increased, the thermo-neutral temperature increased but the water conversion decreased.

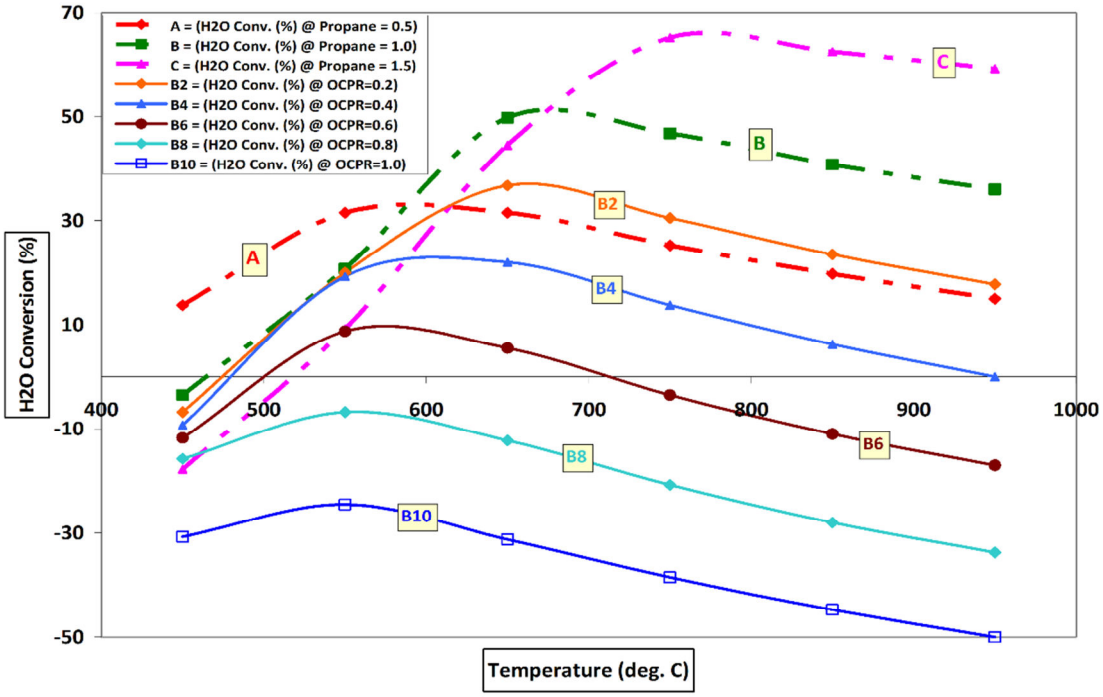

Figure 6.11: H_2O conversion in combined reforming of propane

6.4 Conclusion

The thermodynamic feasibility of a new process scheme of CLC coupled DATR is studied. The CLC of propane with $CaSO_4$ as oxygen carrier and CR of propane seem thermodynamically feasible. The thermal energy obtained by traditional air combustion from 2 moles of C_3H_8 is -4092 kJ (750ºC), but it leads to flue gas containing NO_x, N_2, CO_2 and H_2O, where the separation of components is expensive and hence it is emitted to atmosphere, which increases the carbon footprint. In the new scheme presented in this chapter, the net energy obtained from 2 moles (total) of C_3H_8 is -2046.07 kJ (~1/2 of the traditional process) and a pure N_2 stream for ammonia manufacture and a syngas rich stream for FT synthesis of liquid fuels / petrochemicals is also obtained. The dry autothermal combined reformer operating at thermoneutral temperatures provides a good syngas ratio for FT synthesis. The maximum syngas moles (5.98 moles per mole propane fed) of syngas ratio 1.73 with negligible methane and carbon formation is obtained at TNP 702.12 ºC and

this was identified as the best condition for the CR reactor operation. In DATR combined reformer, the CO_2 conversion is very important and it decreased with increase in OCPR. Hence, lower OCPR and higher temperature seemed optimum for CO_2 conversion from the CLC stream. Lower OCPR would need additional heat from CLC process. This might be permissible as the net heat from CLC process is huge. Positive CO_2 conversion is observed at C (all cases), B (above 550ºC), A (above 650ºC), B2 (above 650ºC), B4 (above 750ºC), B6 (above 925ºC), while the enthalpy requirements for the process operating above 650ºC are low in the order B6 > B4 > A > B2 > B > C. The moles of syngas generated above 650ºC followed the pattern A < B6 < B4 < B2 < B < C. It was concluded that higher CO_2 conversion to syngas would require higher energy from the CLC reactor. Operation of the DATR reactor with OCPR 0.2 above 650ºC was found to be the best operating point from view of balanced CO_2 conversion – enthalpy requirements – syngas generation with zero carbon and low methane formation. The process scheme takes care of the hot CO_2 and steam obtained in CLC to generate syngas, thus solving the expensive CO_2 sequestration issue. This process scheme can be used for a variety of fossil fuels.

6.5 References

Abad A., Mattisson T., Lyngfelt A., Rydén M., 2006, Chemical-looping combustion in a 300W continuously operating reactor system using a manganese-based oxygen carrier, Fuel, 85(9), 1174–1185.

Adanez J., De Diego L.F., Garcia-Labiano F., Gayán P., Abad A., Palacios J.M., 2004, Selection of oxygen carriers for chemical-looping combustion, Energy Fuel, 18(2), 371–377.

Blanchard J., Oudghiri-Hassani H., Abatzoglou N., Jankhah S., Gitzhofer F., 2008, Synthesis of nanocarbons via ethanol dry reforming over a carbon steel catalyst, Chem. Eng. J., 143(1), 186-194.

Cho P., Mattisson T., Lyngfelt A., 2004, Comparison of iron-, nickel-, copper- and manganese-based oxygen carriers for chemical-looping combustion, Fuel, 83(9), 1215–1225.

Cho P., Mattisson T., Lyngfelt A., 2005, Carbon formation on nickel and iron oxide containing oxygen carriers for chemical-looping combustion, Indus. Eng. Chem. Res., 44(4), 668–676.

Choudhary V.R., Mondal K.C., 2006, CO_2 reforming of methane combined with steam reforming or partial oxidation of methane to syngas over $NdCoO_3$ perovskite-type mixed metal-oxide catalyst, Appl. Energy, 83(9), 1024–1032.

De Diego L.F., García-Labiano F., Adánez J., Gayán P., Abad A., Corbella B.M., 2004, Development of Cu-based oxygen carriers for chemical-looping combustion, Fuel, 83(13), 1749–1757.

HSC Chemistry [software], version 5.1, 2002, Pori: Outokumpu Research, Oy.

Ishida M., Jin H., Okamoto T., 1996, A fundamental study of a new kind of medium material for chemical-looping combustion, Energy Fuel, 10(4), 958–963.

Ishida M., Jin H., Okamoto T., 1998, Kinetic behavior of solid particle in chemical looping combustion: suppressing carbon deposition in reduction, Energy Fuel, 12(2), 223–229.

Jankhah S., Abatzoglou N., Gitzhofer F., 2008, Thermal and catalytic dry reforming and cracking of ethanol for hydrogen and carbon nanofilaments' production, Int. J. Hydrogen Energy, 33(18), 4769-4779.

Jin H., Okamoto T., Ishida M., 1998, Development of a novel chemical-looping combustion: synthesis of a looping material with a double metal oxide of CoO–NiO, Energy Fuel, 12(6), 1272–1277.

Jin H., Okamoto T., Ishida M., 1999, Development of a novel chemical-looping combustion: synthesis of a solid looping material of $NiO/NiAl_2O_4$, Indus. Eng. Chem. Res., 38(1), 126–132.

Johansson E., Mattisson T., Lyngfelt A., Thunman H., 2006, A 300W laboratory reactor system for chemical-looping combustion with particle circulation, Fuel, 85(10–11), 1428–1438.

Le H., Hoang T., Mallinson R., Lobban L., 2004, Combined steam reforming and dry reforming of methane using AC discharge, Stud. Surf. Sci. Catal., 147, 175–180.

Li Y., Wang Y., Zhang X., Mi Z., 2008, Thermodynamic analysis of autothermal steam and CO_2 reforming of methane, Int. J. Hydrogen Energy, 33(10), 2507–2514.

Lyngfelt A., Leckner B., Mattisson T., 2001, A fluidized-bed combustion process with inherent CO_2 separation; application of chemical-looping combustion, Chem. Eng. Sci., 56(10), 3101–3113.

Maestri M., Vlachos D.G., Beretta A., Groppi G., Tronconi E., 2008, Steam and dry reforming of methane on Rh: microkinetic analysis and hierarchy of kinetic models, J. Catal., 259(2), 211–222.

Mattisson T., Lyngfelt A., Cho P., 2001, The use of iron oxide as an oxygen carrier in chemical-looping combustion of methane with inherent separation of CO_2, Fuel, 80(13), 1953–1962.

Mattisson T., Järdnäs A., Lyngfelt A., 2003, Reactivity of some metal oxides supported on alumina with alternating methane and oxygen – application for chemical looping combustion, Energ Fuel, 17(3), 643–651.

Mattisson T., Johansson M., Lyngfelt A., 2004, Multicycle reduction and oxidation of different types of iron oxide particles-application to chemical-looping combustion, Energy Fuel, 18(3), 628–637.

Mattisson T., Johansson M., Lyngfelt A., 2006, The use of NiO as an oxygen carrier in chemical-looping combustion, Fuel, 85(5–6), 736–747.

Michael B.C., Donazzi A., Schmidt L.D., 2009, Effects of H_2O and CO_2 addition in catalytic partial oxidation of methane on Rh., J. Catal., 265(1), 117–129.

Naqvi S., Johnson E., 2004, Reforming: syngas solution?, EuroChem News, 81, (2116):21.

Panczyk M., Giecko G., Gac W., Pasieczna S., Stasinska B., Borowiecki T., 2001, Nickel promoted catalysts in the reforming of n-butane with CO_2 or H_2O, Adsorpt. Sci. Technol., 19(6), 455–464.

Qin D., Lapszewicz J., 1994, Study of mixed steam and CO_2 reforming of CH_4 to syngas on MgO-supported metals, Catal. Today, 21(2–3), 551–560.

Smith W.R., 1996, Computer software reviews, HSC chemistry for windows, 2.0, J. Chem. Inf. Comput. Sci., 36(1), 151–152.

Song C., Pan W., Srimat S.T., Zheng J., Li Y., Wang Y.H., 2004, Tri-reforming of methane over Ni catalysts for CO_2 conversion to Syngas with desired H_2/CO ratios using flue gas of power plants without CO_2 separation, Stud. Surf. Sci. Catal., 153, 315–322.

Tomishige K., Nurunnabi M., Maruyama K., Kunimori K., 2004, Effect of oxygen addition to steam and dry reforming of methane on bed temperature profile over Pt and Ni catalysts. Fuel Process. Technol., 85(8–10) 1103–1120.

Villa R., Cristiani C., Groppi G., Lietti L., Forzatti P., Cornaro U., 2003, Ni based mixed oxide materials for CH_4 oxidation under redox cycle conditions, J. Mol. Catal. A: Chem., 204/205, 637–646.

York A.P.E., Xiao T.C., Green M.L.H., Claridge J.B., 2007, Methane oxyforming for synthesis gas production, Catal. Rev. Sci. Eng., 49(4), 511–560.

Chapter 7

Concluding remarks

CHAPTER 7: Concluding remarks

7.1 Conclusions

In this doctorial thesis, we were successful in establishing the thermodynamic feasibility of dry autothermal reforming in many industrial sectors with important applications. This thermodynamic analysis vital step was successful in establishing process feasibility to mark the domain of process operation, evaluate the trends of product compositions and also find the optimum operating conditions. The DATR process theme can be used for CO_2 utilization to produce syngas that has many uses. The thermodynamics of the DATR process was successfully studied using a variety of fuels and the results obtained can pitch for the process and catalyst development programs to make the DATR process commercial similar to the steam and autothermal reforming processes. Steam addition to DATR also produced positive results in specific cases. This research work also focused on the important aspects of thermoneutral conditions in autothermal processes taking the example of DATR. The available literature on “thermoneutral conditions in autothermal processes” is very limited and hence the research work related to the thermoneutral conditions in DATR, presented in this work, can be used as guideline for different autothermal processes. The results obtained in this work are highly encouraging to start further R & D in this area.

7.2 Recommendations

Although thermodynamics is a basic step for process feasibility analysis, the later steps of catalyst and process development can be started provided the results of the thermodynamic analysis are encouraging for process development. Since thermodynamics defines the maximum possible conversions and product yield for the specific feed conditions, the data presented in the thesis can be used as benchmark for catalyst development programs. These steps can vary from fuel to fuel and system to system can themselves form the basis for future research thesis programs. For e.g. the

dry autothermal reforming of glycerol can further researched branching into catalyst development, reactor development and bench scale process development and can form a future thesis work. Similarly the other chapters can be extended to further thesis works.

7.3 Publications from the work done in this thesis

Kale G.R., Kulkarni B.D., 2010, Thermodynamic analysis of dry autothermal reforming of glycerol, Fuel Processing Technology, 91, 520-530.

Kale G.R., Kulkarni B.D., 2010, Thermoneutral point analysis of ethanol dry autothermal reforming, Chemical Engineering Journal, 165, 864-873.

Kale G.R., Kulkarni B.D., 2011, An alternative process for gasoline fuel processors, International Journal of Hydrogen Energy, 36, 2118-2127.

Kale G.R., Kulkarni B.D., Chavan R.N., 2014, Combined gasification of lignite coal: A thermodynamic study, Journal of the Taiwan Institute of Chemical Engineers (Elsevier), 45, 163-173.

Kale G.R., Kulkarni B.D., Joshi A.R, 2010, Thermodynamic study of combining chemical looping combustion and combined reforming of propane, Fuel, 89, 3141–3146.

Kale G.R., Sonar S.S., 2011, Combined reforming of chemical looping combustion products: A thermodynamic analysis, Chemical Technology: An Indian Journal, 6(2), 98-106.